REGULATION AND FUNCTION OF THE CEREBRAL CAVERNOUS MALFORMATION 2 PROTEIN

Lisa Eileen Stalheim Crose

A dissertation submitted to the faculty of the University of North Carolina at Chapel Hill in partial fulfillment of the requirements for the degree of Doctor of Philosophy in the Department of Pharmacology.

Chapel Hill
2009

Approved by:

Gary L. Johnson, Ph.D.

Leslie V. Parise, Ph.D.

Lee M. Graves, Ph.D.

Rudolph L. Juliano, Ph.D.

Adrienne D. Cox, Ph.D.

ABSTRACT

LISA EILEEN STALHEIM CROSE: Regulation and Function of the Cerebral Cavernous Malformation 2 Protein
(Under the direction of Gary L. Johnson, Ph.D.)

Cerebral cavernous malformations (CCM) are vascular lesions of the central nervous system characterized as clusters of dilated, thin-walled blood vessels. CCM lesions are fragile and prone to vascular leakiness and rupture, leading to hemorrhages that cause seizure and stroke. Familial CCM has been shown to be genetically linked to three genes: *CCM1*, *CCM2*, and *CCM3*. The proteins encoded by these genes have no apparent catalytic activity, suggesting they are scaffolds to organize and localize functional protein complexes in cells. This scaffolding function has been appreciated for *CCM2*, which encodes Osmosensing Scaffold for MEKK3 (OSM). CCM2 (OSM) coordinates a signaling complex that consists of Rac1, MEKK3, and MKK3 to activate p38 in response to osmotic stimuli. The studies described here analyze the function of CCM2 in the context of cerebral cavernous malformations. Using proteomic, biochemical, and *in vivo* models, we characterize CCM2 as a critical regulator of endothelial cell signaling and function. We show that CCM2 binds and localizes the CCM1 protein. The CCM2 phosphotyrosine binding (PTB) domain is necessary for a canonical interaction with NPxY motifs within CCM1. We provide evidence of co-

immunoprecipitation and fluorescence resonance energy transfer (FRET) between CCM1 and CCM2, implicating a common genetic and molecular pathway in CCM pathogenesis. We also characterize CCM2 as a Smurf1 binding partner. Through a novel CCM2 PTB domain – Smurf1 HECT domain interaction, CCM2 recruits Smurf1 to specific locations at the plasma membrane where it specifically degrades RhoA. Knockdown of CCM2 in brain endothelial cells leads to increased RhoA protein levels and ROCK signaling. Functionally, this leads to deficiencies in cell migration, tube formation, and maintenance of a permeability barrier. To determine the role of CCM2 *in vivo*, we used *Danio rerio* as a model for vertebrate development. Loss of CCM2 expression leads to decreased blood flow due to restrictions and abnormalities of the aortic arch. The findings presented here indicate that CCM2 regulates protein complexes and signaling pathways important in endothelial cell function and provide insight into the molecular mechanisms involved in cerebral cavernous malformation pathogenesis.

To my teachers

ACKNOWLEDGEMENTS

This work would not have been possible without the outstanding mentorship of Dr. Gary Johnson. Gary has provided all the tools, both experimental and intellectual, to ensure the success of this project and my success as a scientist. I am also indebted to the members of the Johnson Lab for their scientific training and support. I would especially like to thank Dr. Amy Abell who always made time to teach me new techniques, troubleshoot experiments, discuss ideas, and be my “go-to” person for all things science. I feel very fortunate to have been surrounded by such an outstanding and creative group of scientists.

I would also like to thank the members of my thesis committee, Drs. Leslie Parise, Lee Graves, Rudy Juliano, and Adrienne Cox for their scientific guidance and assistance in writing my dissertation.

We have had many collaborators that were generous with their time and reagents for this work. Drs. Doug Marchuk and Jon Zawistowski at Duke University were our collaborators on the CCM1/CCM2 interaction project. Dr. Elwood Linney at Duke University allowed us to spend many months in his lab to do the CCM2 zebrafish project.

I am grateful for funding from the Integrated Vascular Biology Program, which is coordinated by Dr. Nobuyo Maeda, and a predoctoral fellowship from the American Heart Association.

I would like to thank Drs. Mark Vitha and Ron Torry at Drake University and Drs. Peter Anderson and Craig Moneypenny at University of Florida for being my first scientific mentors and for encouraging me to go to graduate school. If not for this early guidance and support I would have never considered graduate school as an option. I would also like to thank Drs. Rob Nicholas and Lee Graves for making sure I did my graduate work at UNC.

Finally, I would like to thank my Mom and Dad for teaching me all the skills I needed to be successful, Julie and Amy for always encouraging me and supporting me in everything I have done, Sherry for teaching me the value of a long walk, and Michael for always being by my side.

TABLE OF CONTENTS

LIST OF TABLES

TABLE

LIST OF FIGURES

FIGURE

LIST OF ABBREVIATIONS

BAEC: Bovine aortic endothelial cell

bEND.3: Mouse brain endothelioma cell

C2: Calcium-dependent phospholipid binding domain

CCM: Cerebral cavernous malformations

CCM1: Cerebral cavernous malformation 1 gene

CCM1: Protein encoded by cerebral cavernous malformation 1 gene, also known as KRIT1

CCM2: Cerebral cavernous malformation 2 gene

CCM2: Protein encoded by cerebral cavernous malformation 2 gene; also known as OSM, malcavernin

CCM3: Cerebral cavernous malformation 3 gene

CCM3: Protein encoded by cerebral cavernous malformation 3 gene; also known as PDCD10

CFP: Cyan fluorescent protein

Dab: Disabled homolog 1

DAF-16: abnormal DAuer Formation-16; *Caenorhabditis elegans* homolog of FOXO-1

DAF2-DA: 4,5-diaminofluorescein diacetate

DAPI: 4′,6′-diamidino-2-phenylindole

DIC: Differential interference contrast

E1: Ubiquitin-activating enzyme

E2: Ubiquitin-conjugating enzyme

E3: Ubiquitin ligase

EGTA: ethylene glycol tetraacetic acid

FERM: Band four-point-one, Ezrin, Radixin, Moesin

FLAG: Polypeptide tag consisting of DYKDDDDK

FRET: Fluorescence resonance energy transfer

$FRETN^{C}$: Fluorescence resonance energy transfer normalized and corrected

GFP: Green fluorescent protein

GST: glutathione S-transferase

HA: Hemagglutinin polypeptide tag

HECT: Homologous to the E6-AP carboxyl terminus

Hpf: Hours post fertilization

HUVEC: Human umbilical vein endothelial cell

ICAP1: Integrin cytoplasmic adapter protein-1

KRI-1: *Caenorhabditis elegans* homolog of KRIT1/CCM1

KRIT1: Krev Interaction Trapped 1

MAPK: Mitogen activated protein kinase

MAP2K: Mitogen activated protein kinase kinase

MAP3K: Mitogen activated protein kinase kinase kinase

MAPKK: Mitogen activated protein kinase kinase

MAPKKK: Mitogen activated protein kinase kinase kinase

MEEC: Mouse embryonic endothelial cell

MEF: Mouse embryonic fibroblast

MLC2: Myosin light chain 2

MO: Morpholino

NEDD4: neural precursor cell expressed, developmentally down-regulated 4

NLS: Nuclear localization sequence

OSM: Osmosensing scaffold for MEKK3; also known as CCM2, malcavernin

PCR: Polymerase chain reaction

PDCD10: Programmed cell death 10 protein

PTB: Phosphotyrosine binding

RNA: Ribonucleic acid

RNAi: RNA interference

RT-PCR: Reverse transcription polymerase chain reaction

SDS-PAGE: sodium dodecyl sulfate polyacrylamide gel electrophoresis

shRNA: short hairpin RNA

siRNA: small interfering RNA

Smurf1/2: Smad ubiquitination regulatory factor 1/2

WW: Proline-rich binding domain; named for critical tryptophan (W) residues within the domain

YFP: Yellow fluorescent protein

I. Introduction

Cerebral cavernous malformations (CCM) are vascular lesions of the central nervous system characterized as clusters of dilated, thin-walled blood vessels. These vascular "caverns" are surrounded by connective tissue, preventing innervation of the surrounding neural parenchyma (Clatterbuck et al., 2001). CCM lesions are fragile and prone to vascular leakiness and rupture, leading to hemorrhages that cause seizure and stroke (Marchuk et al., 2003; Plummer et al., 2005). In the general population, it is believed that 0.5 – 1.0% individuals will be affected by CCM in their lifetime.

Cavernous malformations (also known as cavernous angiomas) can occur sporadically or through autosomal dominant inheritance of mutations in one of three genes: *CCM1*, *CCM2*, and *CCM3*. Although there is incomplete penetrance of the CCM phenotype, this familial form accounts for over 20% of CCM cases. Therefore, understanding the roles of *CCM1*, *CCM2*, and *CCM3* in cell physiology is critical for our understanding of CCM pathogenesis.

CCM1

Mutations in *CCM1* lead to truncations of the protein Krev Interaction Trapped 1, or KRIT1 (Sahoo et al., 1999; Zhang et al., 2000b). To date, over 100 germline mutations have been identified in *CCM1*, most involving premature stop codons due to nonsense, frameshift, or spice-site mutations (Cave-Riant et

al., 2002; Chen et al., 2002; Couteulx et al., 2002; Davenport et al., 2001; Eerola et al., 2001; Laberge-le Couteulx et al., 1999; Laurans et al., 2003; Lucas et al., 2001; Marini et al., 2003; Marini et al., 2004; Musunuru et al., 2003; Sahoo et al., 2001; Sahoo et al., 1999; Verlaan et al., 2002; Xu et al., 2003; Zhang et al., 2000b). It is widely believed that these mutations in *CCM1* lead to loss of function of this gene.

CCM1/KRIT1 had previously been identified in a yeast two-hybrid screen for proteins that interact with the Ras family GTPase Krev1/Rap1A. Initial characterization of CCM1 found that the carboxy- terminus of CCM1 shared a weak homology to the Band 4.1 protein. This region of homology would later be characterized as a FERM domain, based on the domains of Band four-point-one, Ezrin, Radixin, and Moesin. CCM1 also contains three ankyrin domains in the central region of the protein, assumed to be for additional protein interactions. The FERM domain of CCM1 was determined to be necessary for interaction with Krev1/Rap1A and CCM1 itself did not bind strongly to Ras. It was speculated that because of its binding to Krev/Rap1A and not Ras, CCM1 could be specifically regulating Krev/Rap1A signaling (Serebriiskii et al., 1997).

Following the initial study of CCM1 as a Rap1A binding protein, this data was contested when additional groups could not confirm this association. In these studies, a longer CCM1 bait was used. This was due to the identification of additional *CCM1* exons at the 5' end of the sequence, extending CCM1 by 207 amino acids (Eerola et al., 2001; Sahoo et al., 2001; Zhang et al., 2000a). Surprisingly, this longer CCM1 did not associate with Krev1/Rap1A, suggesting

that either the amino-terminus of CCM1 masks the Krev1/Rap1A binding site, or previous data using the shorter CCM1 needed further confirmation (Zawistowski et al., 2002; Zhang et al., 2001). The CCM1-Rap1A interaction was therefore re-examined. Using multiple biochemical assays, CCM1 was confirmed as a Rap1A binding protein, but binding was regulated by a CCM1 conformational change (Sophie Béraud-Dufour, 2007). CCM1 was found to exist in an open or closed conformation, and this conformational change regulated Rap1A binding. This work confirmed the CCM1-Rap1A interaction, and resolved the discrepancy associated with previous studies of CCM1-Rap1A interactions.

The CCM1-Rap1A interaction was determined to function as a mechanism to recruit CCM1 to endothelial cell junctions. Endogenous CCM1 localized at endothelial cell junctions, as determined by co-localization with β-catenin. Endogenous β-catenin also associated with endogenous CCM1 by co-immunoprecipitation. Expression of an active form of Rap1A (Rap1A-G12V) increased association of CCM1 with β-catenin, while expression of an inhibitor of Rap1A activity (Rap1GAP) decreased association of CCM1 with β-catenin. Knockdown of CCM1 expression led to loss of β-catenin at cell junctions, increased stress fiber formation, and increased endothelial cell permeability. Further, expression of exogenous CCM1 was able to reverse increased permeability induced by expression of Rap1GAP. Taken together, CCM1 plays an important role in endothelial permeability through Rap1A-mediated association with endothelial cell junctions (Glading et al., 2007).

A second binding partner for CCM1 is Integrin Cytoplasmic Adapter Protein-1 (ICAP1) (Zawistowski et al., 2002; Zhang et al., 2001). ICAP1 is a negative regulator of β_1 integrin signaling implicated in osteoblast proliferation and differentiation (Bouvard et al., 2007). ICAP1 contains a Phosphotyrosine Binding (PTB) domain, which is responsible for its association with the β_1 tail through a conserved Asparagine – Proline – any amino acid – Tyrosine (NPxY) motif (Chang et al., 1997; Zhang and Hemler, 1999). An NPxY motif was also found within the amino acid sequence of CCM1 (N192-Y195), suggesting that the ICAP1 PTB domain could interact with this CCM1 NPxY motif. Mutation of the CCM1 NPxY motif led to a decrease in ICAP1 binding demonstrated by GST pulldown and by liquid beta-galactosidase assay (Zawistowski et al., 2002). Because of the critical role of β_1 integrins in endothelial cell function, it was hypothesized that loss of CCM1 may lead to defects in endothelial cell adhesion and migration through ICAP1 binding.

The importance of the CCM1-ICAP1 interaction was defined when ICAP1 was found to regulate the open/closed conformation of CCM1 (Sophie Béraud-Dufour, 2007). The CCM1 intermolecular interaction was shown to be between CCM1 NPxY motifs and the CCM1 FERM domain. Presumably, this was occurring between the CCM1 NPxY motifs and the F3 subdomain of the CCM1 FERM domain, which shares structural similarity to PTB domains (Calderwood et al., 2002). The interaction between the CCM1 NPxY motif and CCM1 FERM domain was lost upon addition of ICAP1. Furthermore, in GST-pulldown experiments, CCM1, ICAP1, and Rap1A were found to exist as a ternary protein

complex. Based on these data, it was suggested that ICAP1 could induce the open conformation of CCM1 by binding CCM1 NPxY motifs. In the open conformation, CCM1 would then be available to interact with Rap1A. Based on our current knowledge of CCM1 as a Rap1A effector, this would imply that ICAP1 could act to regulate the availability CCM1 as a Rap1A effector to regulate cell junctions (Figure 1.1).

CCM2

MGC4607 was identified as the *CCM2* gene in 2003. In nine families analyzed, eight unique mutations, predominantly deletions leading to frameshift changes, were found within the *CCM2* gene. Based on the amino acid sequence of *CCM2*, a PTB domain was identified in the amino-terminus of CCM2. Interestingly, the amino-terminal end of *CCM2*, including the PTB domain, harbored all of the mutations identified in the cohort (Liquori et al., 2003). Further analysis identified more pronounced genetic lesions in *CCM2* patients, including large deletions of almost the entire *CCM2* gene (Liquori et al., 2007).

Concomitant with the discovery of MGC4607 as the CCM2 gene, the mouse homolog of CCM2 was characterized as Osmosensing Scaffold for MEKK3 (OSM). Although there are many upstream MAPKKKs that activate p38, MEKK3 was found to be specifically involved in hypertonic activation of this pathway (Uhlik et al., 2003). MEKK3 knockdown cells were found to be deficient in their activation of p38 in response to sorbitol. OSM was found to be an important regulator of this pathway. Identified in a yeast two-hybrid screen using

MEKK3 as bait, OSM was found to associate with MEKK3 and MKK3 by immunoprecipitation. Expression of OSM with MEKK3 was found to synergistically increase MKK3 phosphorylation. Further, joint knockdown of OSM with MEKK3 synergistically decreased activation of p38 in response to sorbitol treatment. Endogenous OSM was found to associate with actin ruffles, and sorbitol treatment of COS-7 cells induced OSM and MEKK3 association in live cells by fluorescence resonance energy transfer (FRET). The GTPase Rac1 was also found to associate with OSM, and this association was induced by sorbitol treatment in live cells. Therefore, it was hypothesized that the signaling module of Rac1-OSM-MEKK3-MKK3 to activate p38 was analogous to the Hog1 osmotic signaling pathway in *Saccharomyces cerevisiae* (Uhlik et al., 2003).

In response to high osmotic conditions, cells rapidly lose water and shrink. Yeast counter this loss of water by accumulating intracellular glycerol through closure of glycerol channels and up-regulation of genes for glycerol synthesis. This is in part coordinated by the Hog1p mitogen activated protein kinase (MAPK) signaling pathway. In response to extracellular hyperosmotic stress, an osmotic signaling complex consisting of Cdc42p, Ste20p, Ste50p and Ste11p is recruited to the plasma membrane. Ste50p recruits the p21-activated kinase Ste20p to the MAP kinase kinase kinase (MAPKKK) Ste11p. Ste11p then phosphorylates and activates Pbs2 (MAPKK) which phosphorylates Hog1p. Hog1p is then translocated to the nucleus where it regulates gene expression (both positively and negatively) by phosphorylation of transcription factors. Out of all the genes that are upregulated in response to hyperosmotic stress, only

20% of these genes are fully Hog1p-dependent, based on Hog1-deficient cells. Yet, the genes that are fully Hog1p-dependent include genes that are the most strongly upregulated in response to hyperosmotic stress (Hohmann et al., 2007; Willem H Mager, 2002). Therefore, the Hog1p pathway is necessary for osmotic adaptation, and this pathway is coordinated by Ste50p, the OSM homolog (Figure 1.2).

Since OSM is the mouse homolog of CCM2, the MEKK3-p38 signaling pathway could therefore be involved in CCM pathology. Indeed, MEKK3 and p38 knockout animals have defects in vascularization in utero (Adams et al., 2000; Yang et al., 2000). However, if deficiencies in p38 signaling lead to CCM is not known.

CCM3

The *CCM3* gene was documented in 2005 by two independent groups (Bergametti et al., 2005; Guclu et al., 2005). Similar to *CCM1* and *CCM2*, most mutations in the *CCM3* gene led to premature stop codons or gene deletions. The *CCM3* gene encodes the protein Programmed Cell Death protein 10. CCM3/PDCD10 was first identified in a screen for genes upregulated in the human myeloid cell line TF-1 upon apoptotic induction. Analysis of the primary structure of CCM3 does not identify any functional domains. CCM3 is ubiquitously expressed and is highly conserved, from *Caenorhabditis elegans* to human.

CCM3 is a binding partner for Mammalian Sterile Twenty-like 4 (MST4). MST4 is a Ste20-like kinase capable of activating the ERK MAPK pathway and promoting cell proliferation (Lin et al., 2001). CCM3 and MST4 co-localize in distinct perinuclear regions in HeLa cells. Expression of exogenous CCM3 in PC-3 cells demonstrated that CCM3 could also induce cellular proliferation. RNAi-medated knockdown of CCM3 inhibits normal cellular proliferation as well as MST4-induced proliferation. CCM3 expression increased phosphorylation of ERK, which could be abrogated by treatment with MST4 siRNA. Therefore, CCM3 and MST4 could act in a common pathway to activate ERK signaling (Ma et al., 2007). Although these studies demonstrate a clear role for CCM3 and MST4 in ERK signaling and cell proliferation, to date there has been no examination of CCM3 in endothelial cells.

Animal models of CCM

Mus musculus

In order to understand the role of the CCM genes in development and angiogenesis, gene knockout models were generated for *CCM1*. The first mouse *CCM1* knock-out was a *CCM1* gene-trap model, generated by insertion of the beta-galactosidase gene in CCM1 exons 6-7. The resulting *CCM1*-null homozygotes led to embryonic lethality at E8.5-9.5 with predominant vascular defects. At this stage, these embryos displayed dilated vessels of the cephalic mesenchyme and an undeveloped yolk sac. The dorsal aortae of these embryos also exhibited a distended morphology that was suggested to be due to

differences in proliferation rates of the endothelial cells in this region. Furthermore, these vessels were defective in their ability to recruit smooth muscle cells and expressed significantly less *EphrinB2*, *Dll4*, and *Notch4,* which are arterial markers. It was suggested that CCM1 was necessary for arterial identity and morphogenesis (Whitehead et al., 2004).

These studies were the first to examine the physiological importance of *CCM1* in vascular development. However, this model was not adequate for modeling CCM pathogenesis. Human CCM patients are not homozygous for mutations in CCM genes. For all CCM genes identified, patients are heterozygous for familial mutations in CCM genes. Therefore, in order to determine if the *CCM1* knock-out mouse was a proper animal model for CCM, it was important to determine if mice that were heterozygous for the *CCM1* gene had an increased chance of CCM formation. In 20 adult mice heterozygous for *CCM1* (aged 8 weeks to 14 months), no brain lesions were seen by gross dissection. This suggested that a "two hit" genetic model (described below) may be needed to generate a proper mouse model for CCM. With this in mind, a *CCM1*+/- *Trp53-/-* double knock-out mouse line was generated. Because of the increased rate of mutation in a p53-null background, it was believed that this could induce somatic muations and increase the prevalence of CCM lesions. This rationale led to brain vascular malformations in five of the nine *CCM1+/- Trp53-/-* mice analyzed. No vascular malformations were found in *CCM1+/- Trp53+/-* mice or *CCM1+/+ Trp53-/-* mice. However, no loss of heterozogosity at *CCM1* was observed, nor were any mutations in *Trp53* found in any CCM

patients (Plummer et al., 2004). This suggested that a second mutation, a somatic mutation, was necessary to model CCM1 pathogenesis in mice.

Interestingly, *CCM2* heterozygous gene-trap mice displayed cerebral hemorrhage without knockout of *Trp53.* The penetrance of such lesions was low (about 10% of adult animals), but the morphology of the lesions was similar to those seen in *CCM1+/- Trp53-/-* knockout mice. Similar to *CCM1*, the *CCM2* knockout was generated by insertion of a gene-trap vector into the *CCM2* gene. The insertion of βGeo into exon 6 of *CCM2* caused a deletion of 45 base pairs of this exon leading to a transcript that contained the amino terminus of CCM2 through the PTB domain, but truncation of the carboxy terminus. Similar to *CCM1* knockout mice, *CCM2* homozygous null mice died during gestation. Due to the low penetrance of lesions it was hypothesized that a two-hit model was also likely for a mouse model of CCM2 (Plummer et al., 2006). To date, no mouse models of CCM3 have been published. These mouse models show that CCM can be modeled in mice; however the molecular events that trigger CCM lesion formation are not known.

Caenorhabditis elegans

The *C. elegans* homologue of CCM1, KRI-1, was identified in a screen for genes involved in organism longevity. In this model, longevity is regulated by intestinal-reproductive tract interactions. A key signaling pathway involved in reproductive system regulation of longevity is the IGF-1-Akt pathway. IGF-1 signaling activates Akt leading to phosphorylation of the transcription factor

FOXO1. The FOXO1 homolog in *C. elegans* is DAF-16. Phosphorylation of DAF-16 sequesters it in the cytoplasm, preventing its ability to regulate gene expression. Loss of KRI-1 expression in the sterile longevity model suppressed longevity. Examination of intestinal DAF-16 showed that in KRI-1 RNAi treated animals DAF-16 had reduced nuclear localization. This nuclear localization defect was independent of DAF-16 phosphorylation, as the mislocalization could be overcome by expression of a DAF-16 whose Akt phosphorylation sites were mutated to alanine. This suggested a role for KRI-1 in DAF-16 localization, either by preventing Akt phosphorylation of DAF-16, or through an independent localization function of KRI-1 (Berman and Kenyon, 2006). However, the mechanism of this regulation has not been determined, either in *C. elegans* or mammalian systems.

CCM cell of origin

CCM lesions are predominantly in the central nervous system. What causes lesions to specifically occur in the CNS? As neural, astrocytic, and pericytic innervations regulate the cerebral microvasculature (Figure 1.3), the cell of origin for CCM has been relatively controversial. An initial study of the *CCM1* expression pattern in the mouse embryo suggested that CCM1 was predominantly expressed in neural cells but not endothelial cells. Using in situ hybridization, *CCM1* mRNA was ubiquitously detected in E7.5-E9.5 mouse embryos. Later term embryos displayed predominant nervous system expression of *CCM1*, as well as epithelial tissues such as lung and intestine.

The tissues of the cardiovascular system showed embryonic expression of *CCM1* in the heart and aorta, but not in capillaries. Furthermore, in adult human and mouse tissues, *CCM1* was expressed in the neuronal layers of the cerebral cortex, the brainstem, and epithelial tissues. *CCM1* expression was not detected in the adult vasculature (Denier et al., 2002). Similar expression patterns were observed for *CCM2* RNA. In adult murine brain tissue, *CCM2* expression was strong in neuronal populations but undetectable in brain vascular endothelium (Plummer et al., 2006). This suggested that cells other than endothelium may be involved in the pathogenesis of CCM.

A more complex view of CCM gene expression in the mouse was observed by Petit and colleagues in 2005. By *in situ* hybridization, strong expression of *CCM1*, *CCM2*, and *CCM3* was observed in the developing nervous system, including the ventricular zone, intermediate zone, cortical plate and ganglionic eminence in the brain, as well as the spinal cord. Similarly, neuronal cell layers at P8 and P19 displayed strong expression of the 3 CCM genes as well as the motor neurons of the grey matter of the adult spinal cord. In the cardiovascular system, *CCM1*, *CCM2*, and *CCM3* were expressed in the heart, aorta, and cardinal vein at E10.5, and at E14.5 this expression persisted in the superior vena cava and aorta, internal carotid, and vertebral and basilar arteries. Examination at P0 showed loss of expression in these regions. In the cerebral vasculature, weak or no expression was observed prenatally, but postnatally weak expression was observed for *CCM2* and *CCM3* at P0 and P8. This expression was lost by P19. Altogether, these experiments suggested restricted

and transient expression of CCM genes in the cerebral vasculature and predominant expression of these genes in neuronal cells. In regards to CCM pathogenesis, a prominent role for perenchymal cells and perenchymal-endothelial cell interactions could not be discounted (Petit et al., 2006).

CCM is believed to be due to endothelial defects, based on ultrastructural data that shows defective cell to cell contacts within CCM lesions (Clatterbuck et al., 2001). This is supported by the *CCM1* knockout mouse, which displayed vascular abnormalities but normal brain development (Whitehead et al., 2004). However, mRNA expression data implies a potential role for CCM genes in neuronal cells. The cellular interactions within the cerebral vasculature are complex, including a prominent role for neuronal, astrocytic, and pericytic innervation in the microvasculature of the brain (Figure 1.3). The importance of these supporting cells has become clearer through use of conditional knockout animals. One example of the importance of the cerebrovascular support cells is with the $\alpha_v\beta_8$ integrin. Knockout of the α_v integrin leads to embryonic (E10.5-E12.5) and perinatal lethality due to intracranial and intestinal hemorrhage. The α_v-null embryos displayed normal vascular patterning and vascularization of the placenta; however, at E11.5-E12.5 blood vessels within the brain were dilated and distended. This led to subsequent hemorrhage (Bader et al., 1998). The mouse knockout for the β_8 integrin displayed a similar phenotype, with lethality occurring due to insufficient vascularization of the yolk sac and placenta or intracerebral hemorrhage from distended blood vessels (Zhu et al., 2002). Elegant studies done by McCarty et. al, subsequently showed that conditional

knockout of the α_v integrin in endothelial cells (using Tie2-Cre) did not lead to intracerebral hemorrhage, but knockout of the α_v integrin in astrocytes (using GFAP-Cre) or neurons and astrocytes (using Nestin-Cre) caused intracerebral hemorrhage (McCarty et al., 2005). Further, the endothelial conditional knockout of β_8 integrin displayed no cerebral hemorrhages with but did display cerebral hemorrhages in a neural-astrocytic conditional knockout model. To further elucidate what cell type is involved in the cerebral hemorrhages, a β_8 integrin conditional knockout for postmitotic neurons (using Nex-Cre) was used, which did not cause cerebral hemorrhage (Proctor et al., 2005). Taken together, these studies suggested that the astrocytic interactions with endothelial cells were the cause of cerebral hemorrhage. Indeed, conditional β_8 integrin knock out mice with hemorrhages had disorganized cortical glia and endothelial cells, and $\alpha_v\beta_8$ integrin was found to be localized on glial cell processes in wild type mice (McCarty et al., 2005; Proctor et al., 2005). As CCM is a disease predominantly manifested in the blood vessels of the central nervous system, similar neural, glial, and endothelial interactions may prove important in the pathogenesis of the disease. Ideally, similar conditional knockout studies in mice will be performed with *CCM1*, *CCM2*, and *CCM3* to elucidate these mechanisms.

The two-hit hypothesis

Familial CCM shows incomplete penetrance. In humans, there is lesion formation in ~60% of individuals that are genetically heterozygous for inherited mutations in CCM genes (Labauge et al., 2007). In mouse models there is a

near absence of lesions in animals that are heterozygous for CCM1 or CCM2 expression. When crossed into a *Trp53-/-* background to induce genetic instability and somatic mutations, mice heterozygous for the CCM1 gene-trap allele had significantly more CCM lesions than those without *Trp53* knockout (Plummer et al., 2004). Therefore it was hypothesized that there must be a second genetic hit associated with CCM lesion formation, analogous to what is observed in retinoblastoma (Goodrich and Lee, 1993).

Recent studies definitively prove the "two hit" hypothesis for induction of CCM. A recent study was able to demonstrate that bi-allelic mutations in CCM genes existed in endothelial cells from CCM lesions. These somatic mutations were not seen in cells surrounding the lesion (Akers et al., 2009). Further support of the two hit hypothesis was a study of CCM protein immunoreactivity in CCM lesions. Loss of immunoreactivity of CCM1, CCM2, or CCM3 was observed in endothelial cells from CCM lesions with the corresponding mutations in CCM1, CCM2, or CCM3, but not adjacent vascular beds (Pagenstecher et al., 2009). These studies show that in human CCM, mutation of both alleles and subsequent loss of expression of CCM1, CCM2, or CCM3 are critical steps in CCM pathogenesis.

CCM2, structure and function

The CCM2 protein contains a PTB domain in the amino terminal region. By homology, the CCM2 PTB domain is most similar to the Dab-like PTB domains (Uhlik et al., 2005). Dab-like PTB domains contain a PH-domain

superfold, which is a structural feature common to all PTB domains. As the name implies, the PH domain superfold is similar to the prototypical phospholipid-binding PH domain. Indeed, numerous PTB domains have been shown to bind to phospholipids, likely regulating their cellular localization.

A distinguishing feature of Dab-like PTB domains is their peptide binding specificity. The canonical binding motif for PTB domains is Asn-Pro-X-Tyr (NPxY), which forms a β turn. The prototypical PTB domains of Shc and IRS-1 bind to these NPxY motifs when the tyrosine is phosphorylated. Dab-like PTB domains bind to unphosphorylated tyrosines in this motif, and in some cases prefer phenylalanine (NPxF). Therefore, interactions between Dab-like PTB domains and their interacting peptides are due to extensive hydrophobic contacts and hydrogen bonds within and surrounding the NPxY or NPxF motif.

Interestingly, the CCM2 PTB domain is most similar to the ICAP1 PTB domain, which binds to CCM1 (Uhlik et al., 2005). Thus, there is the potential that CCM2 could be utilizing its PTB domain to bind to CCM1. This would link CCM1 and CCM2 genetically and molecularly, suggesting that a common signaling pathway is involved in CCM pathogenesis.

Objectives of this project

CCM signaling pathways

Examination of the primary sequence of CCM1, CCM2, and CCM3 illustrates that these three proteins do not contain any identifiable catalytic domains. However, they do contain protein interaction domains (Figure 1.1). We

hypothesize that CCM pathogenesis could be caused by improper protein scaffolding and subsequent cell signaling abnormalities. Since mutations in *CCM1*, *CCM2*, or *CCM3* all lead to the same disease, there is the potential that CCM1, CCM2, and CCM3 are involved in a common signaling pathway. This sole pathway may be responsible for CCM. It is also possible that individual pathways mediated by CCM1, CCM2, or CCM3 could lead to similar phenotypes. In order to understand these signaling pathways, we would like to determine proteins that interact with CCM2. We can then begin to elucidate the functions of these proteins both in normal cell physiology and how loss of these proteins could lead to CCM. We plan to utilize proteomic strategies to find binding partners for CCM2.

CCM proteins also need to be examined in the context of cerebral microvascular cells. To date, studies that have utilized endothelial cell culture systems have used either HUVECs or BAECs. These are good models for primary endothelial cells, but different models are needed for study of CCM. The endothelial cells of the brain are specialized to maintain the blood brain barrier, and their physiology is quite different from other endothelial cells. Because cerebral cavernous malformations lesions frequently occur in the central nervous system, the most logical cell system to use would be cerebral endothelial cells. Therefore, we plan to examine role of endogenous CCM2 in brain endothelial cells using RNAi.

CCM2 protein function in vivo

Loss of CCM2 expression in a mouse gene-trap model leads to embryonic lethality at E9.5. Such early embryonic lethalities are difficult to study, and mouse colony breeding and maintenance for examination of embryonic lethalities are costly and time consuming. Since CCM2 is necessary for embryonic development, we plan to utilize a common model for vertebrate development, *Danio rerio*. The zebrafish developmental model has many advantages when compared to mouse. Zebrafish undergo major developmental processes in a short period of time. By 72 hours post fertilization (hpf), zebrafish embryos have undergone major morphogenic events for the majority of organ systems, allowing rapid screening for defects associated with early embryonic lethalities. Zebrafish are amenable to genetic manipulation by translational-blocking morpholios. What many consider the greatest advantage of the zebrafish model is that embryo development occurs externally and embryos are optically clear. We will be examining the role of CCM2 in vertebrate development by using CCM2 translational-blocking morpholinos and characterizing defects associated with CCM2 loss.

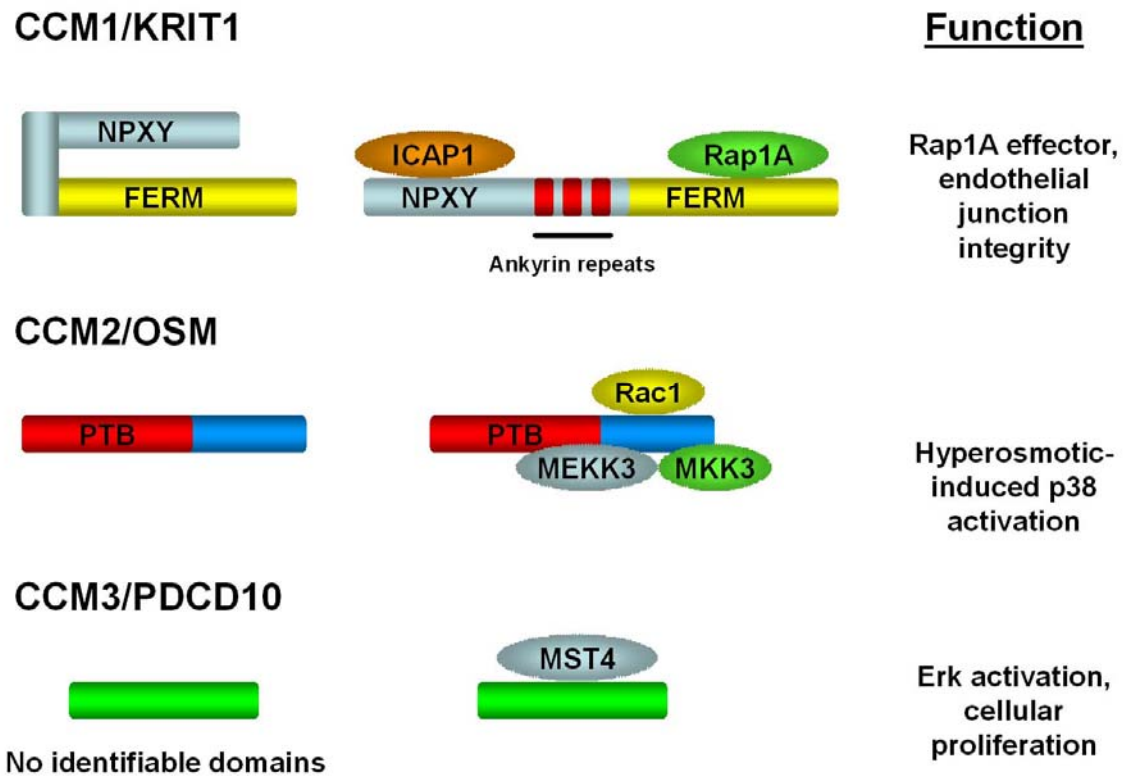

Figure 1.1: Domain structure, interacting proteins, and known function of CCM1, CCM2, and CCM3. CCM1 exists in a closed or open conformation, which is regulated by ICAP1. This can regulate association of CCM1 with Rap1A. CCM2 associates with Rac1, MEKK3, and MKK3 to activate p38 in response to osmotic stress. CCM3 has no identifiable domains, but has been shown to associate with the MST4 kinase to activate Erk signaling pathways.

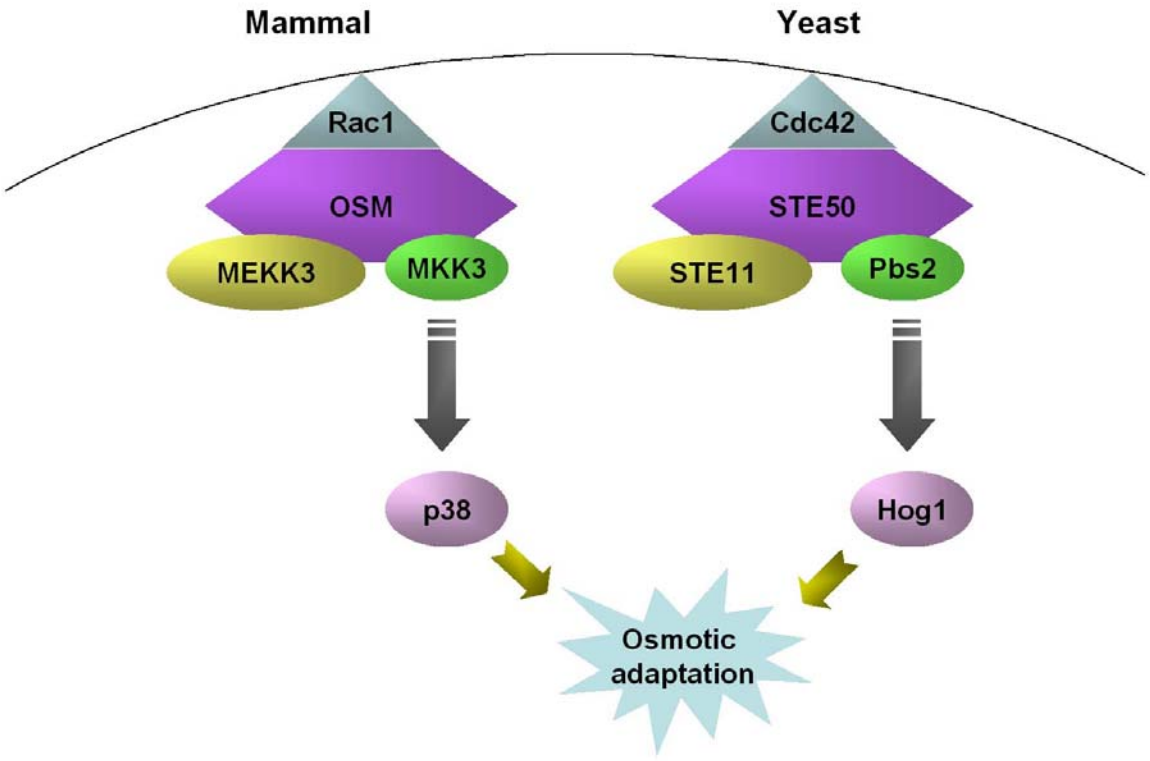

Figure 1.2: Osmotic signaling to p38 via OSM/MEKK3 in mammals is analogous to signaling to Hog1 via STE50/STE11 in yeast. Rac1 and OSM associate at the plasma membrane. Upon hyperosmotic stimulus, OSM coordinates a signaling complex of MEKK3 and MKK3 to activate p38. Yeast utilizes a signaling complex of Cdc42, STE50, STE11, and Pbs2 to activate Hog1 in response to osmotic stimuli.

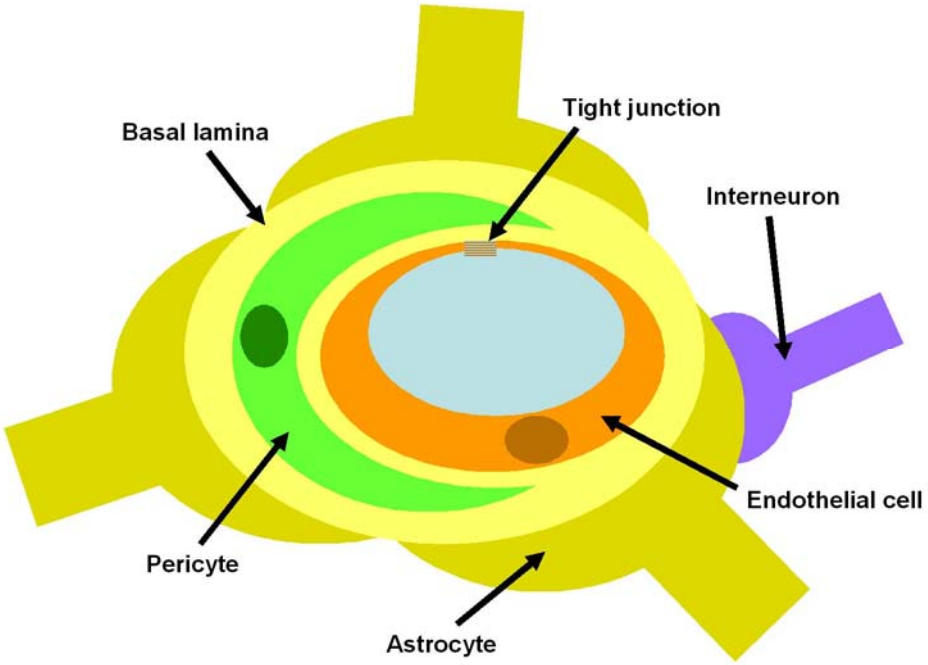

Figure 1.3: The neurovascular unit. The microvasculature of the central nervous system contains endothelial cells supported by pericyte and astrocytic innervations. Endothelial cells maintain tight junctions with each other as well as complex interactions with supporting cells. The cerebral vasculature also receives input from interneurons through astrocytic processes. Adapted from (Abbott et al., 2006).

II. Materials and Methods

Chapter 3

Plasmids and cell culture

Full-length cDNAs for human CCM1 and ICAP1α were isolated by RT–PCR from HUVEC RNA, N-terminally FLAG-tagged by PCR and subsequently cloned into the mammalian expression vector pRK5. Full-length cDNA for CCM2 was N-terminally FLAG-tagged by PCR using human IMAGE Consortium clone 3501896 was used as template and subsequently cloned into pRK5. For CFP and YPF fusion proteins, full-length human CCM1 cDNA was inserted in-frame to the coding sequence of EYFP of pEYFPC1 (Clontech) and full-length human ICAP1α cDNA was inserted in-frame to the coding sequence of ECFP of pECFPC1 (Clontech). CFP-CCM2 and hemagglutinin (HA)-MEKK3 have been described previously (Uhlik et al., 2003). Missense mutations were made using QuickChange™ (Stratagene) site-directed mutagenesis kit and confirmed by sequencing.

293T cells and COS-7 cells were maintained in Dulbecco's modified Eagle medium (DMEM, Invitrogen)/10% fetal bovine serum (FBS, Invitrogen) and supplemented with amphotericin B (GensiaSicor Pharmaceuticals) and penicillin/streptomycin (Invitrogen) at the manufacturers' recommended concentrations.

Immunoprecipitation and western blotting

For co-immunoprecipitation assays, 293T cells were transfected with the constructs listed using FuGene6™ reagent (Roche). Transfected 293T cells or MEFs were lysed in a buffer containing 0.6% Triton X-100, 137 mM NaCl, 10% glycerol and 20 mM Tris pH 7.4 supplemented with Complete™ protease inhibitor tablets (Roche). About 500 µg of cell lysate was incubated with a rabbit polyclonal CCM2 (OSM) antibody (Uhlik et al., 2003) with gentle rocking at 4°C for 2 hours followed by incubation with protein G-sepharose 4B beads (Amersham) at 4°C for 1 hour. The beads were washed five times with lysis buffer, boiled for 5 min in SDS-loading buffer and resolved by SDS–PAGE.

For western blotting, the following antibodies were used: anti-FLAG antibody (M2, Sigma), anti-HA antibody (Sigma), and affinity-purified anti-CCM1 antibody (Bethyl Laboratories, Inc.).

Fluorescence resonance energy transfer

For live-cell fluorescence microscopy and CFP-YFP FRET experiments, COS-7 cells were grown on 25 mm round glass coverslips. Cells were subsequently transfected using Lipofectamine Plus™ (Invitrogen). After 24 hours, cells were placed in a media-filled imaging chamber (Molecular Probes) at room temperature. Cells were treated with 0.2 M sorbitol for the indicated times. CFP-YFP FRET image acquisition and analysis were performed by the three-filter micro-FRET image subtraction method as described previously (Sorkin et al.,

2000). Briefly, images for YFP excitation/YFP emission, CFP excitation/CFP emission and CFP excitation/YFP emission (raw FRET) were obtained using an Axiovert 200M microscope from Zeiss (Germany) and imaging software from Intelligent Imaging Innovations (Denver, CO). Background-subtracted YFP and CFP images were then fractionally subtracted from raw FRET images on the basis of measurements for CFP bleed-through (CFP-CCM2=0.55 and CFP-CCM2 F217A=0.52) and YFP cross-excitation (YFP-CCM1=0.021 and YFP-CCM1 N192A=0.024). This fractional subtraction generated corrected FRET images ($FRET^C$) that function as visual representations of interacting proteins.

MEF isolation

E10.5 primary MEF cultures were established from wild type embryos and littermate embryos heterozygous for a LacZ gene trap insertion in the mouse *Ccm2* gene (cell line RRG051, Bay Genomics, allele designation $Ccm2^{Gt(pGt0Lxf)1Dmar}$). Cells were maintained in Iscove's modified Dulbecco's medium (IMDM, Invitrogen)/10% FBS (Invitrogen) and supplemented with penicillin/streptomycin (Invitrogen) and amphotericin B (GensiaSicor Pharmaceuticals) at the manufacturers' recommended concentrations. Established MEF cell lines were genotyped by PCR using the following primers: 5'-CATCCCTGTCTGGGAACCTA-3' (CCM2 intron 6, reverse), 5'-TCTAGGACAAGAGGGCGAGA-3' (gene trap, reverse) and 5'-GAAGAGTTGTGCTCCCTGCT-3' (CCM2 exon 6, forward).

MAPK activation assay

Spontaneously immortalized wild type and *CCM2*$^{+/-}$ MEFs were serum-starved in OptiMEM™ (Invitrogen) overnight. Cells were then treated with 0.2 M sorbitol or 10 µg/ ml anisomycin for the indicated times and harvested in lysis buffer containing 0.6% Triton X-100, 137 mM NaCl, 10% glycerol and 20 mM Tris pH 7.4 supplemented with Complete™ protease inhibitor tablets (Roche). Fifty µg of cell lysate was resolved by SDS–PAGE. For western blotting, anti-p38 MAP kinase (Santa Cruz Biotechnology, sc-7149) and anti-phospho-p38 MAP kinase (Thr180/Tyr182, Cell Signaling, #9211) were used. Phosphorylated p38 was quantified using densitometry and normalized to levels of total p38 to yield an activation index. Fold induction was calculated as the activation index of the sample divided by the activation index of the untreated sample. For add-back experiments, *CCM2*$^{+/-}$ MEFs were transfected with pRK5-FLAG-CCM2 using the Amaxa Nucleofector™. Cells were used 24 hours post-transfection for p38 activation experiments.

Immunofluorescence

COS-7 cells were grown and transfected on fibronectin-coated coverslips (Becton Dickinson). Cells were washed with phosphate-buffered saline (PBS) and subsequently fixed for 14 minutes in 3% paraformaldehyde/3% sucrose/PBS, washed three times with PBS and permeabilized for 6 min in 0.1% Triton X-100/PBS. Coverslips were washed an additional three times and blocked for 30

minutes in a blocking solution consisting of DMEM containing 10% goat serum. Coverslips were then incubated for 2 hours at room temperature with anti-FLAG antibody (M2, Sigma) diluted in blocking solution. After washing with PBS, coverslips were incubated for 1 hour at room temperature with goat anti-mouse antibody conjugated to AlexaFluor™ 594 (1:1000, Molecular Probes™, Invitrogen). After final washes with PBS, coverslips were mounted with ProLong Gold™ antifade reagent (Molecular Probes™, Invitrogen).

Chapter 4

Zebrafish husbandry

Wild-type AB* *Danio rerio* were handled in accordance with IACUC approved protocols. Embryos were obtained from natural spawning. Embryos were raised in 30% Danieau solution (17 mM NaCl, 0.21 mM KCl, 0.12 mM $MgSO_4$, 0.18 mM $Ca(NO_3)_2$, 1.5 mM HEPES pH 7.6) and incubated at 28.5º C.

Morpholino injection:

Morpholinos were purchased from Gene Tools (Philomath, OR). Morpholinos were designed to the translational start site of the *Danio rerio CCM2* gene. Two CCM2-specific morpholinos (MO) were used: MO #1: ATCTAATACAGCGAAAATGAAGAGC, MO #2: ATTTGTACGTAGAGATGGAGGAGGA, underlined ATG is translational start site). Morpholinos were diluted to 2 ng/nL and 5 nL were used per injection, unless otherwise specified. As a control, 1X Danieau solution was used for

injection (57 mM NaCl, 0.7 mM KCl, 0.4 mM $MgSO_4$, 0.6 mM $Ca(NO_3)_2$, 5 mM HEPES pH 7.6). Embryos were injected between the 1- and 4- cell stages.

DAF2-DA labeling

The fluorescent nitric oxide (NO) indicator 4,5-diaminofluorescein diacetate (DAF-2DA) was a gift from Dr. Margaret Kirby (Duke University). Live embryos were incubated in 10 µM DAF-2DA for 4 hours in the dark at 28.5º C. After incubation, embryos were then euthanized and imaged for DAF2-DA fluorescence.

Blood flow measurements

In silico microangiography was performed as previously described (Malone et al., 2007).

Chapter 5

Cell culture

HEK293 and COS-7 cells were maintained in Dulbecco's modified Eagle medium (DMEM, Gibco) supplemented with 10% fetal bovine serum (FBS, Gibco) and penicillin/streptomycin (Gibco). Microvascular brain endothelial cells (bEND.3) cells were purchased from ATCC and also cultured in DMEM supplemented with 10% FBS and penicillin/streptomycin. Mouse embryonic endothelial cells (MEECs) were cultured in DMEM supplemented with 3% FBS and penicillin/streptomycin. Transfection of HEK293 and COS-7 was done using

Lipofectamine (Invitrogen) according to the manufacturer's instructions. Human umbilical vein endothelial cells (HUVEC) and EBM-2 growth medium were purchased from Lonza. HUVECs were used below passage five.

Antibodies

Western blotting was performed using the following antibodies: polyclonal anti-FLAG (F7425, Sigma), monoclonal anti-M5 FLAG (Sigma), polyclonal anti-HA (sc-805, Santa Cruz), monoclonal anti-HA (12CA5), anti-MEKK3 (#1673-1, Epitomics), anti-CCM2 (described in (Uhlik et al., 2003)), anti-GFP (sc-8334, Santa Cruz), anti-Smurf1 (#2174, Cell Signaling), anti-Erk2 (sc-154, Santa Cruz), anti-ubiquitin (sc-8017, Santa Cruz), anti-MEKK2 (described in (Kesavan et al., 2004)), anti-RhoA (#05-822, Millipore), anti-Rac1 (#05-389, Millipore), donkey anti-Rabbit (Jackson Immunoresearch), and sheep anti-Mouse (GE). For immunofluorescence, the following reagents were used: anti-phospho (Ser19)-myosin light chain 2 (#3671, Cell Signaling), rhodamine-phalloidin (Molecular Probes), FITC Donkey anti-rabbit (Molecular Probes), and DAPI (4′,6′-diamidino-2-phenylindole; 0.04 ng/ml).

Plasmids

pRK5 HA-CCM2, pECFP-CCM2, pECFP-CCM2 F217A, pCMV5 HA-MEKK3, and pCMV5 HA-MEKK2 have been described previously (Fanger et al., 1997; Uhlik et al., 2003; Zawistowski et al., 2005). pCMV5 Flag-Smurf1 and pCMV5 Flag-Smurf1 C699A were gifts from Dr. Jeff Wrana (Samuel Lunenfeld

Research Institute, Mount Sinai Hospital). pCMV Myc-RhoA was a gift from Dr. Keith Burridge (University of North Carolina). pLL5.0 was a gift from Dr. Jim Bear (University of North Carolina). pCMV5B Flag-Smurf2 C716A and pGEX4T1-Smurf1 C699A were purchased from Addgene (Addgene plasmids 11747 and 13503, respectively).

pcDNA Flag-Smurf1ΔHECT and pcDNA Flag-Smurf1 HECT were constructed by amplifying Smurf1 (bp 28-1104 for Smurf1ΔHECT, bp 1105-2274 for Smurf1 HECT) by PCR from pCMV5 Flag-Smurf1 using Smurf1-specific primers engineered with flanking HindIII restriction sites. The resulting PCR products were digested with HindIII (New England Biolabs) and ligated into the HindIII site of pcDNA3. Smurf1 missense mutants were generated using the Quikchange Mutagenesis Kit (Stratagene) according to the manufacturer's instructions. Plasmids were confirmed by DNA sequencing (UNC-CH Genome Analysis Facility).

RNAi

pLKO.1 and pLKO.1 CCM2 shRNA plasmids were purchased from Open Biosystems. 293T cells were set in 6-well plates and transfected with lentiviral packaging vectors (1 μg each) and either pLKO.1 or pLKO.1 CCM2 shRNA plasmids (1.2 μg each). At 24 hours post transfection, the media was removed and fresh 10% FBS/DMEM was placed on the transfected cells. At 48 hours post transfection, the virus-containing supernatant was removed from the 293T cells and filtered through a 0.45 μM filter (Whatman). Polybrene (10 μg/mL final

concentration) was added before applying the supernatant to bEND.3 or MEEC cells set in 6-well plates. At 24 hours after the final infection, cells were either used for experiments or selected with 2 ug/mL puromycin for 2 days.

FLAG-CCM2 pulldown

Flag-CCM2 pulldown experiments were done exactly as described in (Hilder et al., 2007).

Immunoprecipitation and Western blotting

Cells were washed once with PBS and subsequently lysed on ice in 1% NP-40, 20 mM Tris at pH = 7.5, 100 mM NaCl, 10% glycerol, 0.1 mM EDTA, 0.1 mM EGTA 10 µg/mL leupeptin, 2 µg/mL aprotinin, 1 mM Na_3VO_4, 1 mM phenylmethylsulfonyl fluoride. Cell lysates were cleared by centrifugation for 10 minutes at 4º C. Proteins were resolved by SDS-PAGE on either 8% or 12% polyacrylamide gels and subsequently transferred to nitrocellulose.

For immunoprecipitation, 300-500 µg of protein lysate was incubated with 3-5 µg of either anti-FLAG (F7425, Sigma) or anti-HA (sc-805, Santa Cruz) for 2 hours at 4º C with gentle rocking. 40 µL of a 1:1 dilution of Protein G Separose (Invitrogen) was added and incubated for another hour at 4º C. Sepharose beads were then washed five times with lysis buffer and boiled for five minutes in SDS loading buffer before resolving the immunoprecipitated proteins by SDS-PAGE.

Immunofluorescence

COS-7 cells were grown and transfected on square coverslips. bEND.3 cells were grown on Matrigel-coated glass coverslips (1:50, BD Biosciences) and subsequently washed with PBS and fixed for 14 minutes with 3% paraformaldehyde/3% sucrose in PBS. Cells were then permeabilized for 6 minutes with 0.1% Triton X-100 in PBS. After blocking in 10% donkey serum/DMEM, coverslips were incubated in primary antibody diluted in blocking buffer for 2 hours at room temperature. Coverslips were washed with PBS and incubated with secondary antibody and DAPI for 1 hour at room temperature. After washes in PBS, coverslips were mounted in 90% glycerol/OPDA and sealed with nail polish. Imaging was performed using an Axiovert 200M microscope from Zeiss (Germany) and imaging software from Intelligent Imaging Innovations (Denver, CO). To determine phospho-MLC2 association with stress fibers, five representative images for each experimental condition were masked for rhodamine-phalloidin intensity and the mean intensity of phospho-MLC2 was measured on this mask.

In vitro ubiquitination assay

The *in vitro* ubiquitination assay was adapted from (Wang et al., 2006). COS-7 cells were transfected with Flag-Smurf1 constructs and anti-FLAG immunoprecipitation was done as described above. The immunopurified Flag-Smurf1 was then incubated with 10 µg ubiquitin, 0.35 µg rabbit E1, and 0.5 µg UbcH5c (E2, Boston Biochem) in a reaction buffer containing 50 mM Tris-HCl pH=7.5, 10 mM $MgCl_2$, 10 µM DTT, and 4 mM ATP. The reaction was incubated

for 15 minutes at room temperature before ending the reaction with 2X SDS-PAGE loading buffer and boiling for 5 minutes. The reaction products were then analyzed by Western blot for ubiquitinated species.

In vitro wound healing assay

bEND.3 cells stably expressing pLKO.1 or CCM2 shRNAs were transduced with pLL5.0 for expression of GFP. Cells were grown in 24-well dishes to a monolayer. Using a P200 pipet tip, a wound across the cell monolayer was made across the center of the well. The cells were then washed once with growth medium and incubated at 37º in the BD Pathway High Content Imager. Wounds were imaged on GFP fluorescence every 15 minutes for 16 hours on a 10X objective. Percent wound healing was determined as the area of the wound remaining after 16 hours divided by the initial area of the wound (ImageJ).

Real-time RT-PCR

Twenty-four hours after the final infection of bEND.3 cells or twenty-four hours following puromycin selection, total RNA was isolated using the RNeasy Mini Kit (Qiagen) according to the manufacturer's directions. From this preparation, 3 ug of RNA was used for the RT reaction using High Capacity cDNA Reverse Transcription Kit (Applied Biosystems). The RT-PCR assay used 5 µL of the cDNA reaction combined with 15 µL of 2X Universal Master Mix (Applied Biosystems). The *Mus musculus* CCM2 Taqman probe

(Mm00524581_m1) and *Mus musculus* beta-actin Taqman probe were purchased from Applied Biosystems. Data were collected on the Applied Biosystems 7500 Fast System. Samples were run in triplicate and standardized to beta-actin.

GST-pulldown assay

GST-Smurf1 C699A was produced exactly as described in (Wang et al., 2006). His-CCM2 and His-MEKK3 were purified as described previously (Uhlik et al., 2003). GST-pulldown experiments were done as described in (Nakamura et al., 2006).

In vitro tube formation assay

In a 24 well plate, 350 uL of growth factor-reduced Matrigel (BD Biosciences) was polymerized at 37º for 30 minutes. After polymerization, 1.69 x 10^5 cells/well were placed on top of the Matrigel and incubated at 37º for 16 hours.

HUVEC Permeability Assay

For permeability assays, 12-mm, 0.4-μm pore Transwells (Corning) were coated in Matrigel (BD Biosciences; 1:100 dilution in PBS) for 1 hour. During this time, HUVECs were trypsinized and 5 x 10^5 cells per condition were resuspended in 100μL MEF nucleofector solution 2 (Amaxa). To the suspension, 10 μL of either 20μM siGENOME non-targeting siRNA #2 or CCM2 ON-

TARGETplus SMARTpool siRNA (Dharmacon) was added. The suspension was electorporated using program M-003 on the Nucleofector Device (Amaxa). The cells were removed from the cuvette, added to 900 µL of growth medium, and allowed to recover at 37ºC for 10 minutes. The cell suspension was then split between two Matrigel-coated Transwells; 500 µL of cells were plated in the upper chamber with 1.5 mL of growth medium in the lower chamber. The growth medium was changed after 24 hours. Forty-eight hours post-electroporation, the medium from both chambers was removed and replaced with serum- and growth factor-free EBM-2. FITC-dextran (40 kD molecular weight; Invitrogen) was added to the upper chamber at a final concentration of 0.625 mg/mL. As a control to induce permeability, EGTA at a final concentration of 4 mM was added to one set of control cells to disrupt the Ca^{2+}-dependent cell-cell adhesion (Wittchen et al., 2005). Every 15 minutes for 1.5 hours, 50 µL aliquots were removed from the lower chamber, and FITC intensity was measured using a PHERAstar microplate reader (BMG Labtech). Relative fluorescence units (RFU) were plotted against time and reported as the average change in RFU per minute between duplicate Transwells.

III. CCM1 and CCM2 are binding partners; implications for a common signaling pathway in CCM

Introduction

Three genes have been identified in the autosomal dominant form of cerebral cavernous malformations: *CCM1*, *CCM2*, and *CCM3* (Bergametti et al., 2005; Denier et al., 2004; Laberge-le Couteulx et al., 1999; Liquori et al., 2003; Sahoo et al., 1999). The cellular functions of the CCM1, CCM2, and CCM3 proteins are largely uncharacterized, although CCM1 and CCM2 have both been implicated in cell signaling processes by the proteins that they bind. CCM1 binds the GTPase Rap1A and the integrin adaptor ICAP1 suggesting a role for CCM1 in integrin mediated adhesion and signaling (Serebriiskii et al., 1997; Zawistowski et al., 2002). The mouse homolog of CCM2 was characterized as Osmosensing Scaffold for MEKK3 (OSM). OSM binds Rac1, MEKK3, and MKK3 to activate p38 in response to osmotic stress (Uhlik et al., 2003). CCM3 binds a Ste20-like kinase and is associated with activation of Erk signaling (Ma et al., 2007). However, the molecular mechanism of how loss of CCM1, CCM2, or CCM3 leads to CCM is not known.

CCM1, 2, and 3 are linked genetically and phenotypically, suggesting a common signaling pathway associated with loss of expression of any one of these proteins. However, such a pathway has not been found. The proteins encoded by these genes lack identifiable catalytic domains, but do contain

protein interaction domains. CCM1 contains a C-terminal FERM domain and multiple ankyrin repeats. CCM2 contains a PTB domain in its N-terminus. Mutations in CCM genes are mostly frameshift or nonsense mutations. Therefore, mutations in *CCM1*, *CCM2*, or *CCM3* could lead to truncated proteins or loss of protein expression leading to loss of protein complex formation and impaired cell signaling.

In this study, we show that CCM1 and CCM2 are binding partners. The CCM2 PTB domain is necessary for a canonical interaction with NPxY motifs within CCM1. We provide evidence of co-immunoprecipitation and fluorescence resonance energy transfer (FRET) between CCM1 and CCM2, implicating a common genetic and molecular pathway in CCM pathogenesis.

The data presented in this chapter was done in collaboration with Drs. Jon Zawistowski and Mark Uhlik and was published in Human Molecular Genetics in 2005 (Zawistowski et al., 2005).

Results

CCM2$^{+/-}$ cells have perturbed MAPK activation in response to hyperosmotic shock

CCM2 is an osmosensing scaffold for MEKK3-mediated p38 MAPK phosphorylation (Uhlik et al., 2003). We therefore assessed the role of endogenous CCM2 protein in activation of sorbitol-induced p38 signaling. We isolated mouse embryonic fibroblasts (MEFs) heterozygous for a gene trap insertion in the mouse *CCM2* gene. This gene trap cell line (Bay Genomics

RRG051) has a LacZ insertion in exon 6 of *CCM2* which is predicted to be a loss of function mutation (Plummer et al., 2006). Heterozygous MEFs were used for these experiments because they are the genotypic equivalent of familial CCM patients. We first verified that there was reduced CCM2 protein in heterozygous MEFs by western blot with CCM2 antibody (Figure 3.1A). Cells heterozygous for the *CCM2* mutation had significantly less activated p38 MAPK in response to a sorbitol time course as assessed by p38 Thr180/Tyr182 phosphorylation (Figure 3.1A-B). This decrease of p38 phosphorylation was restored in experiments where exogenous FLAG-CCM2 was transfected into CCM2 +/- MEFs (CCM2 add-back, Figure 3.1B), demonstrating that the effect was specific to the reduction of CCM2. These results are consistent with previous work implicating CCM2 in this signaling pathway (Uhlik et al., 2003).

CCM1 associates with the CCM2/MEKK3 protein complex

CCM2 acts as a scaffold for MEKK3-mediated p38 MAPK phosphorylation following sorbitol stimulation (Uhlik et al., 2003), but the role of CCM1 in this pathway is not known. To determine whether CCM1 is a member of the CCM2/MEKK3 scaffold complex, we expressed epitope-tagged CCM1, CCM2 and MEKK3, and examined associating proteins by immunoprecipitation with anti-CCM2 antibody. All three molecules were detected in the complex (Figure 3.2A).

We hypothesized that the presence of CCM1 in the CCM2/MEKK3 signaling complex may represent an interaction between CCM1 and CCM2. To

examine the potential for the CCM1 and CCM2 to associate, we performed CFP-YFP-FRET analysis in live COS-7 cells. Cells expressing YFP-CCM1 and CFP-CCM2 yield a $FRETN^C$ value of 7.43×10^{-5} (s.e.m. = 1.29×10^{-5}) while control cells expressing YFP and CFP-CCM2 yield a $FRETN^C$ value of 0.35×10^{-5} (s.e.m. = 0.11×10^{-5}) (Table 3.1). Visualization of the corrected FRET value revealed a diffuse interaction signal throughout the cytoplasm (Figure 3.2B).

We then determined if an osmotic stimulus would affect CCM1/CCM2 association. Cells expressing YFP-CCM1 and CFP-CCM2 treated with sorbitol displayed a two-fold increase in the $FRETN^C$ value over non-treated cells (Table 3.1). Localization of CCM1-CCM2 complexes shifted from diffusely cytoplasmic to the cell periphery as a consequence of sorbitol stimulation as revealed by visualization of the corrected FRET signal (Figure 3.2B). Re-localization and interaction of CCM1 and CCM2 may reflect a functional role for these proteins at the plasma membrane.

To confirm the interaction of epitope-tagged CCM1/2, we performed co-immunoprecipitation experiments with endogenous protein. Endogenous CCM1 was efficiently co-immunoprecipitated with CCM2 from MEF lysates (Figure 3.3A). Therefore, we conclude that CCM1 and CCM2 are binding partners *in vivo*.

A functional CCM2 PTB domain is necessary for interaction with CCM1

CCM2 contains a PTB domain that is most similar to the ICAP1 PTB domain, which binds CCM1 (Chang et al., 1997; Uhlik et al., 2005). Therefore,

we hypothesized the CCM1/CCM2 association was occurring through a canonical NPxY/PTB domain interaction. The CCM2 PTB domain is most similar to the Dab-like PTB domains (Uhlik et al., 2005). Based on the structure and binding sites of these domains, we engineered a mutation into CCM2 PTB binding pocket that would be predicted to loose association with NPxY motifs. Point mutation of the corresponding residue in CCM2 (F217A) completely abrogated the ability of FLAG-CCM1 to co-immunoprecipitate with FLAG-CCM2 (Figure 3.3B), suggesting that PTB domain integrity is critical for the CCM1/2 interaction.

We confirmed the effect of the CCM2 F217A mutation on the CCM1/2 interaction using FRET. Consistent with co-immunoprecipitation, COS-7 cells co-expressing YFP-CCM1 and CFP-CCM2 F217A had reduced FRET values ($FRETN^C$= 1.355 X 10^{-5}, s.e.m = 0.355 X 10^{-5}) when compared to the FRET value for the wild type CCM1/2 proteins ($FRETN^C$ = 7.43 x 10^{-5}, s.e.m. = 1.29 x 10^{-5}) (Table 3.1). We observed a similar loss of FRET following sorbitol stimulation (CCM2-F217A $FRETN^C$ = 2.29 x 10^{-5}, s.e.m. = 0.307 x 10^{-5} ; WT $FRETN^C$ = 15.77 x 10^{-5} , s.e.m. = 3.13 x 10^{-5}) (Table 3.1).

Germline mutations in the *CCM1* and *CCM2* genes have been exclusively nonsense, frameshift and splicing mutations predicted to prematurely truncate the message. However, a missense mutation has recently been identified in one CCM2 kindred, CCM2 L198R (Denier et al., 2004). This mutation occurs within the CCM2 PTB domain, which we have found to be necessary for interaction with CCM1. Similar to the CCM2 F217A mutant, the CCM2 F217A mutant was not

capable of association with CCM1 as determined by co-immunoprecipitation (Figure 3.3B). Loss of association of CCM1 with the patient mutation CCM2 L198R suggests that the CCM1-CCM2 interaction may be relevant in CCM pathogenesis.

CCM1/CCM2 interaction is not dependent on the same CCM1 NPxY sequence critical for ICAP1 interaction

Previous work has shown that ICAP1, another PTB domain-containing protein, associates with CCM1 through an ICAP1 PTB domain – CCM1 NPxY motif interaction (Zawistowski et al., 2002). CCM1 contains 3 NPxY motifs. Therefore, we wanted to determine if CCM2 and ICAP1 were binding to the same site on CCM1, or if they could both associate with CCM1 at the same time. We tested this hypothesis by co-immunoprecipitation and found that mutagenesis of the critical asparagine (N192A) residue in the CCM1 NPxY motif critical for ICAP1 binding did not disrupt the CCM1/2 association (Figure 3.3B). FRET experiments found that CCM1-N192A and CCM2 interactions were diminished relative to wildtype CCM1 and CCM2, but interaction was not completely abolished (Table 3.1). The FRET data indicate that the N192A CCM1 mutation has a slight effect on CCM1/2 binding, while in the context of co-immunoprecipitation, it does not perturb the interaction. This data suggests that CCM2 could bind to additional NPXY motifs on CCM1. To examine if CCM1, CCM2, and ICAP1 are able to associate in a ternary complex, we performed a CCM1/2 co-immunoprecipitation assay in the presence of increasing amounts of

ICAP1. ICAP1 overexpression did not prevent CCM1 from associating with CCM2; instead, all three molecules were present in the complex precipitated with the CCM2 antibody (Figure 3.5A). This suggests that ICAP1 and CCM2 do not bind to the same CCM1 binding site and ICAP1, CCM2, and CCM1 can associate as a protein complex.

CCM1 contains a functional nuclear localization sequence

The interaction of CCM1/2 prompted us to compare the subcellular localization of CCM1 with CCM2. Endogenous CCM2 localizes to actin-rich membrane ruffles (Uhlik et al., 2003). In contrast, we observed a whole cell distribution for YFP-CCM1 in COS-7 cells. We hypothesized that the nuclear localization of the CCM1 molecule may be due to a nuclear localization sequence (NLS). Examination of the primary sequence of CCM1 identified a putative NLS using the PSORT II program (EXPASY). A “pat4” four-residue pattern, similar to the NLS of the SV40 large T antigen, was predicted at residues 46, 47 and 48 in the unique N-terminal region of CCM1 (corresponding to 46-KKKRKK-51). In addition, a “pat4” sequence was detected at residue 569 within the FERM domain of CCM1 (corresponding to KKHK).

The putative N-terminal NLS in CCM1 was changed by site-directed mutagenesis from the wild-type KKKRKK to KKAAKK (NLS mutant 1), and also to a more severe mutation of KAAAAK (NLS mutant 2). The resulting constructs were transfected into COS-7 cells and assessed for nuclear localization (Figure 3.4B). The percentage of cells displaying nuclear localization for FLAG-CCM1

NLS mutant 1 was reduced to ~ 40% from the ~ 90% of wild-type FLAG-CCM1 cells displaying nuclear localization, while nuclear localization for the more severe FLAG-CCM1 NLS mutant 2 was reduced to ~ 10% of the cells (Figure 3.4C). These data suggest that the putative N-terminal NLS in CCM1 is functional, and suggest that CCM1 may have nuclear-cytoplasmic shuttling capability.

CCM1 localization is influenced by association with CCM2

In addition to contributions of the CCM1 NLS to CCM1 subcellular localization, we hypothesized that association with CCM2 could influence CCM1 subcellular localization. In COS-7 cells, CCM1 exhibits whole cell localization, while CCM2 exhibits exclusively cytoplasmic localization. In cells co-expressing YFP-CCM1 and CFP-CCM2, YFP-CCM1 nuclear localization is lost and becomes exclusively cytoplasmic (Figure 3.4A). This suggests that CCM2 is capable of interacting with and sequestering CCM1 in the cytoplasm. To see if the cytoplasmic sequestration of CCM1 by CCM2 was dependent on the PTB domain integrity of CCM2, we analyzed the effect of the CCM2-F217A mutant on CCM1 localization. In COS-7 cells expressing YFP-CCM1 and PTB-mutant CFP-CCM2 F217A, CCM2 fails to interact with and sequester CCM1 and nuclear localization of YFP-CCM1 is restored (Figure 3.4A). These data are consistent with our co-immunoprecipitation results and provide support that the cerebral cavernous malformations gene products interact in a PTB domain-dependent manner. These data are also consistent with our CCM1 NLS mutagenesis

experiments suggesting a nuclear-cytoplasmic shuttling role for CCM1. We conclude that CCM1 can act as a nuclear-cytoplasmic shuttling protein and this shuttling of CCM1 can be regulated by CCM2.

ICAP1 influences the subcellular localization of CCM1

We have demonstrated that CCM2 is capable of influencing the localization of CCM1. ICAP1, which also binds CCM1, may similarly influence CCM1 localization. When expressed alone, CFP-ICAP1 exhibits predominantly nuclear localization. When co-expressed with CFP-ICAP1, YFP-CCM1 localization shifts from total-cell to exclusively nuclear (Figure 3.5B). Thus, through PTB-domain interactions, ICAP1 and CCM2 are capable of influencing the localization (and presumably function) of CCM1.

Discussion

CCM1 and *CCM2* have been implicated in the disease cerebral cavernous malformations. Although mutation of these genes leads to the same disorder, there has been insufficient data to understand the mechanism of the pathogenesis of CCM. In this work, we provide evidence that CCM1 and CCM2 are binding partners, placing them in the same molecular pathway. This interaction is abrogated by a patient mutation in CCM2 (CCM2 L198R) suggesting that loss of the CCM1/2 association contributes to the development of the abnormal vessels associated with CCM lesions.

The characterization of CCM2 as Osmosensing Scaffold for MEKK3 (OSM) has shed new light on the potential signaling mechanisms that are impacted by loss of CCM2 expression. OSM was found to coordinate osmotic stress-induced p38 activation via Rac1, MEKK3, and MKK3. Indeed, MEKK3 and p38 knockout mice have shown that these signaling pathways are necessary for vascular development and integrity (Adams et al., 2000; Deng et al., 2007; Yang et al., 2000). In this work we have shown that CCM2 heterozygous MEFs are defective in their ability to activate p38 in response to osmotic stress. Importantly, exogenous expression of CCM2 led to a complete recovery of this phenotype. Further, in this work we demonstrated that CCM1 can associate with the CCM2-MEKK3 protein complex, suggesting a role for CCM1 in MEKK3 mediated signaling pathways. Impaired p38 activation may influence downstream p38-specific transcriptional activation involved in the maturation of new vessels and for the maintenance of the existing vessel architecture. Therefore the loss of p38 activation may ultimately contribute to the formation of the misshapen vascular beds of the cerebral cavernous malformation.

Until now, the localization of CCM1 had not been examined. Our demonstration of CCM1 as a nuclear-cytoplasmic shuttling protein opens a new avenue of study of CCM1 function and regulation. We also demonstrate that the CCM1 binding partners ICAP1 and CCM2 play a role in the localization of CCM1. ICAP1 appears to recruit CCM1 to the nucleus, while CCM2 sequesters CCM1 in the cytoplasm. ICAP1 and CCM2 both utilize their PTB domains in their interactions with the CCM1 NPxY motifs. The relative abundance of ICAP1 and

CCM2 may dictate the cellular localization of CCM1, or there may be a more complex signaling event associated with changes in CCM1 localization. These CCM1-ICAP1 and CCM1-CCM2 complexes clearly warrant further study to determine the nuclear and cytoplasmic roles of CCM1.

ICAP1 is known to regulate integrin-mediated signaling events. Activation of β_1 integrins has been shown to recruit ICAP1 to the cytoplasm where it acts as an adaptor protein. ICAP1 is also capable of redistributing to the nucleus after integrin engagement. Therefore, the shuttling of ICAP1-CCM1 complex could be regulated by integrin signaling. In the cytoplasm, CCM1 could associate with CCM2 to control MAPK activation in response to integrin-mediated signaling. In this way a CCM1-CCM2 complex would be necessary to bridge signaling between integrins and MAPK pathways. It would then be reasonable to believe that loss of expression of CCM1 or CCM2, as is predicted in CCM patients, would lead to abhorrent integrin-mediated signaling. Indeed, endothelial cells in sections of CCM lesions appear to have loss of cell-to-cell contact (Clatterbuck et al., 2001), suggesting loss of adhesion.

In this work, we demonstrate that the genetically and phenotypically linked CCM1 and CCM2 proteins exist as a protein complex. We also show that CCM1 is a nuclear-cytoplasmic shuttling protein, suggesting multifaceted regulation of CCM1 function. We further show that CCM1-CCM2 localization is influenced by osmotic stress, which argues that the CCM complex is dynamic. Assaying the function and regulation of the CCM1-CCM2 complex will provide further insight into the molecular mechanisms of CCM pathogenesis.

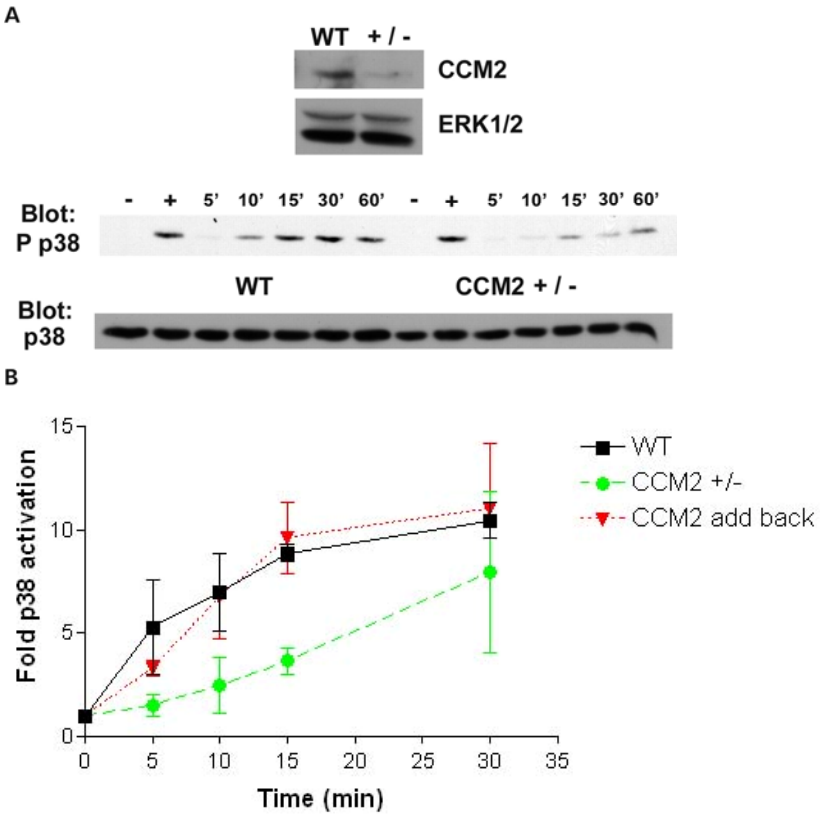

Figure 3.1: MEFs heterozygous for a CCM2 gene trap allele have impaired p38 activation upon hyperosmotic stress. (A) Western blotting with anti-CCM2 antibody confirms reduction of CCM2 protein in CCM2+/– MEFs (top panel). Erk 1/2 was used as a loading control. Wild-type or CCM2+/– MEFs were serum-starved and treated for the indicated times with 0.2 M sorbitol or 15 min with 10 mg ml^{-1} anisomycin as a positive control for p38 activation (+). Lysates were subjected to western blotting with anti-p38 antibody and with anti-phospho (Thr180/Tyr182) p38 antibody. (B) Quantification of impaired p38 activation of CCM2+/– MEFs and rescue by add-back of CCM2. Fold p38 activation was calculated as described in Materials and Methods. Results are representative of three independent experiments. Error bars represent standard error of the mean.

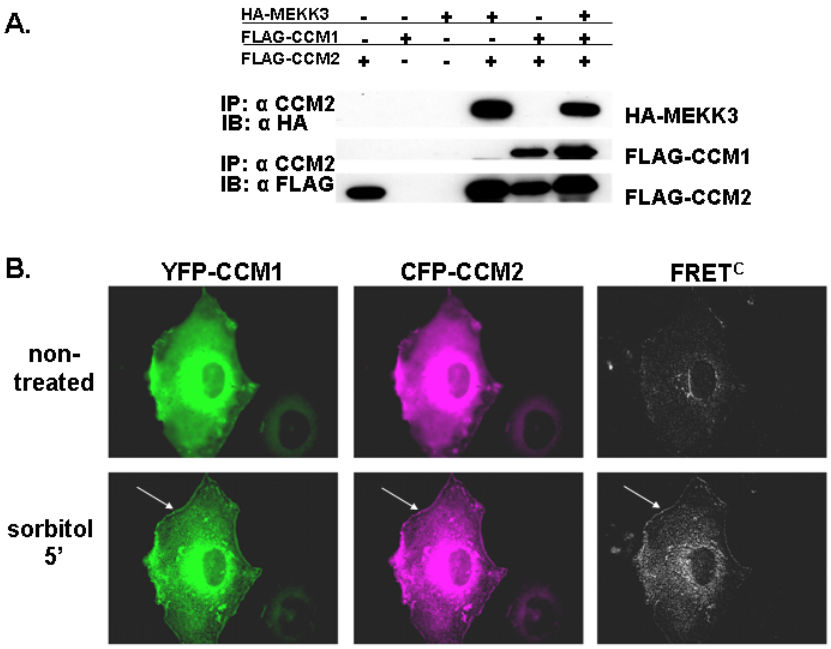

Figure 3.2: CCM1 associates with CCM2. (A) CCM1 is identified in a ternary complex with CCM2 and MEKK3. 293T cells were transfected with the indicated constructs, immunoprecipitated with anti-CCM2 antibody and subjected to western blotting with the indicated antibodies. In addition to HA-MEKK3 and FLAG-CCM1 singly co-immunoprecipitating with FLAG-CCM2, a FLAG-CCM1/FLAG-CCM2/HA-MEKK3 ternary complex is detected. Approximate molecular weights are FLAG-CCM1: 85 kDa and FLAG-CCM2: 60 kDa. (B) CCM1/CCM2 interact in live cells and this interaction is enhanced upon hyperosmotic stress. COS-7 cells transfected with CFP-CCM2 and YFP-CCM1 were visualized at room temperature and analyzed by FRET. CFP fluorescence, YFP fluorescence and corrected FRET ($FRET^C$) were examined for non-treated cells (top) and cells were treated with 0.2 M sorbitol for 5 min (bottom). Non-treated cells yield a diffuse $FRET^C$ signal throughout the cytoplasm. Cells treated with sorbitol display a re-distribution of CFP-CCM2 and YFP-CCM1 to the cell periphery (arrows) and an enhanced $FRET^C$ interaction signal at these sites.

Donor construct	Acceptor construct	Treatment	$FRETN^{C}$/(CFPxYFP)	Standard error
CFP-CCM2	YFP	NT	$0.35x10^{-5}$	$0.11x10^{-5}$
CFP-CCM2	YFP-CCM1	NT	$7.43x10^{-5}$	$1.29x10^{-5}$
CFP-CCM2	YFP-CCM1	0.2M sorbitol	$15.77x10^{-5}$	$3.13x10^{-5}$
CFP-CCM2 F217A	YFP-CCM1	NT	$1.36x10^{-5}$	$0.36x10^{-5}$
CFP-CCM2 F217A	YFP-CCM1	0.2M sorbitol	$2.29x10^{-5}$	$0.31x10^{-5}$
CFP-CCM2	YFP-CCM1 N192A	NT	$3.95x10^{-5}$	$0.78x10^{-5}$
CFP-CCM2	YFP-CCM1 N192A	0.2M sorbitol	$10.28x10^{-5}$	$1.48x10^{-5}$

Table 3.1. FRET values for CCM1/2 interactions. COS-7 cells were treated for 5 min with 0.2 M sorbitol and compared with FRET interaction values of non-treated (NT) cells. Multiple cells were visualized to obtain normalized $FRETN^{C}$/(CFPxYFP) values (n=10 CFP-CCM2/YFP, n=10 CFP-CCM2/YFP-CCM1, n=10 CFP-CCM2 F217A/YFP-CCM1 and n=7 CFP-CCM2/YFP-CCM1 N192A).

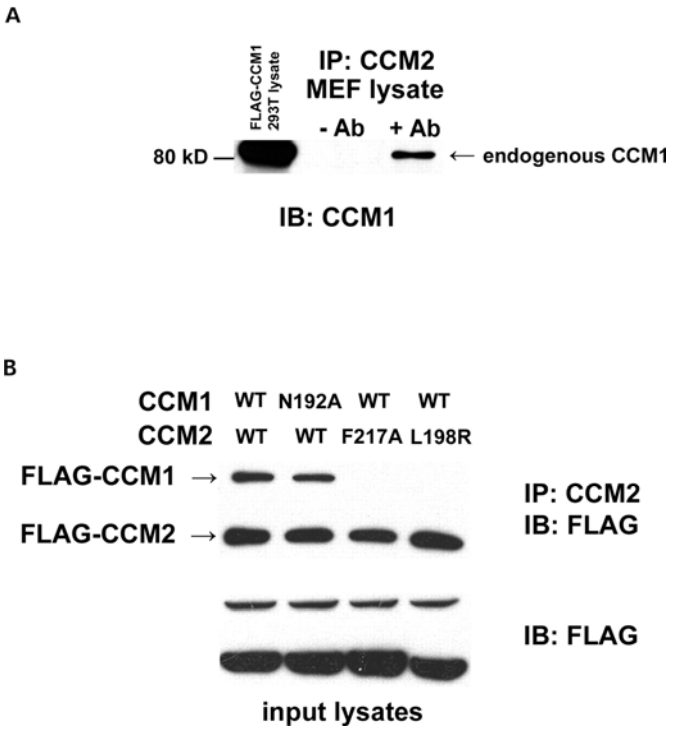

Figure 3.3: The CCM1/2 interaction is dependent on the CCM2 PTB domain. (A) Endogenous CCM1 co-immunoprecipitates with endogenous CCM2. Following immunoprecipitation of MEF lysate with anti-CCM2 and western blotting with anti-CCM1 antibody, CCM1 is detected as a species migrating near the predicted molecular weight of 83 kDa. 100 µg of 293T cell lysate transfected with FLAG-CCM1 was utilized as a size control for endogenous CCM1. (B) Engineered and CCM2 patient PTB domain mutations abrogate the CCM1/2 interaction. FLAG-CCM1 and FLAG-CCM2 with the indicated mutations were expressed in 293T cells, and complexes were immunoprecipitated with anti-CCM2 antibody followed by western blotting with anti-FLAG antibody. The engineered CCM2 PTB domain mutation (CCM2-F217A) and a CCM2 patient PTB domain mutation (CCM2-L198R) completely prevent FLAG-CCM1 from being co-immunoprecipitated with FLAG-CCM2, whereas NPxY mutation N192A in FLAG-CCM1 does not perturb the interaction.

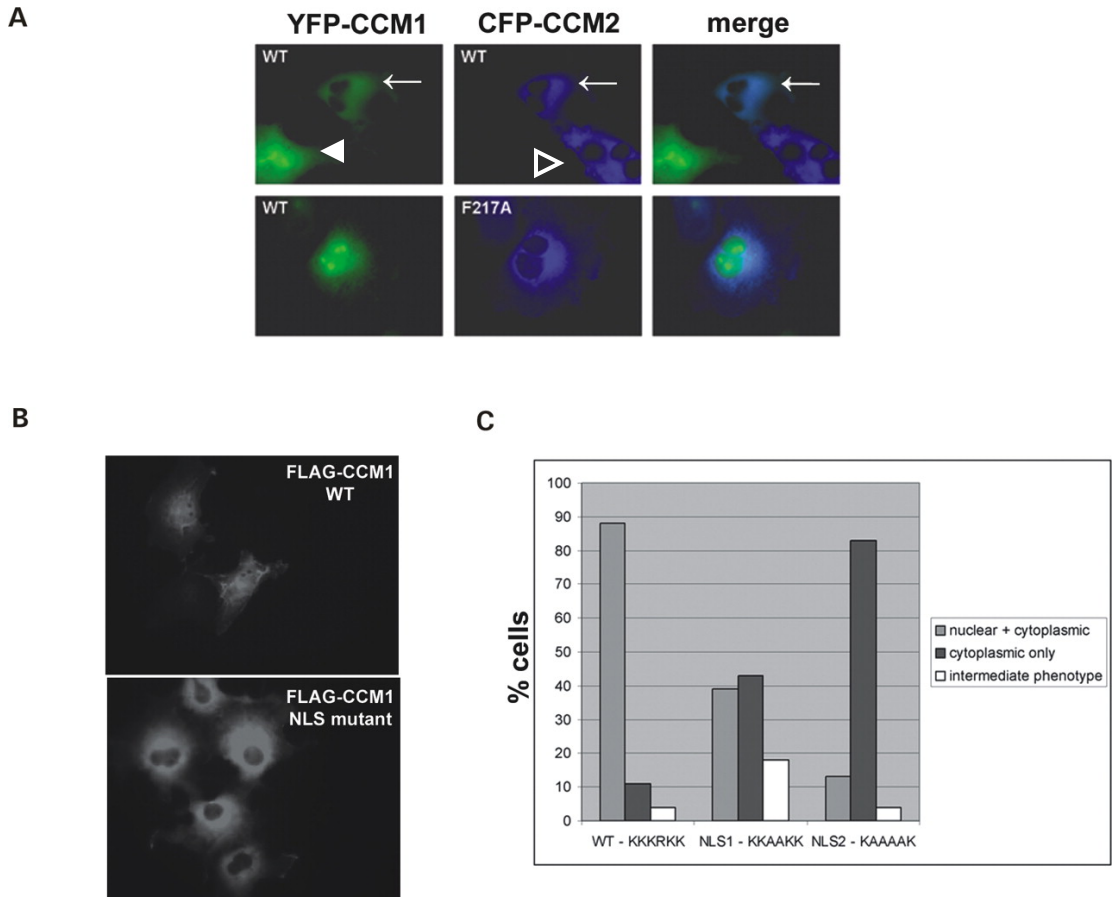

Figure 3.4: CCM1 subcellular localization is influenced by CCM2 and by a CCM1 NLS. (A) The CCM2 PTB domain regulates CCM1 localization. COS-7 cells were transfected with CFP-CCM2 or CFP-CCM2 F217A with YFP-CCM1 and fluorescence was examined in live cells at room temperature. YFP-CCM1 fluorescence is distributed throughout the cell (closed arrowhead), whereas CFP-CCM2 fluorescence is predominantly cytoplasmic (open arrowhead). In cells co-expressing YFP-CCM1 and CFP-CCM2 (arrow), CCM2 is capable of interacting with and sequestering CCM1 in the cytoplasm (top panels). This sequestration phenotype is lost in cells co-expressing PTB-mutant CFP-CCM2 F217A and YFP-CCM1, as YFP-CCM1 exhibits wild-type, whole-cell fluorescence (bottom panels). (B) CCM1 possesses a functional NLS. Wild-type FLAG-CCM1 in COS-7 cells localizes to both the nucleus and the cytoplasm, whereas FLAG-CCM1 NLS mutant 2 (KKRKKK→KAAAAK) is predominantly cytoplasmic in the majority of cells as revealed by anti-FLAG immunofluorescence. Magnification: 40x. (C) Percentage of cells exhibiting FLAG-CCM1 nuclear localization following NLS mutagenesis. n=150

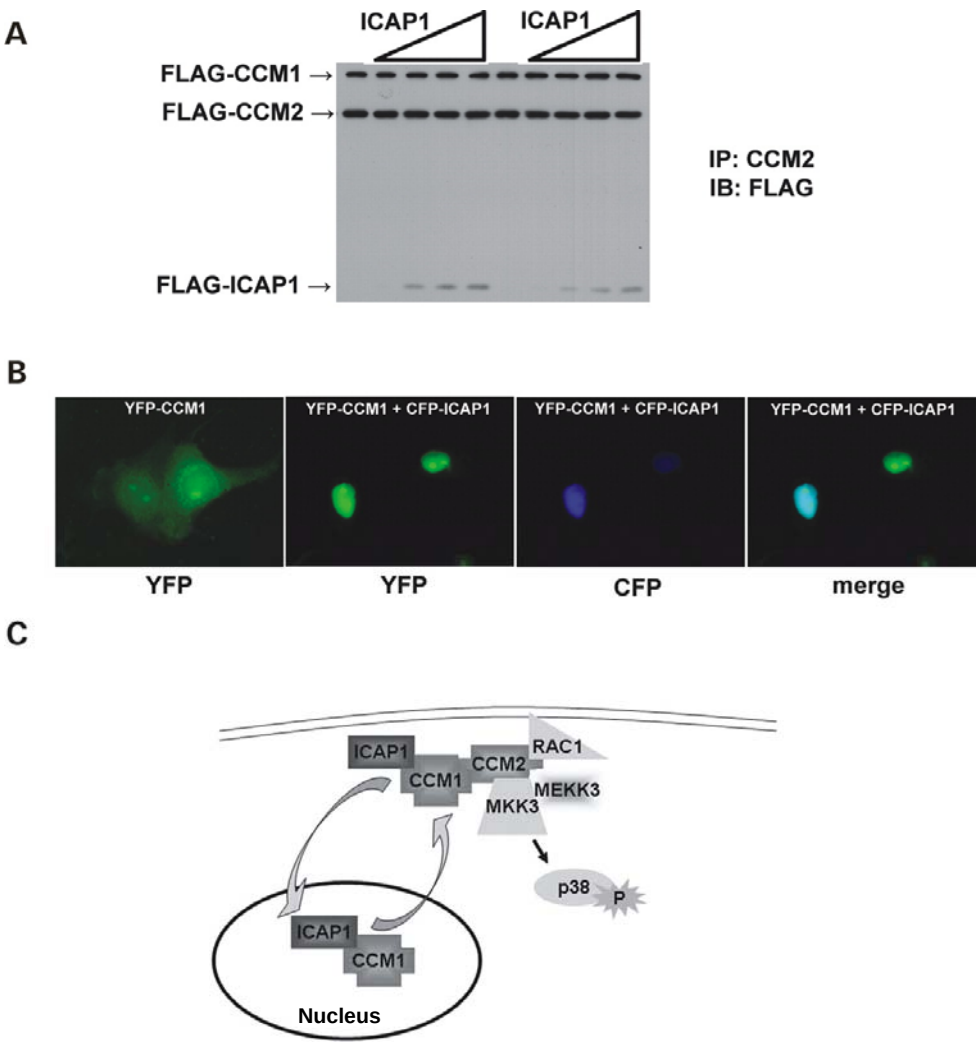

Figure 3.5: ICAP1 associates with CCM1 and CCM2 and sequesters CCM1 in the nucleus. (A) ICAP1 does not compete with CCM2 for binding to CCM1, but is a member of a ternary complex with CCM1 and CCM2. 293T cells were transiently transfected with the indicated constructs. Cell extracts were analyzed by immunoprecipitation using a polyclonal antibody to CCM2 followed by western blotting with anti-FLAG antibody. (B) ICAP1 sequesters CCM1 in the nucleus. COS-7 cells were transfected with YFP-CCM1 alone and co-transfected with CFP-ICAP1. Live COS-7 cells transfected with YFP-CCM1 alone exhibit whole-cell fluorescence, whereas YFP-CCM1 is sequestered in the nucleus when co-expressed with CFP-ICAP1. (C) Molecular model for CCM protein function. CCM1 can act as nuclear-cytoplasmic shuttling protein. In the presence of ICAP1, CCM1 is predominantly nuclear. In the presence of CCM2, CCM1 is predominantly cytoplasmic, where it can associate with the MEKK3 signaling module.

IV. CCM2 regulates aortic arch morphogenesis in Danio rerio

Introduction

Cerebral cavernous malformations (CCMs) are lesions of the central nervous system composed of clusters of dilated thin-walled blood vessels. Patients with this disorder are at high risk of seizures and stroke due to potential hemorrhage of the lesion. To date, three genes have been linked to familial CCM: *CCM1* (KRIT1), *CCM2* (OSM), and *CCM3* (PDCD10). The physiological and cell signaling roles of these proteins are not fully characterized although all appear to exist in a protein complex (Hilder et al., 2007). Knock-out mice for *CCM1* and CCM2 have been generated; however, using the mouse as a model to study the physiological function of these proteins has proven to be problematic due to early embryonic lethality (Plummer et al., 2006; Whitehead et al., 2004). We have utilized zebrafish (*Danio rerio*) as a model organism to better understand the roles of these proteins in embryonic development and in the pathogenesis of CCM. Using translational blocking morpholinos, we can successfully knock-down CCM2 expression. CCM2 morpholino-treated embryos have decreased blood flow at 24 and 48 hours post fertilization (hpf) due to a restriction in the first aortic arch. Zebrafish embryos lacking CCM2 expression also show pronounced defects in the development of the optic tectum and abnormal closure of the cranial neural tube. We conclude that *Danio rerio* is a

viable model organism to examine the physiological role of CCM2 in vertebrate development. We also show that loss of CCM2 in zebrafish leads to developmental vascular abnormalities similar to those seen in CCM1 knockout mice, suggesting a common molecular pathway for CCM protein function.

This work was done in collaboration with Drs. Mike Malone and Elwood Linney. Blood flow analysis was published in BMC Biotechnology (Malone et al., 2007).

Results

The model organism Danio rerio *has a CCM2 homolog*

Danio rerio is a prominent animal model for vertebrate development. This species has been utilized for decades because of its optical clarity, genomic amenability, and most importantly, rapid and external gestation. Lack of *CCM2* expression in the mouse leads to embryonic lethality around E9.5 (Plummer et al., 2006). Therefore we considered using *Danio rerio* as an alternative model vertebrate organism to examine CCM2 function *in vivo*.

To determine if CCM2 had a homolog in *Danio rerio*, we used the program BLAST to compare human CCM2 sequence (Accession NP_113631) to genes of the *Danio rerio* genome. A zebrafish CCM2 homolog was identified (Accession NP_001002315). These two proteins were found to be 75% identical based on their amino acid sequence (Figure 4.1). Similar to human CCM2, the zebrafish CCM2 protein contains a PTB domain in the amino-terminus. Importantly, residues we had previously identified in human CCM2 as crucial for PTB domain

integrity, F217 and L198, are conserved in the zebrafish CCM2 protein (Zawistowski et al., 2005).

CCM2-specific morpholinos knock down CCM2 expression

CCM2-specific morpholinos were designed near the translational start site on *Danio rerio* CCM2 RNA. CCM2 morpholino #1 targeted the mRNA sequence directly adjacent to the start-site ATG. CCM2 morpholino #2 overlapped the start-site ATG and initial 5' coding sequence (Figure 4.2). These two independent CCM2 morpholinos were capable of knocking-down CCM2 expression. Western blots of embryo lysates demonstrated a clear inhibition of CCM2 expression both at 24 and 48 hours post-fertilization (hpf, Figure 4.2).

CCM2 knockdown leads to decreased embryonic blood flow

In order to determine the role of CCM2 in vertebrate development, we injected CCM2 morpholinos into zebrafish embryos. Wild-type embryos at the 1- to 4- cell stage were injected with CCM2 morpholinos or left uninjected as a control. Embryos were monitored at 24 and 48 hours post-fertilization for phenotypes. Embryos injected with CCM2 morpholinos (CCM2 morphant embryos) developed normally until about 24 hpf. CCM2 morphant somite development was normal in both the number and morphology of somites. The yolk sac, tail, and body axis appeared normal. However, beyond 24 hpf differences became more clear between uninjected and CCM2 morphant embryos. CCM2 morphant embryos displayed loss of pigmentation and flat

heads compared to control embryos (Figure 4.3). In addition to these developmental defects, the most pronounced defect we observed was loss of blood circulation.

In the developing zebrafish embryo, blood flow initiates around 24 hpf, when the heart beat initiates. During the first few hours of embryonic blood flow, blood circulates from the yolk ball to the heart and through the dorsal aorta and caudal vein (Kimmel et al., 1995). In our CCM2 morphant embryos, blood flow appeared to be restricted, with an abundance of blood cells accumulated in the yolk sac but not distributed throughout the embryo. We quantified this erythrocyte flux and determined that loss of CCM2 expression led to a dramatic loss of blood flow throughout the embryo (Figure 4.4). Loss of embryonic blood flow was not due to changed diameter of the intersomitic vessels or dorsal aorta (Figure 4.4). These defects were observed with two independent CCM2 morpholinos, implying that loss of embryonic blood flow was specific to CCM2 knockdown.

Morphant embryos have normal vascular patterning and bulbus arteriosus development

To determine the reason for loss of blood flow in CCM2 morphant embryos, we examined the vascular patterning and heart development in these embryos. Using time-lapse microscopy, control and CCM2 morphant embryos were monitored for blood flow. These movies of embryonic blood flow were then used to determine where blood had distributed throughout the embryo. We

termed this technique "*in silico* microangiography", as it essentially replaces the more traditional method of injecting ink or fluorescent dye into the heart and examining where the blood is distributed. Based on these measurements, the CCM2 morphants did have proper vascular patterning, with correct growth of the dorsal aorta, caudal vein, and intersomitic vessels (Figure 4.5).

Another explanation for loss of blood flow was improper heart development. In the zebrafish model, many of the most complex processes in heart development occur before 24 hpf. Fate mapping experiments have identified the paths taken by cardiac precursors from pre-gastrulation to adult. The cardiac progenitors ingress during gastrulation and migrate to the lateral plate mesoderm. At the cranial midline, they fuse to form the primitive heart tube which begins beating around 24 hpf. The atrial and ventricle chambers develop and are easily identifiable by 36 hpf (Stainier et al., 1993). In the developing embryo, the bulbus arteriosus is a component of the teleost heart that is formed during the last stages of heart development. Therefore, the presence of the bulbus arteriosus is indicative of proper heart development. DAF2-DA, a marker for the bulbus arteriosus, was recently characterized (Grimes et al., 2006). In order to examine bulbus arteriosus development in our CCM2 morphant embryos, we treated live embryos with DAF2-DA. Both control and CCM2 morphant embryos had strong DAF2-DA staining, suggesting that heart development was predominantly normal (Figure 4.5). Based on these experiments we concluded that neither vascular patterning nor heart development was inducing the loss of blood flow in CCM2 morphant embryos.

Loss of CCM2 causes malformations of the first aortic arch

Careful examination of CCM2 morphant embryos revealed that blood flow was being restricted near the outflow tract of the heart. Blood cells had accumulated in the yolk sac; even though the heart was developed and pumping. Upon microscopic evaluation of the CCM2 morphant embryos, we discovered a restriction in the proximal dorsal aorta, specifically in the aortic arch. Using *in silico* microangiography, these defects were more clearly seen (Figure 4.6). Control embryos had an aortic arch that was a consistent diameter. CCM2 morphant embryos displayed a restriction in the aortic arch near the outflow tract of the heart that ballooned past the restriction (Figure 4.6). Based on this data we concluded that CCM2 is necessary for morphogenesis of the aortic arch in *Danio rerio*.

CCM2 morphants have developmental defects of the head and trunk

Although the loss of blood flow was the most obvious phenotype we observed in CCM2 morphant embryos, these embryos had additional defects of the head and trunk. The first of these defects was seen in the region of the cranial neural tube. At 30 hpf, a developmental timepoint past neural tube closure, CCM2 morphants had heads that were more flat than uninjected controls (Figure 4.3). In many vertebrate systems, flat head phenotypes are indicative of neural tube defects. Indeed, the neural tube closure in CCM2 morphant embryos was not normal. Microscopic examination of the ventral cranial region of the

CCM2 morphant embryo found that the neural tube was closed, but the ventral point of closure contained less contact compared to the control embryos (Figure 4.7). This could indicate some form of developmental delay, or a true neural tube closure defect.

CCM2 morphants also lacked development of the optic tectum (Figure 4.8). Around 24 hpf, the embryonic brain undergoes segmentation. One of the final regions to undergo segmentation is the midbrain. The midbrain primordium subdivides horizontally to form the dorsal and ventral sections, the optic tectum and midbrain tegmentum, respectively. Upon both microscopic inspection of live embryos and embryo sections, CCM2 morphant embryos lacked development of the optic tectum. This data suggests that in addition to the aortic arch defects, neural developmental defects are also occurring in CCM2 morphant embryos.

Discussion

Danio rerio has proven to be a beneficial tool in our understanding of vertebrate development. Many developmental processes that occur in mammalian systems are conserved in zebrafish, making this system a cost-effective alternative to mouse models. For early embryonic lethalities zebrafish are a more desirable model since the embryos develop externally. Furthermore, zebrafish can survive without a functioning cardiovascular system until 48 hpf. Since much of the early vasculature forms before 48 hpf, this makes Danio rerio ideal for studying vascular abnormalities. Using translational blocking morpholinos to CCM2, we have begun to characterize the developmental defects

associated with CCM2 loss. We have found that morpholino knockdown of CCM2 leads to decreased embryonic circulation, due in part to constriction of the first aortic arch.

Our observations in zebrafish suggest a common evolutionary role for CCM2 in vascular development. A gene-trap knockout model for *CCM2* in mice demonstrated that complete loss of CCM2 expression leads to embryonic lethality at E9.5 (Plummer et al., 2006). Mice heterozygous for the CCM2 gene-trap allele developed CCM lesions, albeit at a low penetrance. Recently the mechanism of this embryonic lethality of the CCM2 gene-trap model was characterized and found to be strikingly similar to our zebrafish CCM2 knockdown model. At E8.5, mouse embryos null for CCM2 expression had a narrow and irregular dorsal aorta which prevented embryonic blood flow (Whitehead et al., 2009). Another recently published work examined CCM2 morphant embryos (Kleaveland et al., 2009). In this work, CCM2 morphant zebrafish were analyzed for vascular patterning and heart development. Similar to our results, CCM2 morphant zebrafish demonstrated proper vascular patterning and blood flow in CCM2 morphant embryos was diminished due to a proximal aortic constriction. Therefore, based on two independent studies in zebrafish and mouse model systems, CCM2 is clearly involved in aorta morphogeneic processes.

The zebrafish homologs of *CCM1* and *CCM2* have been identified in N-ethyl-N-nitrosourea (ENU) mutagenesis screens for genes necessary for cardiovascular development (Chen et al., 1996; Stainier et al., 1996). *CCM1* and

CCM2 homologs, *santa* and *valentine* respectively, both exhibited large, distended hearts by 48 hours post fertilization (hpf, (Mably et al., 2006). These mutants were unable to circulate blood, even though there was a beating heart. Further examination of the *santa* and *valentine* embryos were found to have a myocardial layer of only one cell thick, when the normal embryo should have 2-3 cell thick layer. These hearts displayed differentiated cardiac markers but lacked endocardial cushions. As the number of myocytes and number of endocardial cells were found to be equal between wild type, *santa*, and *valentine* embryos, it was hypothesized that *santa* and *valentine* were required for the concentric growth of the heart. In this condition, the cells proliferate to the normal cell number, but the growth occurs around the perimeter of the heart instead of in layers, leading to very large, dilated heart chambers. In our CCM2 morphant embryos, we did observe pericardial edema in a fraction of embryos (data not shown); although our measure of heart development, DAF2-DA staining, suggested that heart development was predominantly normal. We believe that since the major events in heart development (heart tube formation, looping, atrium and ventricle specification) did occur, that these hearts would be DAF2-DA positive, meaning the loss of concentric growth associated with mutations in *santa* and *valentine* may not be sufficient to block bulbus arteriosus development.

Our CCM2 morphants also exhibited developmental defects of the optic tectum and neural tube. The expression patterns determined for *santa* and *valentine* may explain these additional phenotypes (Mably et al., 2006). By in

situ hybridization, at 28 hpf *santa* and *valentine* were expressed throughout most of the brain, with strong expression in the ventricular zone. In mice, significant neuronal expression of CCM2 has also been observed (Plummer et al., 2006). Based on these expression patterns, neural abnormalities would be predicted with CCM2 knockdown. Neural defects have not been characterized in other CCM2 animal models, suggesting that this defect could be specific to zebrafish.

The aortic arch defects observed in CCM2 morphant embryos are strikingly similar to defects seen in the *CCM1* gene-trap mouse model, suggesting a genetic link between *CCM1* and *CCM2* (Whitehead et al., 2009; Whitehead et al., 2004). Studies have proven a genetic link between *CCM1* and *CCM2* in zebrafish. *Santa* and *valentine* were found to be genetically in the same pathway based on treatment of embryos with *santa* and *valentine* morpholinos in combination (Mably et al., 2006). Injection of both *santa* and *valentine* morpholinos led to a dramatic increase in the number of embryos with heart defects compared to embryos injected with either *santa* or *valentine* morpholinos alone, suggesting alteration of a common signaling pathway. This is consistent with our characterization of CCM1 and CCM2 as molecular binding partners (Zawistowski et al., 2005).

How do the morphogenic processes in aortic arch formation relate to human CCM? Of all the animal models generated for the CCM genes, the only model to consistently have brain malformations similar to CCM patients was the *CCM1 +/- Trp53 -/-* mouse model (Plummer et al., 2004). This implies that a somatic mutation event leads to endothelial defects and CCM formation post-

natal. Although our model does not form brain lesions, it is possible to gain information pertinent to CCM from animal models that do not form brain lesions. The same signaling pathways involved in morphogenesis of the aortic arch could well be involved in maintenance of the vasculature of the brain. Further study is necessary to determine these signaling pathways associated with CCM1, CCM2, or CCM3 loss in endothelial cells.

In this work we characterize a zebrafish model for CCM2. We show that loss of CCM2 expression leads to decreased embryonic blood flow due to aorta morphogenic defects. The phenotypes characterized here confirm the importance of CCM2 in vascular development. As these defects phenocopy defects in CCM1-null mice and zebrafish, we provide additional support that CCM1 and CCM2 are in a common signaling pathway relevant to CCM pathogenesis.

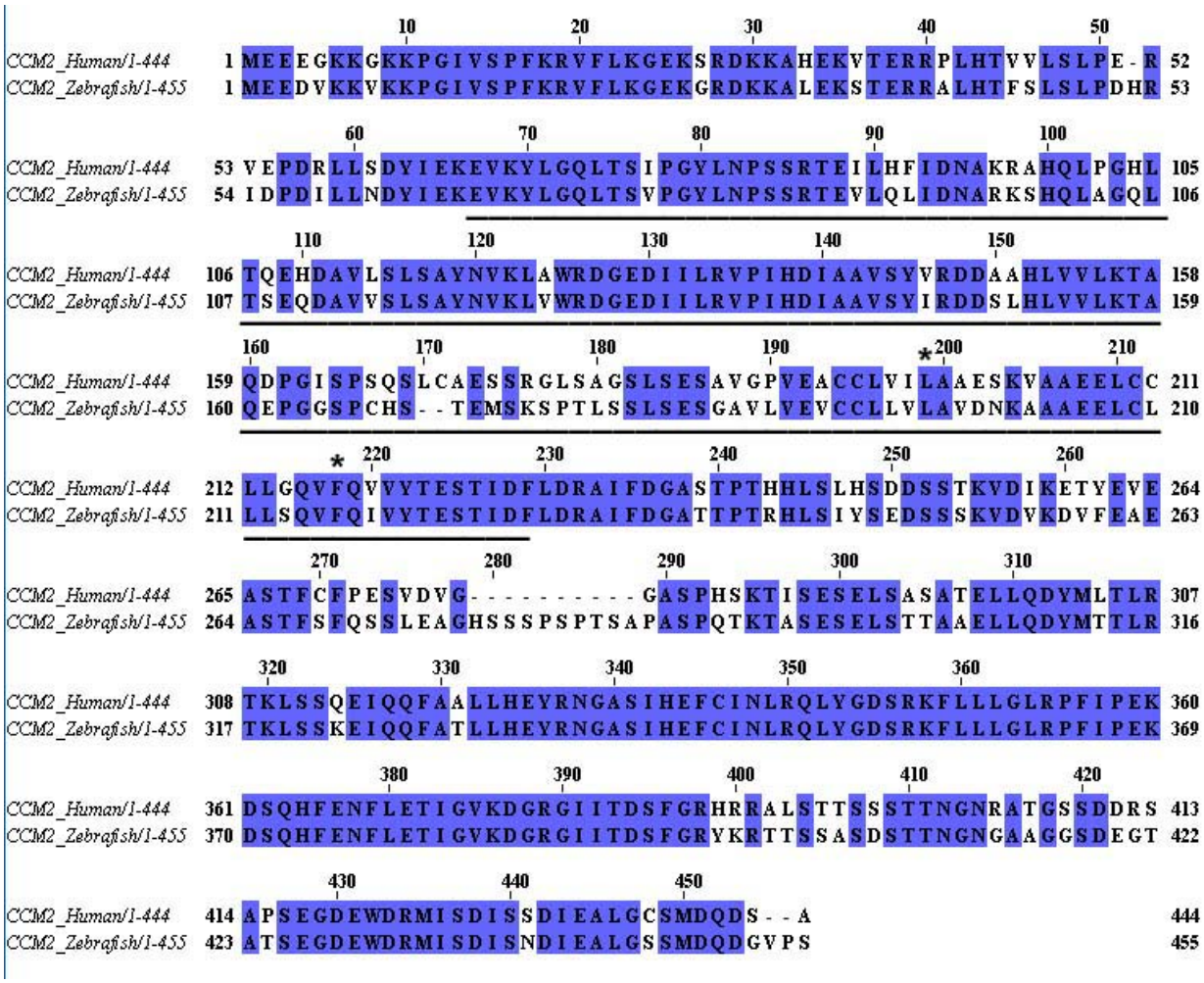

Figure 4.1: The Danio rerio CCM2 homolog. T-Coffee alignment (EMBL-EBI) of the human CCM2 amino acid sequence (Accession NP_113631) and the Danio rerio CCM2 amino acid sequence (Accession NP_001002315). The predicted PTB domain of *Danio rerio* CCM2 is underlined. The conserved residues that have been previously shown to be necessary for PTB domain integrity are designated with an asterisk.

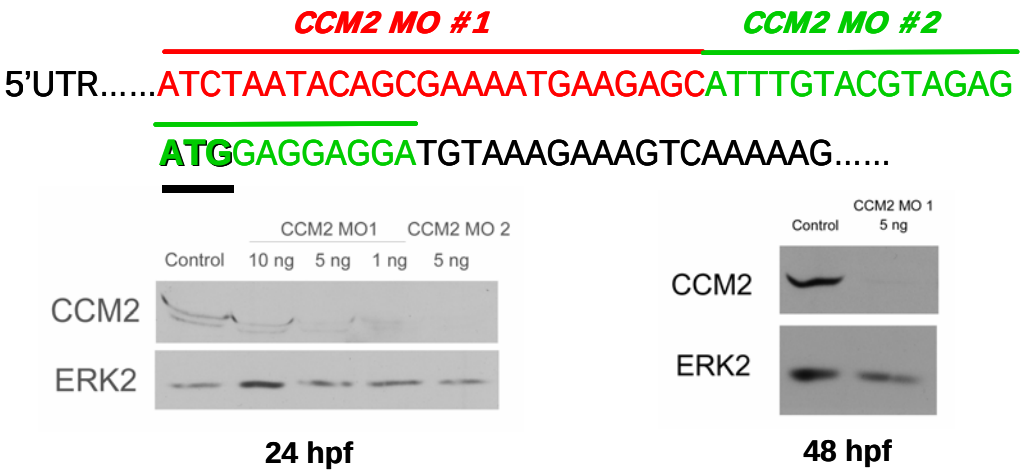

Figure 4.2: CCM2 knockdown strategy. Translational blocking morpholinos were designed to the region surrounding the translational start site of CCM2 mRNA. The start site ATG is underlined. Morpholinos were injected into 1 to 4 cell stage zebrafish embryos. After 24 or 48 hours, whole embryo lysate was analyzed for CCM2 protein knockdown using a polyclonal CCM2 antibody.

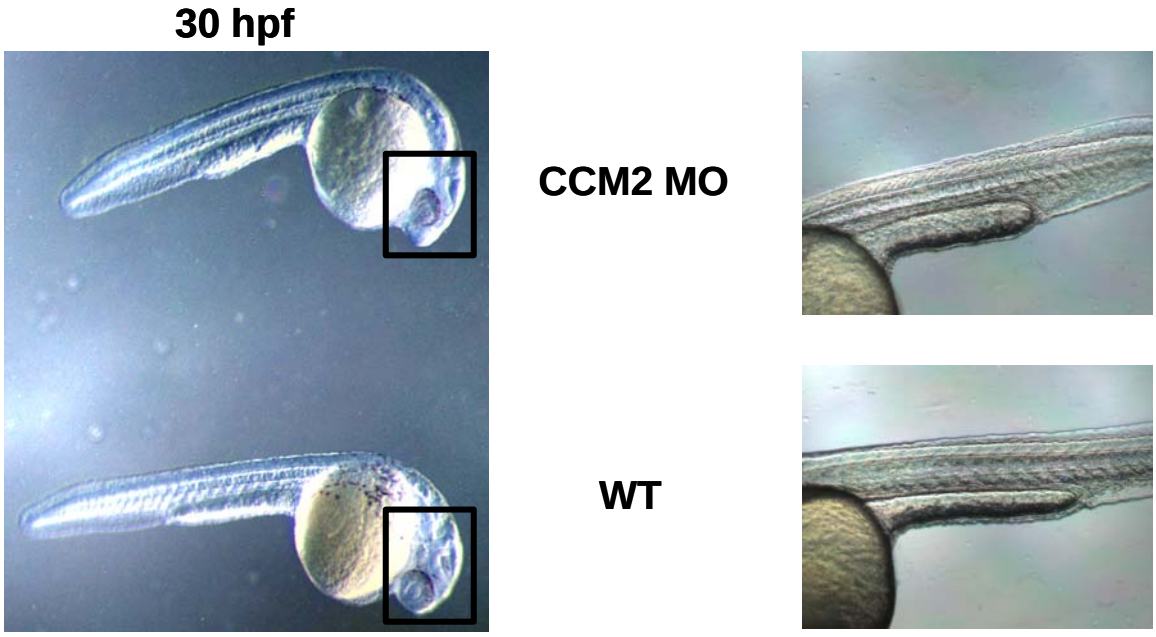

Figure 4.3: CCM2 morphant phenotype. Thirty hours post fertilization (hpf), embryos were analyzed by light microscopy. CCM2 morpholino-treated embryos displayed a flat head compared to wild type embryos. Morpholino-treated embryos also appear to be hypo-pigmented. Embryos have the proper number and size of somites.

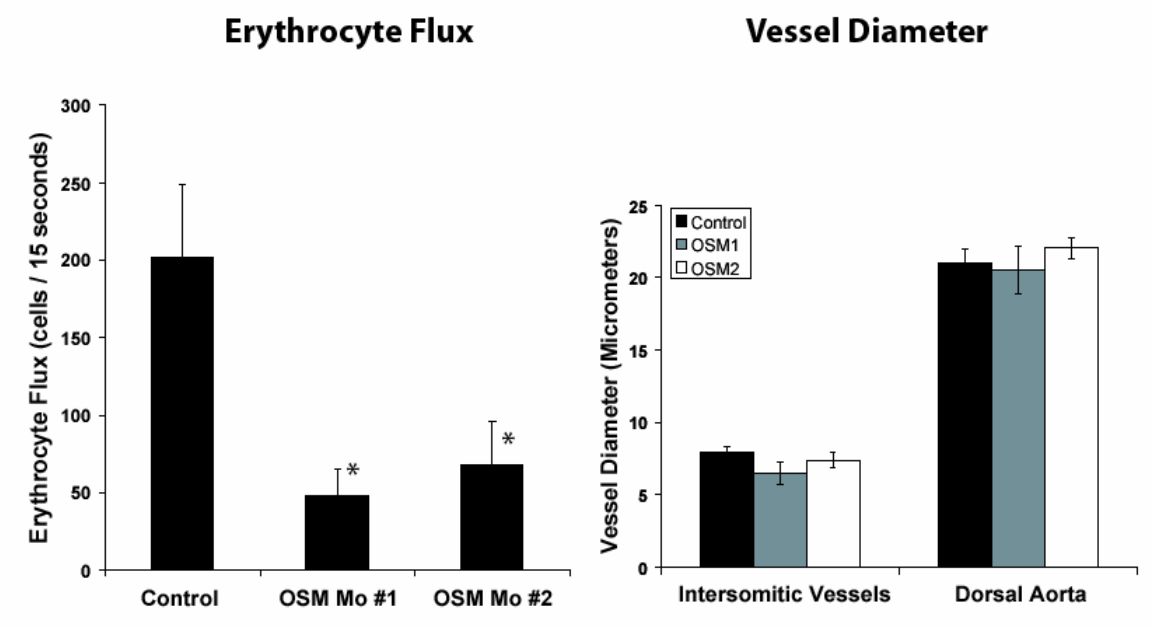

Figure 4.4: CCM2 (OSM) morphants have decreased blood flow in comparison to wild type embryos while blood vessel diameter is unaffected. 2-D DIC images were obtained from 48 hpf embryos. Erythrocyte flux and vessel diameter was measured using linescan imaging across the dorsal aorta and intersomitic vessels.

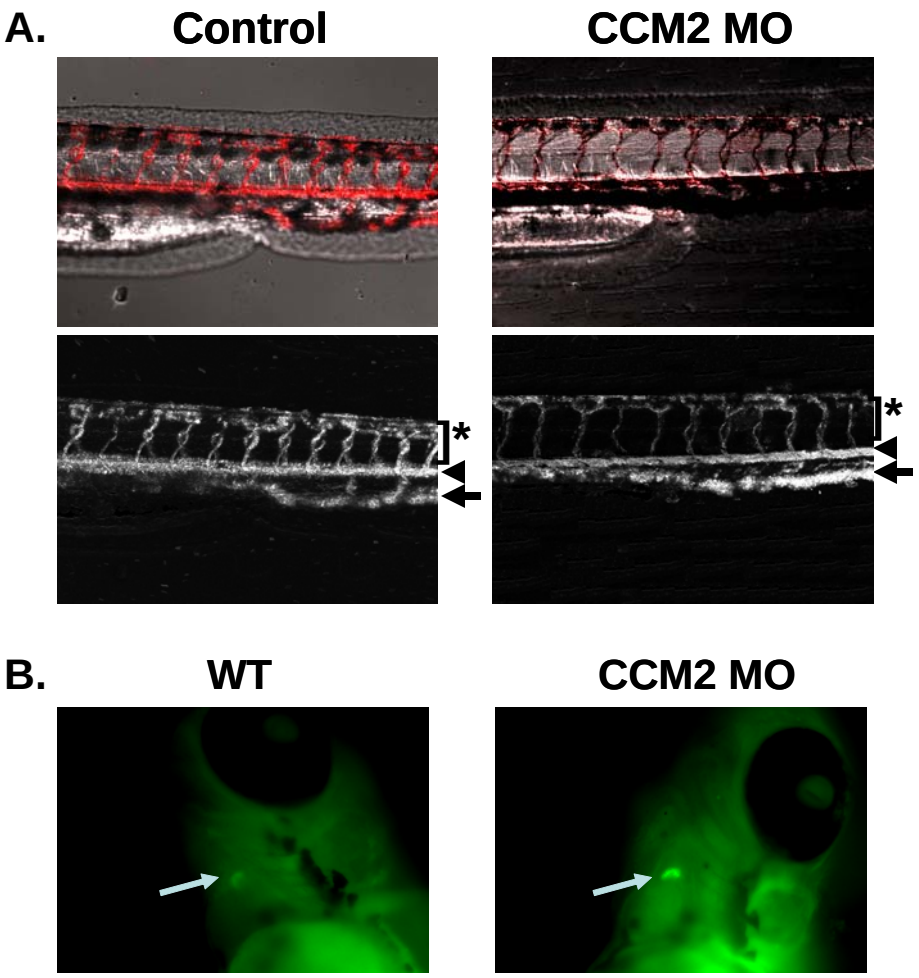

Figure 4.5: CCM2 morphant embryos have normal vascular patterning and bulbus arteriosus development. A) Top: *In silico* microangiography was performed on wild type and CCM2 morpholino-treated embryos at 48 hpf. The red tracings denote where blood has circulated. Bottom: *In silico* microangiographs of control and CCM2 morphant zebrafish embryos. Arrowheads denote the position of the aorta, the arrows denote the caudal vein, and the asterisk denotes the position of the intersomitic vessels. Note that intersomitic vessels are in the proper orientation and make complete dorsal and ventral connections. B) Live wild type and CCM2 morpholino treated embryos were incubated with DAF2-DA for 4 hours to label the bulbus arteriosus (arrow). Note that the bulbus arteriousus is present and in the proper size and shape in CCM2 morpholino-treated embryos.

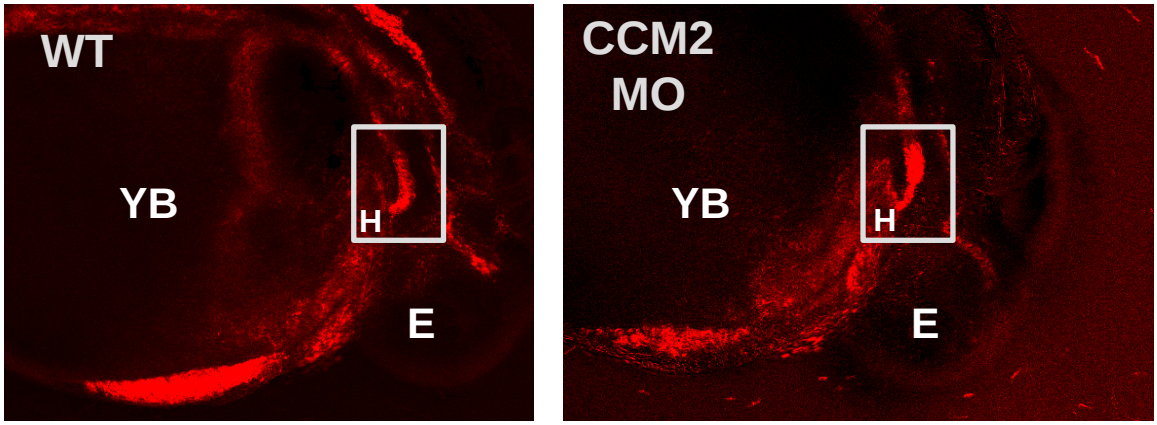

Figure 4.6: Aortic arch malformation in CCM2 morphant embryos. Wild type and CCM2 morpholino-treated embryos were analyzed by *in silico* microangiography at 24 hpf. In morpholino-treated embryos, the aortic arch (boxed) is constricted. H = Heart, E = Eye, YB = Yolk ball.

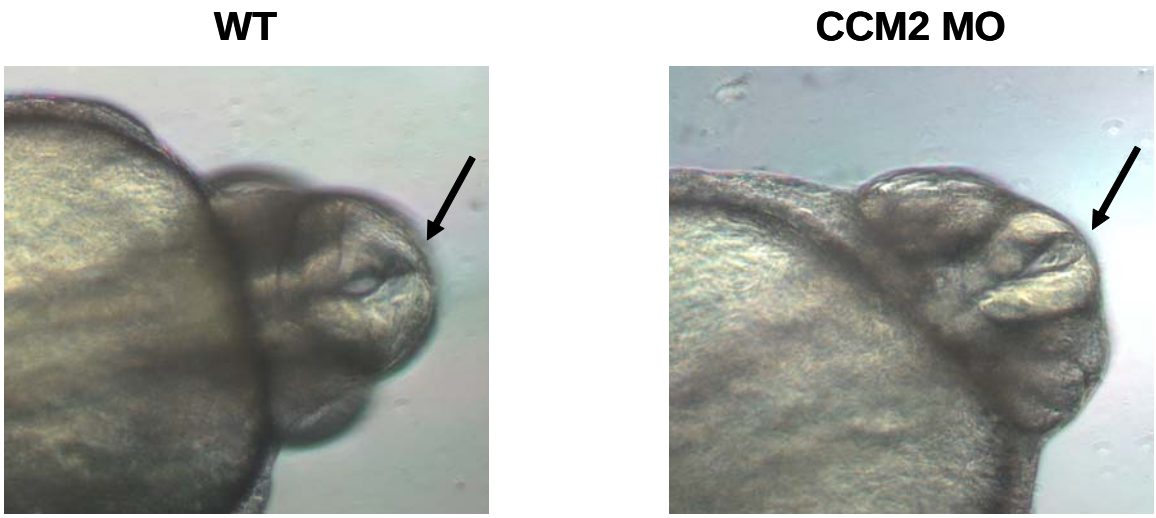

Figure 4.7: CCM2 morpholino-treated embryos have abnormal neural tube closure. Examination of embryos at 30 hpf dorsally revealed atypical neural tube closure in morpholino-treated embryos (arrow).

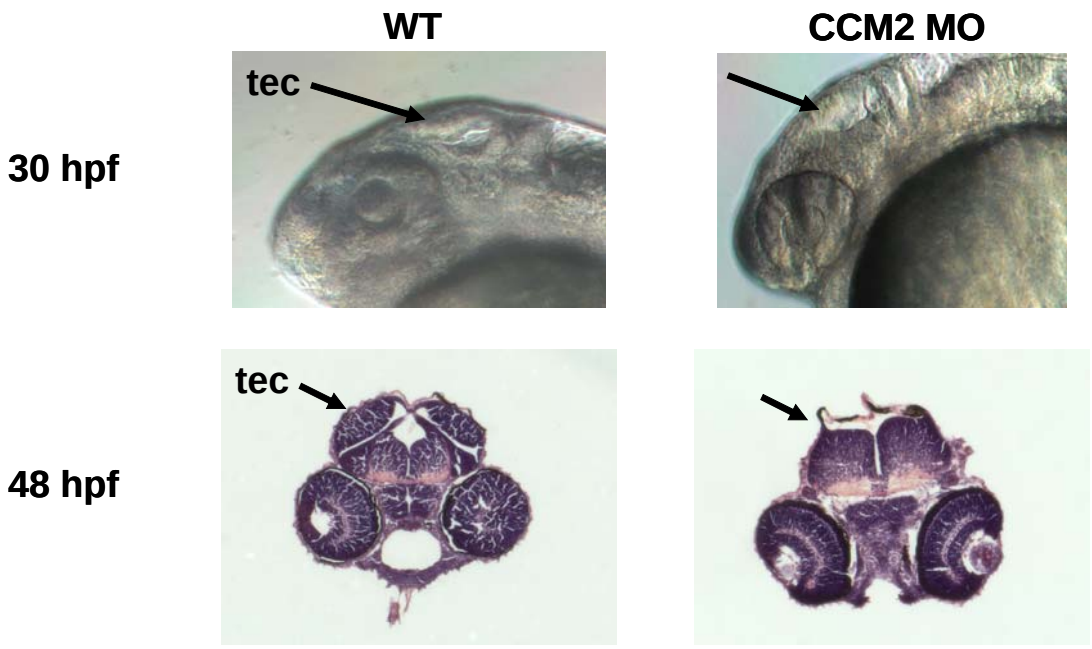

Figure 4.8: CCM2 morphant embryos do not develop an optic tectum. Top: Live embryos 30 hpf do not appear to have an optic tectum (tec). Bottom: Cross-sections of 48 hpf embryos confirms lack of tectum developent. Paraformaldehyde-fixed embryos were cryosectioned at 6 μm and stained with hematoxylin and eosin.

V. CCM2 acts as a negative regulator of ROCK signaling by promoting Smurf1-mediated degradation of RhoA

Introduction

We previously characterized a scaffold-like protein named Osmosensing Scaffold for MEKK3, (OSM), for its ability to bind actin, localize to Rac-containing membrane ruffles, and its obligate requirement for p38 activation in response to hyperosmotic stress (Uhlik et al., 2003). Simultaneously, the gene encoding OSM, *CCM2*, was found to be mutated in the human disease cerebral cavernous malformations (Liquori et al., 2003). Cerebral cavernous malformations (CCM) are vascular lesions of the central nervous system characterized as clusters of dilated, thin-walled blood vessels. CCM lesions are fragile and prone to vascular leakiness and rupture, leading to hemorrhages that cause seizure and stroke (Marchuk et al., 2003; Plummer et al., 2005).

In addition to *CCM2*, the familial form of CCM has been mapped to mutations in 2 other genes, *CCM1* and *CCM3* (Bergametti et al., 2005; Sahoo et al., 1999; Zhang et al., 2000b). *CCM1* encodes KRIT1, a Rap1A effector protein that is required for maintenance of endothelial cell junctions (Glading et al., 2007). CCM1/KRIT1 contains multiple ankyrin repeats, a carboxy-terminal FERM domain, and NPxY motifs which interact with the PTB domain of CCM2/OSM (Zawistowski et al., 2005). The *CCM3* gene encodes Programmed Cell Death 10 (PDCD10), a gene up-regulated in the human myeloid cell line TF-

1 upon induction of apoptosis (Bergametti et al., 2005). Although CCM3 does not have any predicted domain structure, it also binds CCM2 (Hilder et al., 2007). Based on these data, we have proposed a CCM protein complex that contains these proteins.

Bi-allelic germline and somatic mutations and loss of specific CCM protein expression have been seen in endothelial cells of CCM lesions but not interstitial cells (Akers et al., 2009; Pagenstecher et al., 2009). This finding confirms the two-hit hypothesis for CCM pathogenesis and also suggests that CCM is a disease associated with complete loss of specific CCM gene expression in endothelial cells and subsequent endothelial cell dysfunction. Recently, CCM2 knockdown endothelial cells were shown to have increased activation of RhoA (Whitehead et al., 2009), although the mechanism was not defined. Herein, we demonstrate a molecular mechanism for activation of this pathway. Through a novel CCM2 PTB domain interaction with the Smurf1 HECT domain, we now show that CCM2 binds the E3 ligase Smurf1 for the control of RhoA degradation.

This work was done in collaboration with Dr. Tom Hilder, who provided permeability assay data and CCM2 pull-down of endogenous Smurf1.

Results

CCM2 binds Smurf1

We have previously demonstrated that MEKK3, a Ste11-like MAP3K that regulates the p38 pathway in mammalian cells in response to hyperosmolarity (Uhlik et al., 2003), binds to CCM2 and is a component of a larger CCM1-CCM2-

CCM3 protein complex (Hilder et al., 2007). MEKK3 is highly homologous to MEKK2, and both contain a conserved PY motif that, in MEKK2, has been shown to bind the E3 ubiquitin ligase Smurf1 (Yamashita et al., 2005). Therefore, we asked if Smurf1 was found in the CCM protein complex, possibly by binding to the PY motif of MEKK3. Cells stably expressing FLAG-tagged wild type CCM2 or a CCM2 PTB domain mutant that is unable to bind NPxY motifs in target proteins (CCM2-F217A), were used in co-immunoprecipitation assays to define endogenous proteins that bind to the CCM protein complex (Hilder et al., 2007). Figure 5.1A shows that endogenous Smurf1 co-immunoprecipitated with FLAG-CCM2 but not CCM2 F217A, indicating that Smurf1 associates with the CCM2 protein complex in a PTB domain-dependent manner.

MEKK3 binds CCM2 independent of the CCM2 PTB domain (Hilder et al., 2007), suggesting that Smurf1 association with the CCM complex may be independent of MEKK3. We utilized a catalytically inactive mutant of Smurf1, Smurf1 C699A, to examine these protein-protein interactions, as it is unable to ubiquitinate and degrade Smurf1 substrates (Wang et al., 2006). We expressed Smurf1 C699A with MEKK3, CCM2, or MEKK2, a known substrate of Smurf1 (Yamashita et al., 2005). Figure 5.1B shows that MEKK2, MEKK3 and CCM2 are all able to co-immunoprecipitate with Smurf1C699A.

We used GST-Smurf1 protein purified from bacteria and MEKK3 and CCM2 expressed and purified from SF-9 cells to examine if interactions between the E3 ligase and MEKK3 and CCM2 are direct. CCM2 and MEKK3 both directly

bind GST-Smurf1 (Figure 5.1C), demonstrating that Smurf1 and CCM2 are binding partners both *in vivo* and *in vitro*.

CCM2 binds Smurf1 via a PTB domain - HECT domain interaction

Smurf1 is a member of the NEDD4 family of E3 ligases, which have a common domain structure of an amino-terminal C2 domain followed by multiple WW domains and a carboxy-terminal HECT domain (Ingham et al., 2004). Smurf1 constructs were generated that encoded either the N-terminal moiety of Smurf1 (FLAG-Smurf1 ΔHECT containing the C2 and WW domains), or the C-terminal moiety of Smurf1 (FLAG-Smurf1 HECT encoding only the HECT domain). Co-expression of the Smurf1 moieties with CCM2 indicated that CCM2 predominantly bound the HECT domain with little binding to the N-terminal portion of Smurf1 (Figure 5.2A), indicating that CCM2 was binding specifically to the HECT domain. Consistent with this, the HECT domain of Smurf1 was sufficient to bind CCM2 by co-immunoprecipitation. Smurf1 and Smurf2 are highly homologous in their HECT domains (Lin et al., 2000). Figure 5.2B demonstrates that CCM2 binds both Smurf1 and Smurf2, as would be predicted. Consistent with the CCM2 pull down of endogenous Smurf1 (Figure 1A), the interaction between full length Smurf1 or the Smurf1 HECT domain requires a functional CCM2 PTB domain (Figures 5.2C and D). To our knowledge this is the first demonstration of a PTB domain-HECT domain interaction.

The consensus PTB-binding motif is Asn-Pro-X-Tyr (NPxY), where X is any amino acid (Smith et al., 2006). Examination of the amino acid sequence of

the Smurf1 HECT domain identified an NPYY motif (AA 457-460) that is also conserved in the Smurf2 HECT domain. The tyrosine of the NPxY motif is critical for interaction of binding partners with many PTB domains (Smith et al., 2006). Mutation of Y460 within the Smurf1 NPYY motif to alanine had little effect on interaction with CCM2 by co-immunoprecipitation (data not shown). Engineering combinations of mutations involving two mutations within the NPYY motif of Smurf1 determined that N457A/Y460A (APYA) had a partial inhibition of association, while mutation at residues Y459 and Y460 (NPAA referred to as Smurf1 YY-AA below) caused a loss of detectable association with CCM2 (Figure 5.2E). These results indicate that CCM2, via its PTB domain, requires the NPYY motif within the Smurf1 HECT domain for binding.

CCM2 is not a Smurf1 substrate, nor does it affect Smurf1 catalytic activity

Since CCM2 is a Smurf1 binding protein, it was not known if CCM2 was a substrate for Smurf1-mediated degradation. In cells expressing Smurf1 WT, or Smurf1 C699A, there was no change in abundance of CCM2 relative to control transfected cells, although a loss of known Smurf1 substrates, RhoA and MEKK2, was observed (Figure 5.3A). These results indicate that CCM2 is not a substrate for Smurf1-mediated ubiquitination and degradation. This is consistent with what is known about substrate recognition by NEDD4 family E3 ligases. Most NEDD4 family members interact with their substrates via their WW domains (Ingham et al., 2004). In most cases, this occurs through a canonical interaction of the WW domain with a PY motif within the substrate (Ingham et al., 2005;

Ingham et al., 2004). CCM2 interacts with the Smurf1 HECT domain via its PTB domain, and negligibly with the amino-terminal moiety of Smurf1 that contains the WW domains. This is consistent with CCM2 not being a substrate for Smurf1.

The HECT domain catalyzes the ubiquitination of Smurf1 substrates. Binding of CCM2 to the Smurf1 HECT domain could therefore regulate the catalytic activity of Smurf1. Expression of CCM2 with Smurf1 neither significantly increased nor decreased the catalytic activity of Smurf1 in a Smurf1 ubiquitination assay (Figure 5.3B). Furthermore, the Smurf1 YY-AA mutation, which cannot bind CCM2, was still catalytically active in a Smurf1 *in vitro* ubiquitination assay (Figure 5.3C), indicating that the CCM2 interaction with the NPYY motif of the Smurf1 HECT domain does not affect the catalytic activity of Smurf1.

Co-expression of CCM2 and Smurf1 leads to cell rounding

When expressed in COS-7 cells CCM2 was localized in the cytoplasm with enhanced localization at the plasma membrane (Figure 5.4A). Smurf1 was also localized at the cell periphery, a function of the C2 domain of NEDD4 family members (Plant et al., 1997). When co-expressed, Smurf1 and CCM2 co-localized to the plasma membrane and induced a dramatic rounding of cell morphology (Figure 5.4B). Cell rounding was not observed in cells expressing CCM2 or Smurf1 alone, nor in cells expressing CCM2 and Smurf1 C699A (Figure 5.4A and D). The phenotype induced by co-expression of CCM2 and

Smurf1 suggested that the CCM2-Smurf1 complex is altering the cytoskeleton and adherence of COS-7 cells. Cells co-expressing CCM2 and Smurf1 YY-AA, which cannot bind CCM2, did not show a cell rounding phenotype (Figure 5.4C), suggesting a CCM2-Smurf1 complex is required for inducing the rounded morphology.

CCM2 localizes Smurf1 by binding the HECT domain

The C2 domain localizes Smurf1 to the plasma membrane. Therefore, CCM2 binding is not required for membrane localization of Smurf1, but would be predicted to localize Smurf1 to CCM2 protein complexes. As expected, the Smurf1 HECT domain, when expressed alone, was not able to localize to the cell membrane and remains cytoplasmic because it lacks a C2 domain (Figure 5.4E). Expression of CCM2 with the Smurf1 HECT domain resulted in relocalization of the Smurf1 HECT domain to the plasma membrane, where it co-localized with CCM2 (Figure 5.4E). Thus, the CCM2 PTB-Smurf1 HECT domain interaction localizes Smurf1 to CCM2 complexes primarily at the cell periphery.

CCM2 regulates RhoA degradation

Smurf1 is an E3 ligase for RhoA, whose degradation could result in the morphological changes we observed in cells expressing CCM2 and Smurf1 (Figure 5.4, (Wang et al., 2003)). We hypothesized that CCM2 regulates Smurf1-mediated degradation of RhoA. To define the function of CCM2 in brain endothelial cells, RNAi was used to knockdown CCM2 expression. Using a

lentivirus-based shRNA system, brain microvascular endothelial cells (bEND.3) were infected with either a control vector (pLKO.1) or two independent CCM2 shRNA vectors. The bEND.3 cells were analyzed for CCM2 RNA knockdown by RT-PCR assay. Both shRNA constructs were found to be effective at knocking down CCM2 RNA by 90% (Figure 5.5C). Cells expressing shRNA for CCM2 had increased levels of RhoA as determined by immunoblotting (Figure 5.5A). These cells did not show a significant increase in RhoA transcription (Figure 5.5D), suggesting that the increased RhoA detected was occurring post-transcriptionally. Importantly, knockdown of CCM2 did not affect abundance of the Smurf1 substrate MEKK2, the Smurf1 interacting protein MEKK3, or the GTPase Rac1 (Figure 5.5A). These findings indicate that loss of CCM2 expression selectively facilitates degradation of RhoA, but not other Smurf1 substrates such as MEKK2.

In order to determine if CCM2 could be facilitating Smurf1-mediated degradation of RhoA, we expressed increasing amounts of CCM2 in combination with Smurf1 and RhoA (Figure 5.5B). Cells expressing Smurf1C699A and increasing amounts of CCM2 had little effect on RhoA levels. In contrast, increasing amounts of CCM2 in the presence of wild type Smurf1 led to significant loss of RhoA protein, consistent with CCM2 regulating Smurf1 dependent RhoA degradation.

Knockdown of CCM2 in brain microvascular endothelial cells leads to dysregulation of the actin cytoskeleton

Expression of Smurf1 and CCM2 in COS-7 cells led to increased cell rounding (Figure 5.4B), suggesting that the Smurf1-CCM2 complex is involved in cytoskeletal regulation. Furthermore, CCM2 knockdown in bEND.3 cells resulted in increased RhoA protein levels, consistent with CCM2 controlling RhoA-dependent cytoskeletal dynamics. Figure 5.6 shows that CCM2 knockdown in the bEND.3 brain endothelial cells resulted in increased stress fiber formation when compared to cells expressing the control vector. Two different shRNAs for CCM2 each gave similar increases in stress fiber formation, demonstrating these are likely on-target effects of CCM2 knockdown (Figure 5.7). Because CCM2 regulates RhoA abundance and increases stress fiber formation, we examined if CCM2 knockdown affected downstream signaling pathways by measuring the phosphorylation of MLC2, a substrate for Rho kinase (Amano et al., 1996). CCM2 knockdown cells have a significant increase in phospho-MLC2 associated with stress fibers compared to control cells. (Figure 5.7). Treatment of CCM2 knockdown cells for 24 hours with 10 μM Y-27632, an inhibitor of Rho kinase, resulted in a loss of phospho-MLC2 levels associated with stress fibers to levels similar to control cells. These findings are consistent with the increased RhoA levels associated with loss of CCM2 expression. Further, this suggests that there is increased signaling downstream of RhoA in CCM2 knockdown cells that can be reversed with the Rho kinase inhibitor Y-27632.

CCM2 regulates endothelial cell migration

Knockdown of CCM2 led to increased stress fiber formation in brain endothelial cells. In order to determine if this impacted cell migration, we performed wound healing assays. Confluent monolayers of brain endothelial cells expressing GFP were wounded and imaged every 15 minutes for 16 hours. Cells expressing a control vector were capable of healing 50% of the wound; however, cells lacking CCM2 were significantly less capable of closing the wound in the same period of time (Figure 5.8A-B). This is consistent with increased RhoA signaling, as cessation of RhoA signaling is necessary for cytoskeletal turnover and migration.

Endothelial tubule formation and maintenance of a permeability barrier requires CCM2

Consistent with an impairment of endothelial cell migration, knockdown of CCM2 expression markedly inhibits in vitro tubule formation in Matrigel of mouse embryonic endothelial cells (MEECs). MEECs were used in the study because bEND.3 cells do not readily form tubules *in vitro*. After 16 hours of culture on a Matrigel plug, MEECs expressing the pLKO.1 control vector were able to form a network of branched tubules, while cells lacking CCM2 expression were impaired in this function (Figure 5.9B).

An *in vitro* endothelial permeability assay was used to determine if CCM2 was also important for endothelial monolayer integrity. HUVECs were used because of the strong permeability barrier formed by HUVEC monolayers. CCM2 knockdown in HUVECs resulted in increased permeability compared to

cells treated with the control siRNA (Figure 5.9A). Furthermore, the CCM2 knockdown HUVECs induced permeability to the extent that was comparable with control cells treated with EGTA to induce permeability. Thus, CCM2 is required for proper endothelial cell functions including migration, morphogenesis, and permeability. We hypothesize these defects are due in part to aberrant regulation of Smurf1-mediated degradation of RhoA.

Discussion

CCM is a disease of the vasculature of the central nervous system. However, the pathogenesis of CCM remains unclear. Analysis of the amino acid sequence of the three genes known to be mutated in the familial form of CCM has not identified any catalytic domains. This suggests that the function of these three proteins is to organize signaling complexes in the cell. Indeed, we have acknowledged this role for CCM2 as an osmosensing scaffold for activation of the p38 MAPK pathway (Uhlik et al., 2003; Zawistowski et al., 2005). It is now clear that scaffolding proteins play major roles in both the stimulus-dependent activation of a signaling cascade as well as the subcellular localization of the signaling module (Lu et al., 2006; Miller and Lefkowitz, 2001). We have previously shown that the CCM2 PTB domain is responsible for localizing CCM1 to the cytoplasm of cells (Zawistowski et al., 2005). Our lab has shown further that the proteins EF1A1, RIN2, and tubulin also interact with CCM2 in a PTB-domain dependent manner (Hilder et al., 2007). How CCM2 is regulating the function of these proteins remains to be determined; however, the diversity of

binding partners suggests a complex and varied role for CCM2 in cell physiology. In our current work we provide evidence that CCM2 acts to recruit the E3 ligase Smurf1 to specific locations at the cell membrane to regulate localized degradation of RhoA. Again, the PTB domain of CCM2 was necessary for this interaction. What makes this phenomenon novel is the interaction of the CCM2 PTB domain with the Smurf1 catalytic HECT domain. To our knowledge this is the first example of a PTB-HECT domain interaction. We have found that PTB binding motifs are conserved in many other HECT domains (Table 5.1) and this may be the first example of a yet unappreciated role for PTB domains.

Although the CCM2 interaction with Smurf1 does not appear to change the catalytic activity of Smurf1 or act to recruit CCM2 as a Smurf1 substrate, this interaction does appear to play a role in localization of Smurf1 to the membrane to degrade RhoA. Studies of NEDD4 E3 ligases have provided trends associated with the common domain architecture of these proteins. The amino-terminal C2 domain has been shown to be involved in membrane localization of NEDD4 family members. This was first demonstrated in the Ca2+ dependent membrane localization of NEDD4 via its C2 domain (Plant et al., 1997). The C2 domain has also been implicated in an auto-inhibition of the HECT domain (Wiesner et al., 2007). The majority of protein-protein interactions for NEDD4 E3 ligases have been attributed to the WW domains. Within this family, WW domains vary in number as well as primary sequence and are believed to be the source of substrate specificity (Ingham et al., 2005). Furthermore, WW domains have been implicated in phosphorylation-dependent regulation of these proteins

(Gallagher et al., 2006). Roles for intermolecular interactions within the HECT domain have been less clear, aside from the role of E2 binding to this region. However, Smad7, an inhibitory Smad in the TGF-beta signaling pathway, has been shown to interact with the HECT domain of Smurf1 and Smurf2 via the Smad7 N-terminal domain (NTD) and promote association of the Smurf1/2 HECT domain with the E2 (Ogunjimi et al., 2005). A Smad7-Smurf1/2 interaction also occurs between a PY motif within Smad7 and the WW domains of Smurf1/2 (Chong et al., 2006). The MH2 domain of Smad7 binds to the TGF-beta receptor to recruit Smurf1/2 to the receptor and promote downregulation by ubiquitination of the receptor (Ebisawa et al., 2001). Therefore, there is prior evidence for regulation of Smurf activity by localization. In the case of CCM2, it appears that CCM2 may be recruiting Smurf1 to sites of actin remodeling in order to regulate the localized degradation of RhoA.

It should be noted that there has been no evidence thus far that Smurf1/2 are involved in CCM. The initial characterization of Smurf1/2 was in the context of downregulation of the TGFβ signaling pathway. Indeed, knock-out animal models for proteins at many levels of the TGFβ signaling pathway have displayed abhorrent vascular phenotypes (Arthur et al., 2000; Lebrin et al., 2005; Park et al., 2008). Since CCM2 binds and localizes Smurf1, it then seems reasonable to believe that CCM2 may also be involved in regulation of TGFβ signaling. In this way, the TGFβ signaling pathway may be relevant to CCM pathology.

The significance of our work is, in part, the knockdown of CCM2 in a brain microvascular endothelial cell line, bEND.3. Endothelial cells lacking CCM2

expression are defective in cell migration, permeability, and tubule formation. bEND.3 cells display an increase in RhoA abundance, predictably leading to increased signaling via the Rho kinase (ROCK) pathway. Indeed, the importance of ROCK signaling in endothelial cells has been recognized. Subsequent phosphorylation of MLC2 results in actomyosin contractility, loss of cell to cell contact, and increased permeability (Figure 5.10, (Wojciak-Stothard and Ridley, 2002)). We show that CCM2 knockdown leads to increased abundance of RhoA and stress fibers as well as increased phosphorylated MLC2 associated with stress fibers. Further, co-expression of CCM2 and Smurf1 led to cell rounding, likely due to dramatic loss of RhoA and cytoskeletal collapse.

Recent work has shown that CCM2 is a negative regulator of RhoA signaling in HUVECs (Whitehead et al., 2009); however, the molecular mechanism was not determined. We also provide evidence for activation of this pathway, although we observed a decrease in directed cell migration in bEND.3 cells, a response not observed with HUVECs. This suggests variability in endothelial cell physiology between these two cell types. Taken together, these studies strongly imply that defective RhoA regulation is a significant contributor to the pathogenesis of CCM.

We now provide the mechanism of increased RhoA signaling associated with loss of CCM2. For the first time we show that CCM2 associates with Smurf1 to regulate the degradation of the GTPase RhoA. Further, we have characterized a novel interaction between the CCM2 PTB domain and the Smurf1 HECT domain. Although the CCM2 interaction with Smurf1 does not

regulate the catalytic activity of Smurf1 nor act to recruit CCM2 as a Smurf1 substrate, this interaction plays a role in localization of Smurf1 to promote degradation of RhoA.

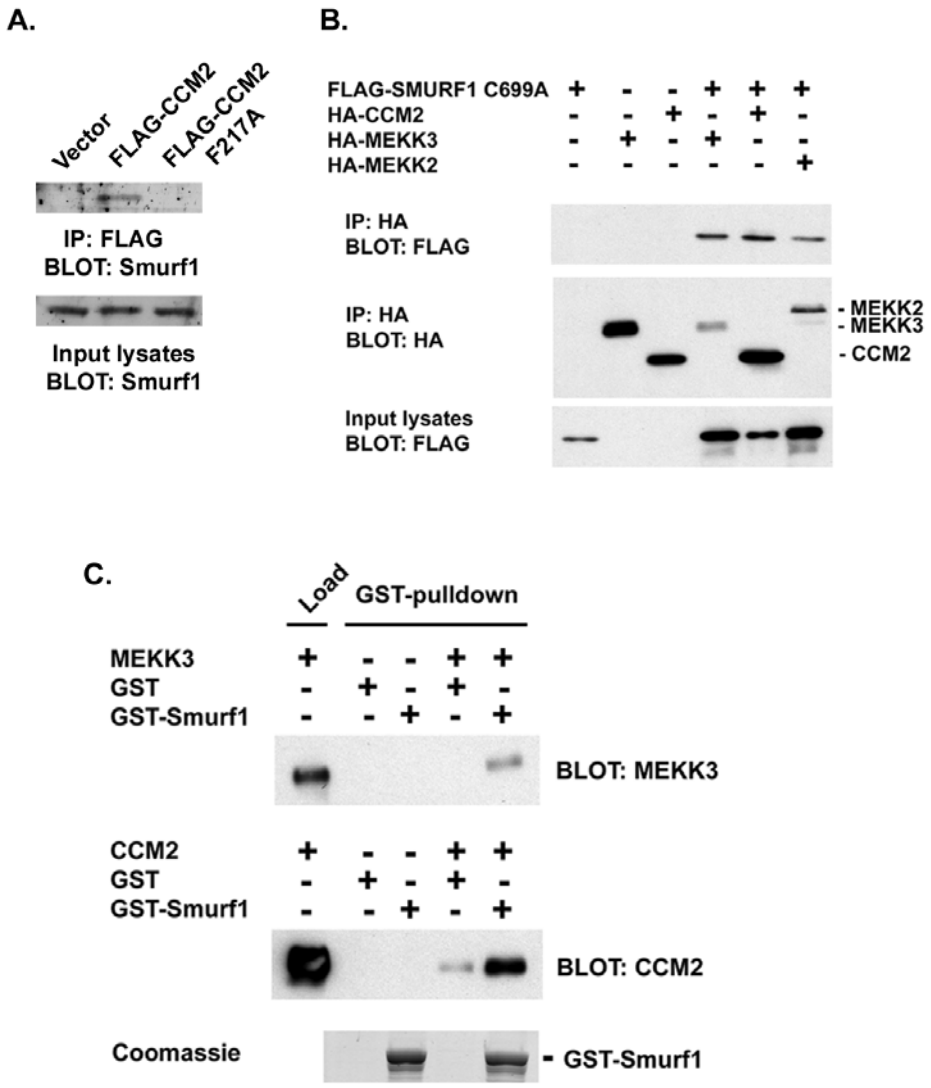

Figure 5.1: Smurf1 binds CCM2, MEKK2, and MEKK3. A) RAW264.7 stable cell lines expressing empty vector, Flag-CCM2, or Flag-CCM2 F217A were lysed and incubated with anti-FLAG-coated sepharose beads. The associated endogenous Smurf1 was examined by western blot. B) Cells expressing HA-tagged CCM2, MEKK2, or MEKK3 with Flag-Smurf1C699A were immunoprecipitated with anti-HA antibody and associated Flag-Smurf1C699A was determined by western Blot. C) The Smurf1-MEKK3 and Smurf1-CCM2 interaction is direct. Purified GST or GST-Smurf1 was incubated with purified His-MEKK3 or His-CCM2 and associating proteins were determined by western blot using anti-MEKK3 antibody or anti-CCM2 antibody.

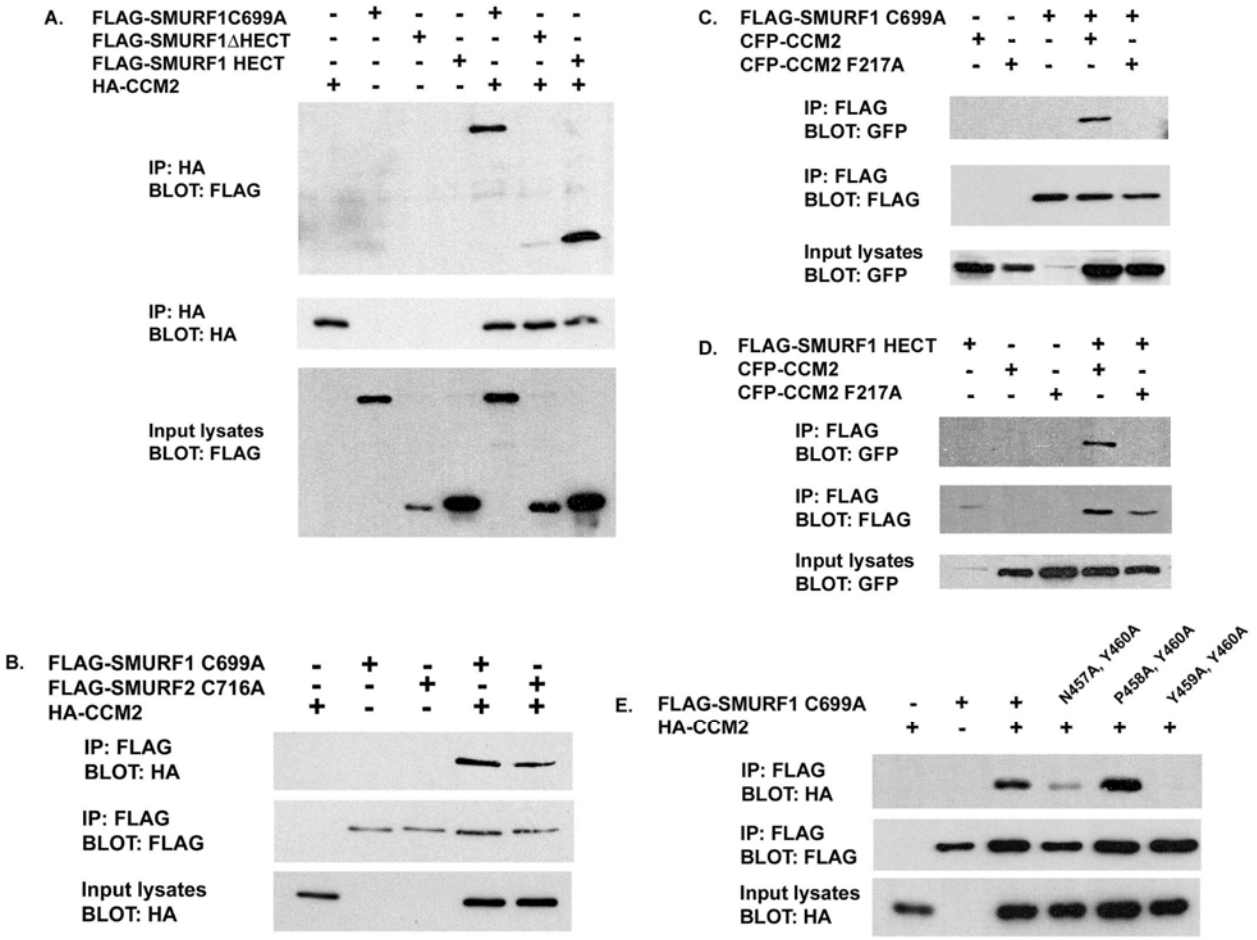

Figure 5.2: CCM2 interacts with Smurf1 via a novel PTB domain – HECT domain interaction. A) CCM2 interacts with the Smurf1 HECT domain. Cells expressing HA-CCM2 with FLAG-Smurf1C699A, FLAG-Smurf1ΔHECT or FLAG-Smurf1HECT were lysed and immunoprecipitated with anti-HA antibody. The associating proteins were determined by western blot for anti-Flag antibody. B) CCM2 interacts with Smurf1 in a PTB domain dependent manner. Cells expressing FLAG-Smurf1C699A and CFP-CCM2 or CFP-CCM2 F217A were lysed and immunoprecipitated with anti-FLAG antibody. Associated CFP-CCM2 was determined by western blot for anti-GFP antibody. C) CCM2 interacts with the Smurf1 HECT domain in a PTB domain dependent manner. FLAG-Smurf1HECT was expressed with either CFP-CCM2 or CFP-CCM2 F217A in cells. Cell lysates were incubated with anti-Flag antibody and associating CFP-CCM2 was determined by western blot. D) CCM2 can associate with either Smurf1 or Smurf2. Cells expressing HA-CCM2 and either FLAG-Smurf1C699A or FLAG-Smurf2C716A were lysed and immunoprecipitated with anti-FLAG antibody. Associating HA-CCM2 was determined by western blot for anti-HA. E) An NPYY motif within the HECT domain of Smurf1 is responsible for interaction with CCM2. Cells expressing HA-CCM2 and FLAG-Smurf1C699A, FLAG-Smurf1 N457A/Y460A/C699A, FLAG-Smurf1 P458A/Y460A/C699A, or FLAG-Smurf1 Y459A/Y460A/C699A were lysed and immunoprecipitated with anti-FLAG antibody. Associated HA-CCM2 was determined by western blot.

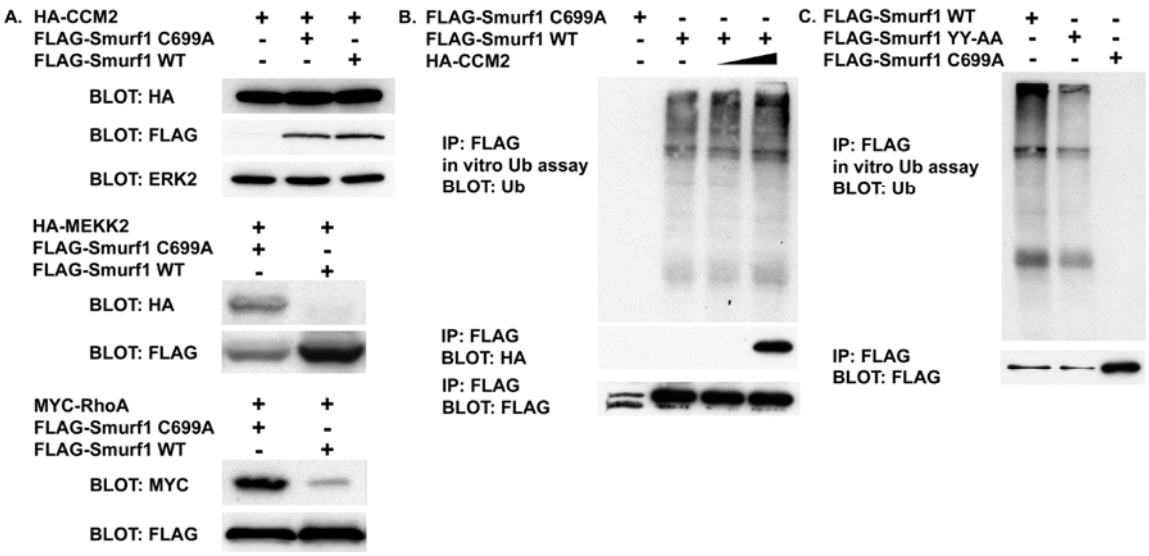

Figure 5.3: CCM2 is not a Smurf1 substrate nor does it impact Smurf1 catalytic activity. A) Cells expressing HA-CCM2, HA-MEKK2, Myc-RhoA, FLAG-Smurf1 C699A, or FLAG-Smurf1 WT were lysed and steady-state levels of HA-CCM2, HA-MEKK2, or Myc-RhoA were determined by western blot. B) Cells expressing FLAG-Smurf1 C699A, FLAG-Smurf1 WT, or HA-CCM2 were lysed, and FLAG-Smurf1 proteins were immunopurified. The immunopurified FLAG-Smurf1 or FLAG-Smurf1 C699A was subsequently used for an in vitro ubiquitination assay. C) Cells expressing FLAG-Smurf1 C699A, FLAG-Smurf1 WT or FLAG-Smurf1 YY-AA were lysed and immunopurified for in vitro ubiquitination.

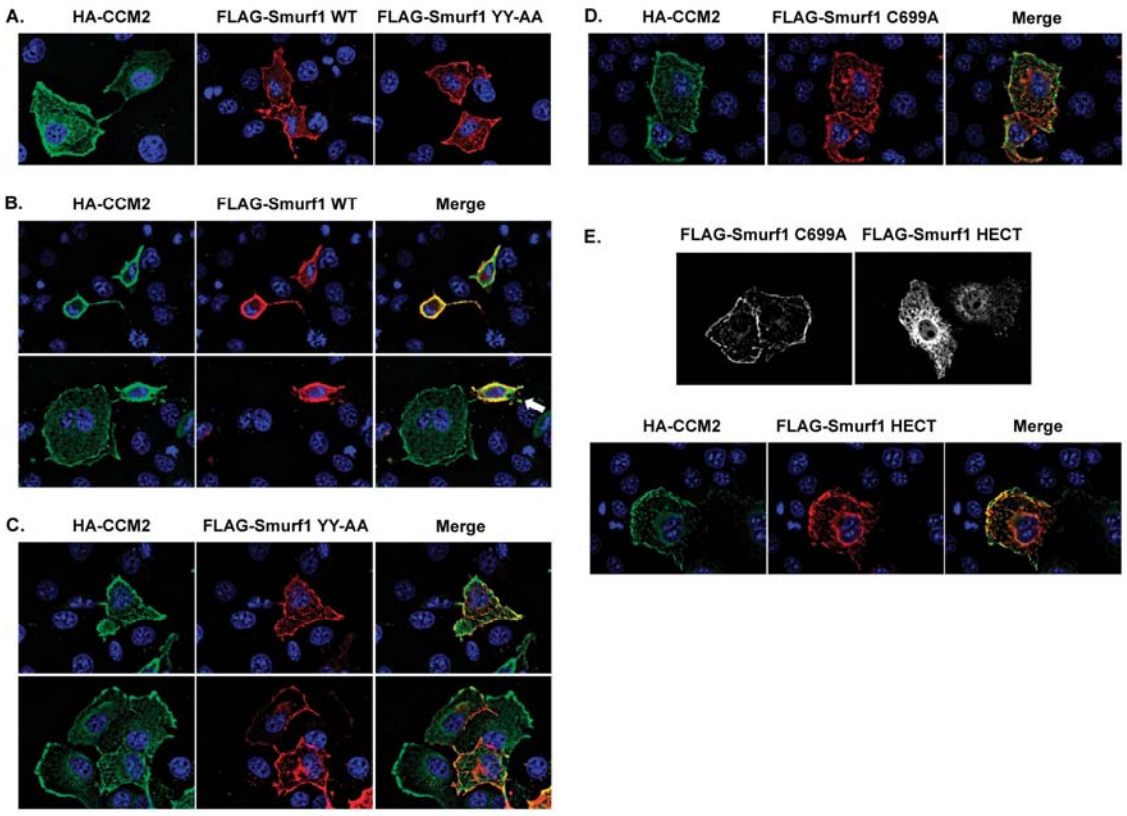

Figure 5.4. Expression of Smurf1 WT and CCM2 leads to cell morphology changes. A) COS-7 cells expressing HA-CCM2, FLAG-Smurf1 WT, or FLAG-Smurf1 YY-AA were fixed and stained with anti-HA antibody or anti-FLAG antibody. B) COS-7 cells expressing HA-CCM2 and Smurf WT display cell rounding (arrow), while cells expressing HA-CCM2 and FLAG-Smurf1 YY-AA (C) or HA-CCM2 and FLAG-Smurf1 C699A (D) do not. CCM2 can recruit the Smurf1 HECT domain to the plasma membrane. E) The Smurf1 HECT domain does not localize to the plasma membrane. CCM2 recruits the Smurf1 HECT domain to the plasma membrane. COS-7 cells expressing HA-CCM2, FLAG-Smurf1 C699A, or FLAG-Smurf1 HECT were fixed and stained with anti-FLAG and anti-HA antibodies.

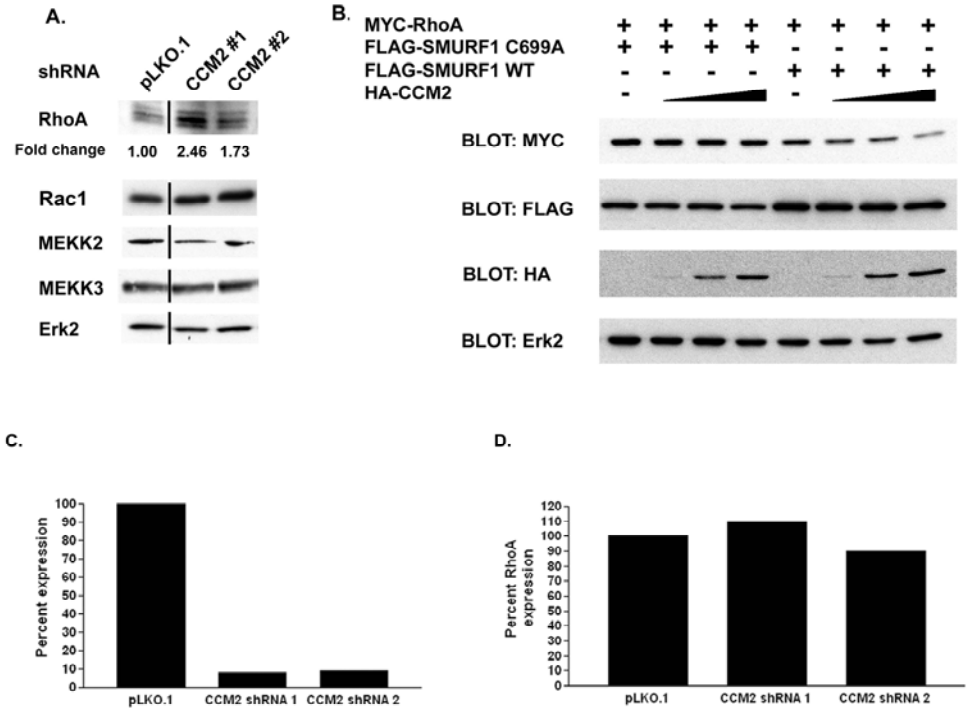

Figure 5.5: CCM2 regulates Smurf1-mediated RhoA abundance. A) bEND.3 cells expressing pLKO.1 or CCM2 shRNAs were lysed and abundance of endogenous RhoA, Rac1, MEKK2, and MEKK3 were analyzed by western blot. Erk2 was measured as a loading control. Fold change was calculated by determining the RhoA intensity relative to the Erk2 intensity for that sample standardized to the RhoA/Erk2 ratio for cells expressing pLKO.1. The line denotes where lanes were removed for clarity. B) HEK293 cells were transfected with Myc-RhoA, FLAG-Smurf1 WT, FLAG-Smurf1 C699A, and increasing amounts of HA-CCM2. Cells were subsequently lysed and analyzed by western blot. C) Relative quantitation of CCM2 RNA expression in bEND.3 cells was determined by real time RT-PCR quantitation. Representative data shown. CCM2 RNA levels were standardized to β-actin RNA levels. D) Relative quantitation of RhoA RNA expression in bEND.3 cells was determined by real time RT-PCR quantitation. Representative data shown. RhoA RNA levels were standardized to β-actin RNA levels.

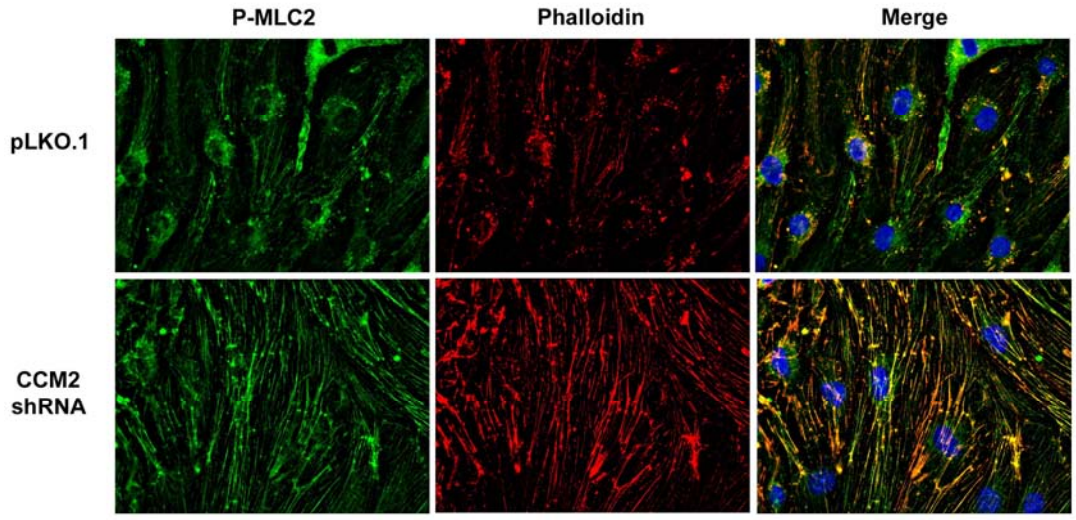

Figure 5.6: CCM2 knockdown leads to cytoskeletal changes in brain endothelial cells. bEND.3 cells stably expressing pLKO.1 or CCM2 shRNA were plated on Matrigel-coated coverslips and stained for phalloidin (red), phospho(Ser19)-MLC2 (green) and DAPI (bule).

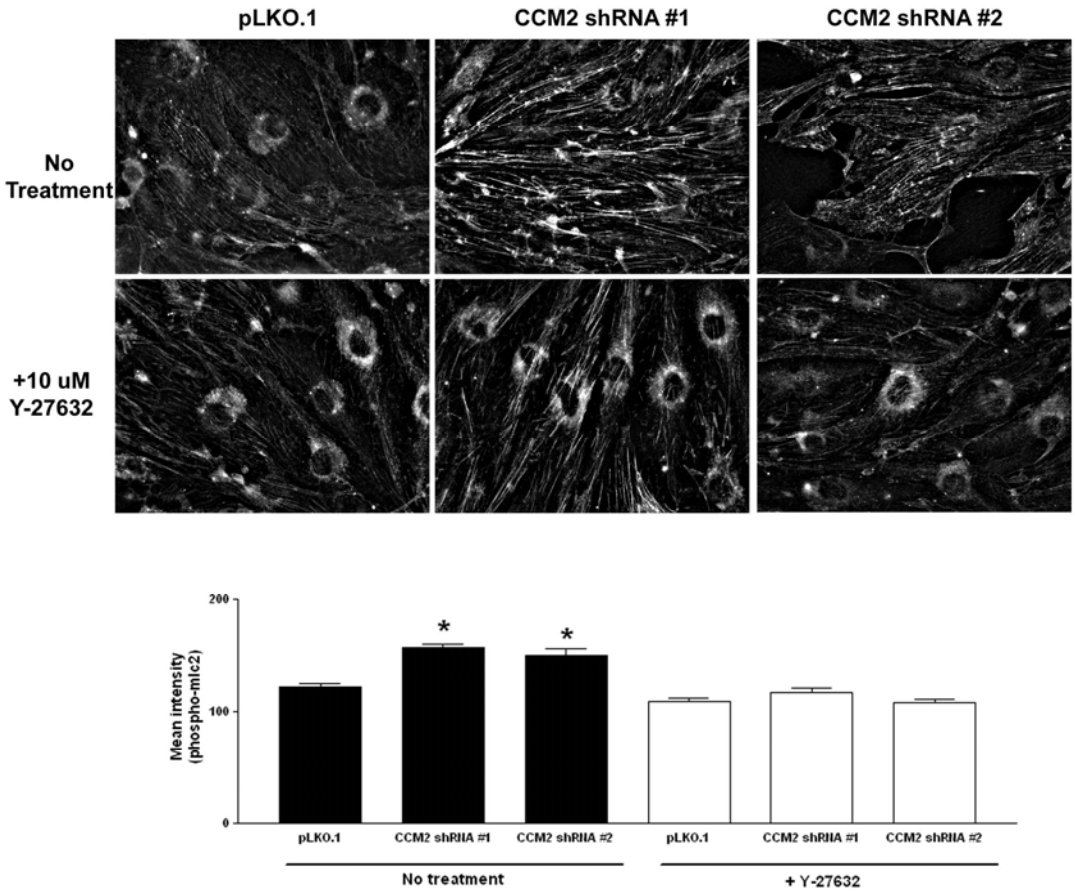

Figure 5.7: Increased association of phospho-MLC2 with stress fibers in CCM2 knockdown cells is abrogated with treatment with the ROCK inhibitor Y-27632. Top: bEND.3 cells grown on coverslips were treated with or without Y-27632 for 24 hours and then stained for phospho(Ser19)-MLC2. Bottom: Intensity of phosphorylated MLC-2 associated with rhodamine-phalloidin was determined as described in Materials and Methods.

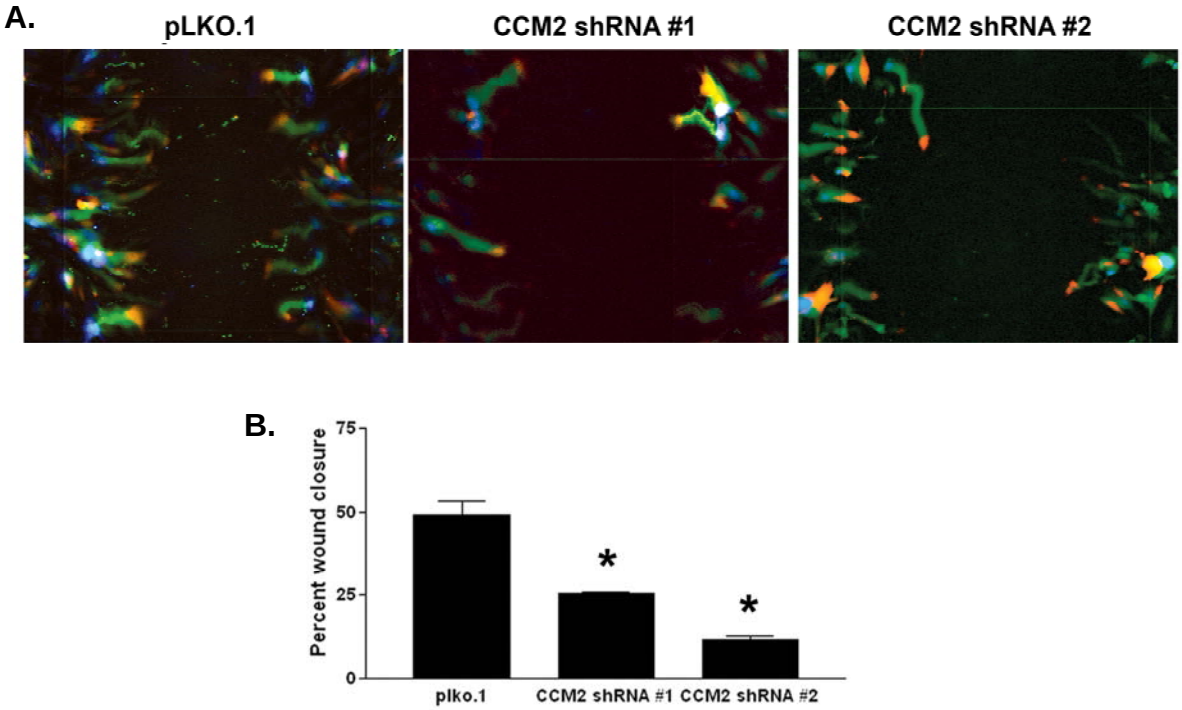

Figure 5.8: Loss of CCM2 expression impairs directed cell migration. A) bEND.3 cells grown to confluency were subjected to an in vitro wound healing assay. Cells were imaged every 15 minutes for 16 hours. The paths taken by cells (green) expressing either pLKO.1 or CCM2 shRNAs demonstrates decreased migration in CCM2-knockdown cells. The cell's starting point is shown in blue and its final location is shown in red. B) Quantitation of in vitro wound healing assays. Cells lacking CCM2 expression are less able to close a wound as measured by percent wound closure. * $p < 0.02$

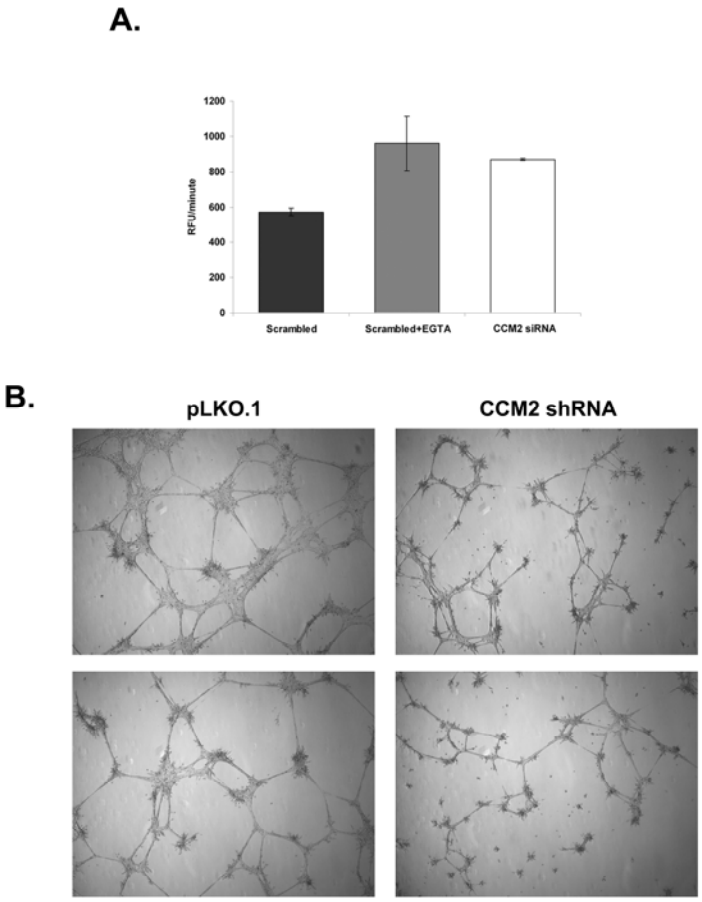

Figure 5.9: CCM2 is necessary for endothelial barrier function and endothelial tubule formation. A) HUVECs electroporated with either CCM2 SMARTpool siRNA or scrambled siRNA were plated on duplicate Matrigel-coated Transwells and were allowed form monolayers for 48 hours. The medium was then removed and replaced with EBM-2 containing 0.625 mg/mL FITC-dextran, with or without 4 mM EGTA. Aliquots (50 µL) were removed from the bottom well at 15 minute increments for 1.5 hours and fluorescence was read using a PHERAstar microplate reader. Data is expressed as the change in relative fluorescence units (RFU) per minute ± the standard deviation of the duplicates. Results are representative of three experiments. The average percent knockdown of CCM2 RNA levels compared to scrambled controls was ~60%. B) Mouse embryonic endothelial cells stably expressing either pLKO.1 or CCM2 shRNA were subjected to an *in vitro* tube formation assay as described in Materials and Methods.

Accession	Protein	Motif	Residues
O00308	WWP2	NPMY	573 - 576
Q8IYU2	HACE1	NPDY	610 - 613
Q76N89	HECW1	NPYY	1317-1320
Q15034	HERC3	NPIY	760-763
Q6ZTQ5	Similar to NEDD4L	NPMY	134-137
Q96PU5-3	NEDD4L isoform 3	NPYY	573-576
Q96PU5-5	NEDD4L isoform 5	NPYY	657-660
Q15751	HERC1	NPYY	3030-3033
Q9HCE7-2	SMURF1 isoform2	NPYY	431-434
O95071	UBR5	NPLY	539-542
Q96PU5	NEDD4L	NPYY	677-680
Q96J02	ITCH	NPMY	606-609
Q9P2P5	HECW2	NPYY	1284-1287
Q9H0M0	WWP1	NPMY	625-628
NP_940682	NEDD4 isoform 2	NPYY	949-952
P46934	NEDD4	NPYY	702-705
Q9HCE7	SMURF1	NPYY	457-460
Q9HAU4	SMURF2	NPYY	451-454
CAI42354	HUWE1	NPMY	4075-4078
CAI17960	ITCHY homolog	NPMY	565-568
Q9H0M0-3	WWP1 isoform 3	NPMY	495-498
Q96PU5-2	NEDD4L isoform 2	NPYY	613-616

Table 5.1: The NPXY motif in the Smurf1/2 HECT domain is conserved in other human HECT domains.

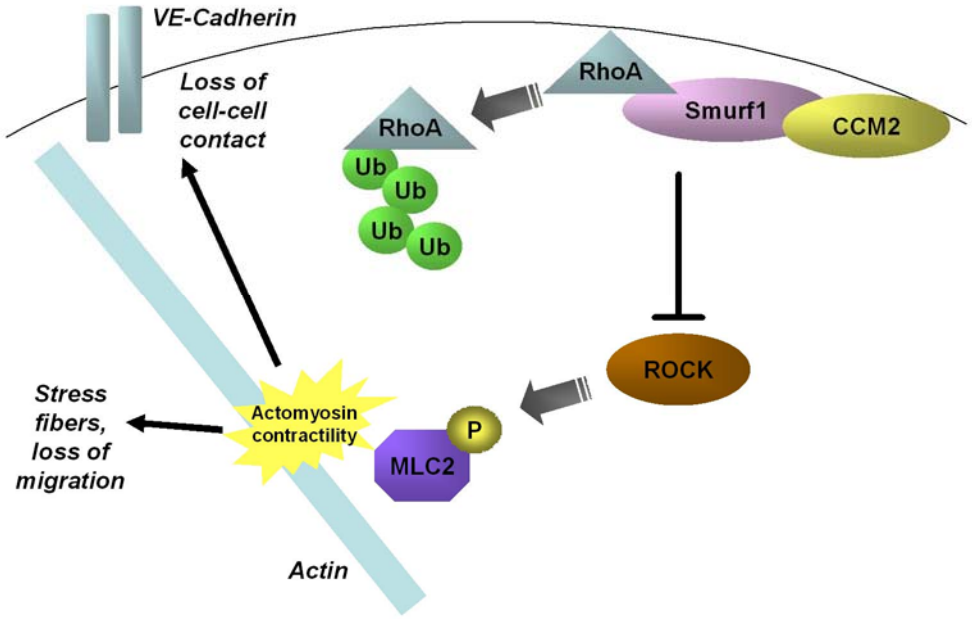

Figure 5.10: Model of CCM2-Smurf1 function. CCM2 recruits Smurf1 to specific locations at the plasma membrane to promote RhoA ubiquitination and degradation. This complex of CCM2 and Smurf1 therefore acts as a negative regulator of signaling downstream of RhoA. In the absence of CCM2, increased abundance of RhoA leads to enhanced RhoA signaling. RhoA signaling causes activation of ROCK and MLC2, resulting in actomyosin contractility and stress fiber formation. In endothelial cells, this leads to increased permeability and decreased cell to cell contact through VE-cadherin.

VI. Conclusion

Recent advancements

Our knowledge of CCM pathogenesis and CCM protein function has been recently expanded due to many high quality CCM research publications. Within the past four months, the two hit hypothesis has been proven, multiple CCM vertebrate models have been characterized, and a receptor upstream of CCM proteins has been described. The field has taken a large step forward and the recent developments are described below.

The two hit hypothesis of CCM pathogenesis had long been suspected, but not proven. Due to high expression levels of CCM mRNA in neural cells and the specificity of CCM lesions to the brain, parenchymal cell involvement was still considered relevant to CCM pathogenesis. A recent publication by Akers et al has shown that endothelial cells are responsible for CCM pathogenesis due to the two hit hypothesis. This study sequenced *CCM1*, *CCM2*, and *CCM3* from endothelial and surrounding cells from CCM lesions. In addition to the familial mutations in *CCM1*, *CCM2*, or *CCM3*, endothelial cells from CCM lesions had a second somatic mutation in these genes. These somatic mutations were not found in the surrounding neural tissue. Therefore, bi-allelic mutations in *CCM1*, *CCM2*, or *CCM3* leading to complete loss of expression in endothelial cells appear to be the cause of CCM lesion formation (Akers et al., 2009).

Conditional knockout mouse models have confirmed that endothelial cells are the tissue responsible for CCM endothelial cell dysfunction. Two independent groups generated CCM2 conditional knockout models to examine the role of endothelial and neural cells in embryonic lethalities associated with loss of CCM2. In both studies, loss of CCM2 in the neuroepithelium did not lead to embryonic lethality. Loss of CCM2 expression in endothelium led to embryonic lethalities due to vascular defects. Interestingly, these endothelial conditional knockout models both phenocopied the CCM1 and CCM2 gene-trap models. Loss of CCM2 in endothelial cells led to defects in aortic development. The aortic arch was of an inconsistent diameter and was collapsed in some regions. Impaired invasion of the embryonic vasculature into the labyrinth layer caused aberrant placenta vascularization. CCM2 knockdown endothelial cells had impaired tube lumen formation *in vitro* and increased RhoA activation. Loss of CCM2 expression caused increased VEGF-induced permeability, which could be blocked with simvastatin. The authors demonstrated that simvastatin blocked the increased signaling downstream of RhoA in CCM2 siRNA treated cells, suggesting that simvastatin should be further examined as a potential treatment for CCM2 patients (Boulday et al., 2009; Whitehead et al., 2009). Based on these studies and the work presented in this dissertation, regulation of RhoA signaling in endothelial cells appears to be a critical function for CCM2.

The signaling events upstream of the CCM protein complex have remained elusive. A recent study has identified a receptor that provides a function for the CCM1/CCM2 protein complex. The heart of glass (HEG1)

receptor was identified in a zebrafish screen for cardiovascular defects. It was hypothesized that this receptor may be in the same pathway as CCM1 and CCM2 as loss of HEG1 expression in zebrafish led to cardiovascular defects that phenocopied *santa* and *valentine* embryos. Loss of HEG1 in mice led to pulmonary hemorrhage and dorsal aorta collapse. The endothelial cell junctions in HEG1-null animals were found to be compromised compared to wild type mice. On a molecular level, HEG1 was found to associate with CCM2 through CCM1. The authors concluded that HEG1 is the receptor upstream of the CCM protein complex and this signaling pathway is necessary for blood vessel morphogenesis and integrity (Kleaveland et al., 2009).

The studies presented in this dissertation agree well with these recent advancements in our knowledge of CCM. We characterized a CCM1/CCM2 protein complex and predicted that it was relevant for CCM pathology. We now know that this interaction is important for signaling through the HEG1 receptor (Kleaveland et al., 2009). Signaling through this pathway appears to be critical for vascular development and integrity. We also showed that CCM2 is necessary for osmotic activation of p38, which is necessary for vascular development. Our examination of the CCM2-Smurf1 interaction characterized the molecular mechanism for enhanced RhoA activation in CCM2 knockdown cells (Whitehead et al., 2009). CCM2 recruits Smurf1 to the membrane, leading to RhoA degradation and downregulation of RhoA signaling. This maintains the proper cytoskeletal turnover in endothelial cells to allow migration and to enhance cell-to-cell contacts. Our study of CCM2 function in zebrafish showed that CCM2 is

necessary for aorta morphogenesis and proper embryonic blood flow, which is consistent with mouse and zebrafish models utilized by other groups. We can therefore appreciate the importance of this work in the context of CCM research and also endothelial cell physiology.

Based on our current knowledge of CCM proteins, we can begin to envision how these proteins may function in endothelial cells and how loss of CCM1, CCM2, or CCM3 could lead to endothelial defects (Figure 6.1). CCM1 is a Rap1 effector that is recruited to tight junctions to maintain junctional integrity. It also serves as an adaptor to link CCM2 to the HEG1 receptor. In the absence of CCM1, endothelial tight junctions are compromised, leading to endothelial leakiness. CCM2 coordinates activation of p38 via MEKK3 signaling, which is necessary for proper embryonic vascular development. CCM2 also recruits Smurf1 to specific sites at the plasma membrane to promote RhoA degradation. In the absence of CCM2, RhoA signaling is enhanced, leading to increased actomyosin contractility and stress fiber formation, which decreases cell-to-cell contact and prevents cell migration. In this way, loss of CCM1 or CCM2 could lead to endothelial cell defects that phenocopy each other, but these defects could occur through distinct mechanisms.

Future directions

We are only at the beginning of our understanding of the function of the proteins associated with cerebral cavernous malformations. The roles of CCM1, CCM2, and CCM3 biochemically and *in vivo* are still largely uncharacterized.

The work presented in this dissertation has led to new questions about CCM proteins and how dysregulation of these proteins could lead to cerebral cavernous malformations.

The heart of glass (HEG1) receptor has emerged as a component of the CCM complex. HEG1 has been linked to CCM both genetically and biochemically. CCM1 interacts with the cytoplasmic tail of the HEG1 receptor, linking it to CCM2. However, the signaling events downstream of HEG1 are completely uncharacterized. Based on what we know about CCM1 and CCM2 function, there are multiple pathways that could be involved in HEG1 signaling. First, HEG1 could signal through CCM1 to regulate CCM1 association with ICAP1, Rap1A, and β-catenin. In this way, HEG1 could be involved with Rap1A or β-catenin signaling pathways. HEG1 could also signal through CCM2 through MEKK3-medated p38 activation. Finally, we have characterized CCM2 as a negative regulator of RhoA signaling through Smurf1-mediated degradation. Thus, HEG1 could facilitate this pathway as well. Alternatively, activation of HEG1 may activate another signaling pathway not known at this time to be linked to CCM proteins. It is clear that significant effort is needed to characterize the signaling pathways downstream of HEG1 and how disruption of these pathways could contribute to CCM pathogenesis.

Smurf1-mediated degradation of RhoA has been characterized as a mechanism for regulation of cell polarity. In response to activation of the TGFβ receptor, Smurf1 associates with the Par6-PKC zeta cell polarity complex to regulate localized degradation of RhoA. In epithelial cells, the localized

degradation of RhoA leads to dissolution of tight junctions and epithelial-mesenchymal transition (EMT). In the work presented here, we have demonstrated that CCM2 binds Smurf1 to regulate Smurf1 localization and degradation of RhoA in endothelial cells. However, a role for CCM2 in cell polarization has not been examined. Therefore, a future direction of this project is to examine the role of CCM2 in regulating cell polarity, both in epithelial cells and endothelial cells.

CCM1, CCM2, and CCM3, have been shown to associate with each other and with proteins outside the CCM protein complex. We hypothesize that CCM1, CCM2, and CCM3 work together as a CCM protein complex but also have distinct roles with individual effectors. An important avenue of research is to understand the mechanisms involved with CCM complex association and dissociation. Using a combined approach of immunopurification of endogenous CCM protein complexes, size-exclusion chromatography, and mass spectrometry, the composition of CCM protein complexes within the cell would be determined. CCM protein complexes and the interactions regulating these complexes would provide significant insight into the signaling roles of CCM1, CCM2, and CCM3.

The findings presented in this dissertation indicate that CCM2 regulates multiple protein complexes and signaling pathways important in endothelial cell function. Analysis of these signaling pathways has provided insights into the molecular mechanisms that could be involved in cerebral cavernous malformation pathogenesis. These developments in our understanding of the

function of CCM2 will hopefully continue to advance the field toward the goal of targeted therapies for cerebral cavernous malformations.

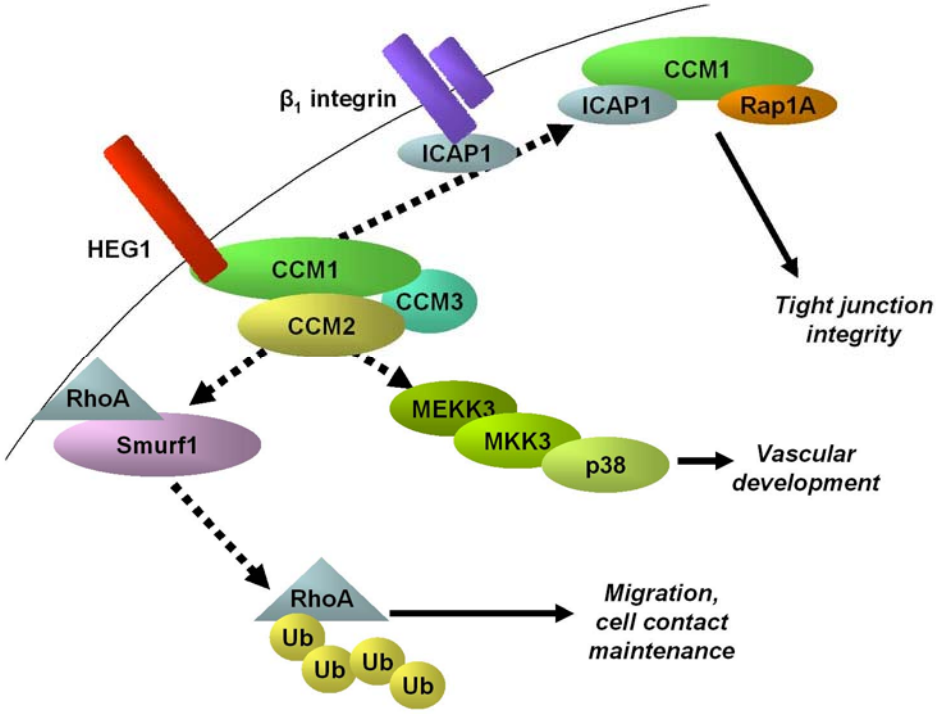

Figure 6.1: Model of CCM protein signaling complexes in endothelial cells. CCM1, CCM2, and CCM3 associate as a multi-protein complex. CCM1 functions to link HEG1 to CCM2, and presumably CCM3. CCM2 activates p38 signaling through MEKK3, which regulates vascular development. CCM2 can also associate with Smurf1 to regulate RhoA degradation. This pathway decreases signaling through RhoA and facilitates migration and cell contact maintenance. Finally, CCM1 can associate with ICAP1 and Rap1A to promote tight junction integrity. Absence of one or more of these pathways may be important in CCM pathogenesis.

References

Abbott, N. J., Ronnback, L., and Hansson, E. (2006). Astrocyte-endothelial interactions at the blood-brain barrier. Nat Rev Neurosci *7*, 41-53.

Adams, R. H., Porras, A., Alonso, G., Jones, M., Vintersten, K., Panelli, S., Valladares, A., Perez, L., Klein, R., and Nebreda, A. R. (2000). Essential role of p38alpha MAP kinase in placental but not embryonic cardiovascular development. Mol Cell *6*, 109-116.

Akers, A. L., Johnson, E., Steinberg, G. K., Zabramski, J. M., and Marchuk, D. A. (2009). Biallelic somatic and germline mutations in cerebral cavernous malformations (CCMs): evidence for a two-hit mechanism of CCM pathogenesis. Hum Mol Genet *18*, 919-930.

Amano, M., Ito, M., Kimura, K., Fukata, Y., Chihara, K., Nakano, T., Matsuura, Y., and Kaibuchi, K. (1996). Phosphorylation and Activation of Myosin by Rho-associated Kinase (Rho-kinase). J Biol Chem *271*, 20246-20249.

Arthur, H. M., Ure, J., Smith, A. J., Renforth, G., Wilson, D. I., Torsney, E., Charlton, R., Parums, D. V., Jowett, T., Marchuk, D. A.*, et al.* (2000). Endoglin, an ancillary TGFbeta receptor, is required for extraembryonic angiogenesis and plays a key role in heart development. Dev Biol *217*, 42-53.

Bader, B. L., Rayburn, H., Crowley, D., and Hynes, R. O. (1998). Extensive Vasculogenesis, Angiogenesis, and Organogenesis Precede Lethality in Mice Lacking All [alpha]v Integrins. Cell *95*, 507-519.

Bergametti, F., Denier, C., Labauge, P., Arnoult, M., Boetto, S., Clanet, M., Coubes, P., Echenne, B., Ibrahim, R., Irthum, B.*, et al.* (2005). Mutations within the programmed cell death 10 gene cause cerebral cavernous malformations. Am J Hum Genet *76*, 42-51.

Berman, J. R., and Kenyon, C. (2006). Germ-Cell Loss Extends C. elegans Life Span through Regulation of DAF-16 by kri-1 and Lipophilic-Hormone Signaling. Cell *124*, 1055-1068.

Boulday, G., Blecon, A., Petit, N., Chareyre, F., Garcia, L. A., Niwa-Kawakita, M., Giovannini, M., and Tournier-Lasserve, E. (2009). Tissue-specific conditional CCM2 knockout mice establish the essential role of endothelial CCM2 in angiogenesis: implications for human cerebral cavernous malformations. Disease Models & Mechanisms *2*, 168-177.

Bouvard, D., Aszodi, A., Kostka, G., Block, M. R., Albiges-Rizo, C., and Fassler, R. (2007). Defective osteoblast function in ICAP-1-deficient mice. Development *134*, 2615-2625.

Calderwood, D. A., Yan, B., de Pereda, J. M., Alvarez, B. G., Fujioka, Y., Liddington, R. C., and Ginsberg, M. H. (2002). The Phosphotyrosine Binding-like Domain of Talin Activates Integrins. J Biol Chem *277*, 21749-21758.

Cave-Riant, F., Denier, C., Labauge, P., Cecillon, M., Maciazek, J., Joutel, A., Laberge-Le Couteulx, S., and Tournier-Lasserve, E. (2002). Spectrum and expression analysis of KRIT1 mutations in 121 consecutive and unrelated patients with Cerebral Cavernous Malformations. Eur J Hum Genet *10*, 733-740.

Chang, D. D., Wong, C., Smith, H., and Liu, J. (1997). ICAP-1, a novel beta1 integrin cytoplasmic domain-associated protein, binds to a conserved and functionally important NPXY sequence motif of beta1 integrin. J Cell Biol *138*, 1149-1157.

Chen, D. H., Lipe, H. P., Qin, Z., and Bird, T. D. (2002). Cerebral cavernous malformation: novel mutation in a Chinese family and evidence for heterogeneity. J Neurol Sci *196*, 91-96.

Chen, J., Haffter, P., Odenthal, J., Vogelsang, E., Brand, M., van Eeden, F., Furutani-Seiki, M., Granato, M., Hammerschmidt, M., Heisenberg, C.*, et al.* (1996). Mutations affecting the cardiovascular system and other internal organs in zebrafish. Development *123*, 293-302.

Chong, P. A., Lin, H., Wrana, J. L., and Forman-Kay, J. D. (2006). An expanded WW domain recognition motif revealed by the interaction between Smad7 and the E3 ubiquitin ligase Smurf2. J Biol Chem *281*, 17069-17075.

Clatterbuck, R. E., Eberhart, C. G., Crain, B. J., and Rigamonti, D. (2001). Ultrastructural and immunocytochemical evidence that an incompetent blood-brain barrier is related to the pathophysiology of cavernous malformations. J Neurol Neurosurg Psychiatry *71*, 188-192.

Couteulx, S. L., Brezin, A. P., Fontaine, B., Tournier-Lasserve, E., and Labauge, P. (2002). A novel KRIT1/CCM1 truncating mutation in a patient with cerebral and retinal cavernous angiomas. Arch Ophthalmol *120*, 217-218.

Davenport, W. J., Siegel, A. M., Dichgans, J., Drigo, P., Mammi, I., Pereda, P., Wood, N. W., and Rouleau, G. A. (2001). CCM1 gene mutations in families segregating cerebral cavernous malformations. Neurology *56*, 540-543.

Deng, Y., Yang, J., McCarty, M., and Su, B. (2007). MEKK3 is required for endothelium function but is not essential for tumor growth and angiogenesis. Am J Physiol Cell Physiol *293*, C1404-1411.

Denier, C., Gasc, J. M., Chapon, F., Domenga, V., Lescoat, C., Joutel, A., and Tournier-Lasserve, E. (2002). Krit1/cerebral cavernous malformation 1 mRNA is preferentially expressed in neurons and epithelial cells in embryo and adult. Mech Dev *117*, 363-367.

Denier, C., Goutagny, S., Labauge, P., Krivosic, V., Arnoult, M., Cousin, A., Benabid, A. L., Comoy, J., Frerebeau, P., Gilbert, B.*, et al.* (2004). Mutations within the MGC4607 gene cause cerebral cavernous malformations. Am J Hum Genet *74*, 326-337.

Ebisawa, T., Fukuchi, M., Murakami, G., Chiba, T., Tanaka, K., Imamura, T., and Miyazono, K. (2001). Smurf1 Interacts with Transforming Growth Factor-beta Type I Receptor through Smad7 and Induces Receptor Degradation. J Biol Chem *276*, 12477-12480.

Eerola, I., McIntyre, B., and Vikkula, M. (2001). Identification of eight novel 5'-exons in cerebral capillary malformation gene-1 (CCM1) encoding KRIT1. Biochim Biophys Acta *1517*, 464-467.

Fanger, G. R., Johnson, N. L., and Johnson, G. L. (1997). MEK kinases are regulated by EGF and selectively interact with Rac/Cdc42. Embo J *16*, 4961-4972.

Gallagher, E., Gao, M., Liu, Y.-C., and Karin, M. (2006). Activation of the E3 ubiquitin ligase Itch through a phosphorylation-induced conformational change. Proceedings of the National Academy of Sciences of the United States of America *103*, 1717-1722.

Glading, A., Han, J., Stockton, R. A., and Ginsberg, M. H. (2007). KRIT-1/CCM1 is a Rap1 effector that regulates endothelial cell cell junctions. J Cell Biol *179*, 247-254.

Goodrich, D. W., and Lee, W.-H. (1993). Molecular characterization of the retinoblastoma susceptibility gene. Biochimica et Biophysica Acta (BBA) - Reviews on Cancer *1155*, 43-61.

Grimes, A. C., Stadt, H. A., Shepherd, I. T., and Kirby, M. L. (2006). Solving an enigma: arterial pole development in the zebrafish heart. Dev Biol *290*, 265-276.

Guclu, B., Ozturk, A. K., Pricola, K. L., Bilguvar, K., Shin, D., O'Roak, B. J., and Gunel, M. (2005). Mutations in apoptosis-related gene, PDCD10, cause cerebral cavernous malformation 3. Neurosurgery *57*, 1008-1013.

Hilder, T. L., Malone, M. H., Bencharit, S., Colicelli, J., Haystead, T. A., Johnson, G. L., and Wu, C. C. (2007). Proteomic identification of the cerebral cavernous malformation signaling complex. J Proteome Res *6*, 4343-4355.

Hohmann, S., Krantz, M., and Nordlander, B. (2007). Yeast Osmoregulation. Methods in Enzymology. In Osmosensing and Osmosignaling, D. H. a. H. Sies, ed. (Academic Press), pp. 29-45.

Ingham, R. J., Colwill, K., Howard, C., Dettwiler, S., Lim, C. S. H., Yu, J., Hersi, K., Raaijmakers, J., Gish, G., Mbamalu, G.*, et al.* (2005). WW Domains Provide a Platform for the Assembly of Multiprotein Networks. Mol Cell Biol *25*, 7092-7106.

Ingham, R. J., Gish, G., and Pawson, T. (2004). The Nedd4 family of E3 ubiquitin ligases: functional diversity within a common modular architecture. Oncogene *23*, 1972-1984.

Kesavan, K., Lobel-Rice, K., Sun, W., Lapadat, R., Webb, S., Johnson, G. L., and Garrington, T. P. (2004). MEKK2 regulates the coordinate activation of ERK5 and JNK in response to FGF-2 in fibroblasts. J Cell Physiol *199*, 140-148.

Kimmel, C. B., Ballard, W. W., Kimmel, S. R., Ullmann, B., and Schilling, T. F. (1995). Stages of embryonic development of the zebrafish. Dev Dyn *203*, 253-310.

Kleaveland, B., Zheng, X., Liu, J. J., Blum, Y., Tung, J. J., Zou, Z., Chen, M., Guo, L., Lu, M.-m., Zhou, D.*, et al.* (2009). Regulation of cardiovascular development and integrity by the heart of glass-cerebral cavernous malformation protein pathway. Nat Med *15*, 169-176.

Labauge, P., Denier, C., Bergametti, F., and Tournier-Lasserve, E. (2007). Genetics of cavernous angiomas. The Lancet Neurology *6*, 237-244.

Laberge-le Couteulx, S., Jung, H. H., Labauge, P., Houtteville, J. P., Lescoat, C., Cecillon, M., Marechal, E., Joutel, A., Bach, J. F., and Tournier-Lasserve, E. (1999). Truncating mutations in CCM1, encoding KRIT1, cause hereditary cavernous angiomas. Nat Genet *23*, 189-193.

Laurans, M. S., DiLuna, M. L., Shin, D., Niazi, F., Voorhees, J. R., Nelson-Williams, C., Johnson, E. W., Siegel, A. M., Steinberg, G. K., Berg, M. J.*, et al.* (2003). Mutational analysis of 206 families with cavernous malformations. J Neurosurg *99*, 38-43.

Lebrin, F., Deckers, M., Bertolino, P., and ten Dijke, P. (2005). TGF-{beta} receptor function in the endothelium. Cardiovasc Res *65*, 599-608.

Lin, J. L., Chen, H. C., Fang, H. I., Robinson, D., Kung, H. J., and Shih, H. M. (2001). MST4, a new Ste20-related kinase that mediates cell growth and transformation via modulating ERK pathway. Oncogene *20*, 6559-6569.

Lin, X., Liang, M., and Feng, X. H. (2000). Smurf2 is a ubiquitin E3 ligase mediating proteasome-dependent degradation of Smad2 in transforming growth factor-beta signaling. J Biol Chem *275*, 36818-36822.

Liquori, C. L., Berg, M. J., Siegel, A. M., Huang, E., Zawistowski, J. S., Stoffer, T., Verlaan, D., Balogun, F., Hughes, L., Leedom, T. P.*, et al.* (2003). Mutations in a gene encoding a novel protein containing a phosphotyrosine-binding domain cause type 2 cerebral cavernous malformations. Am J Hum Genet *73*, 1459-1464.

Liquori, C. L., Berg, M. J., Squitieri, F., Leedom, T. P., Ptacek, L., Johnson, E. W., and Marchuk, D. A. (2007). Deletions in CCM2 Are a Common Cause of Cerebral Cavernous Malformations. The American Journal of Human Genetics *80*, 69-75.

Lu, G., Kang, Y. J., Han, J., Herschman, H. R., Stefani, E., and Wang, Y. (2006). TAB-1 Modulates Intracellular Localization of p38 MAP Kinase and Downstream Signaling. J Biol Chem *281*, 6087-6095.

Lucas, M., Costa, A. F., Montori, M., Solano, F., Zayas, M. D., and Izquierdo, G. (2001). Germline mutations in the CCM1 gene, encoding Krit1, cause cerebral cavernous malformations. Ann Neurol *49*, 529-532.

Ma, X., Zhao, H., Shan, J., Long, F., Chen, Y., Chen, Y., Zhang, Y., Han, X., and Ma, D. (2007). PDCD10 Interacts with Ste20-related Kinase MST4 to Promote Cell Growth and Transformation via Modulation of the ERK Pathway. Mol Biol Cell *18*, 1965-1978.

Mably, J. D., Chuang, L. P., Serluca, F. C., Mohideen, M.-A. P. K., Chen, J.-N., and Fishman, M. C. (2006). santa and valentine pattern concentric growth of cardiac myocardium in the zebrafish. Development *133*, 3139-3146.

Malone, M., Sciaky, N., Stalheim, L., Hahn, K., Linney, E., and Johnson, G. (2007). Laser-scanning velocimetry: A confocal microscopy method for quantitative measurement of cardiovascular performance in zebrafish embryos and larvae. BMC Biotechnology *7*, 40.

Marchuk, D. A., Srinivasan, S., Squire, T. L., and Zawistowski, J. S. (2003). Vascular morphogenesis: tales of two syndromes. Hum Mol Genet *12 Spec No 1*, R97-112.

Marini, V., Ferrera, L., Dorcaratto, A., Viale, G., Origone, P., Mareni, C., and Garre, C. (2003). Identification of a novel KRIT1 mutation in an Italian family with cerebral cavernous malformation by the protein truncation test. J Neurol Sci *212*, 75-78.

Marini, V., Ferrera, L., Pigatto, F., Origone, P., Garre, C., Dorcaratto, A., Viale, G., Alberti, F., and Mareni, C. (2004). Search for loss of heterozygosity and mutation analysis of KRIT1 gene in CCM patients. Am J Med Genet A *130*, 98-101.

McCarty, J. H., Lacy-Hulbert, A., Charest, A., Bronson, R. T., Crowley, D., Housman, D., Savill, J., Roes, J., and Hynes, R. O. (2005). Selective ablation of {alpha}v integrins in the central nervous system leads to cerebral hemorrhage, seizures, axonal degeneration and premature death. Development *132*, 165-176.

Miller, W. E., and Lefkowitz, R. J. (2001). Expanding roles for [beta]-arrestins as scaffolds and adapters in GPCR signaling and trafficking. Current Opinion in Cell Biology *13*, 139-145.

Musunuru, K., Hillard, V. H., and Murali, R. (2003). Widespread central nervous system cavernous malformations associated with cafe-au-lait skin lesions. Case report. J Neurosurg *99*, 412-415.

Nakamura, K., Uhlik, M. T., Johnson, N. L., Hahn, K. M., and Johnson, G. L. (2006). PB1 Domain-Dependent Signaling Complex Is Required for Extracellular Signal-Regulated Kinase 5 Activation. Mol Cell Biol *26*, 2065-2079.

Ogunjimi, A. A., Briant, D. J., Pece-Barbara, N., Le Roy, C., Di Guglielmo, G. M., Kavsak, P., Rasmussen, R. K., Seet, B. T., Sicheri, F., and Wrana, J. L. (2005). Regulation of Smurf2 ubiquitin ligase activity by anchoring the E2 to the HECT domain. Mol Cell *19*, 297-308.

Pagenstecher, A., Stahl, S., Sure, U., and Felbor, U. (2009). A two-hit mechanism causes cerebral cavernous malformations: complete inactivation of CCM1, CCM2 or CCM3 in affected endothelial cells. Hum Mol Genet *18*, 911-918.

Park, S. O., Lee, Y. J., Seki, T., Hong, K.-H., Fliess, N., Jiang, Z., Park, A., Wu, X., Kaartinen, V., Roman, B. L., and Oh, S. P. (2008). ALK5- and TGFBR2-independent role of ALK1 in the pathogenesis of hereditary hemorrhagic telangiectasia type 2. Blood *111*, 633-642.

Petit, N., Blécon, A., Denier, C., and Tournier-Lasserve, E. (2006). Patterns of expression of the three cerebral cavernous malformation (CCM) genes during

embryonic and postnatal brain development. Gene Expression Patterns *6*, 495-503.

Plant, P. J., Yeger, H., Staub, O., Howard, P., and Rotin, D. (1997). The C2 Domain of the Ubiquitin Protein Ligase Nedd4 Mediates Ca2+-dependent Plasma Membrane Localization. J Biol Chem *272*, 32329-32336.

Plummer, N. W., Gallione, C. J., Srinivasan, S., Zawistowski, J. S., Louis, D. N., and Marchuk, D. A. (2004). Loss of p53 sensitizes mice with a mutation in Ccm1 (KRIT1) to development of cerebral vascular malformations. Am J Pathol *165*, 1509-1518.

Plummer, N. W., Squire, T. L., Srinivasan, S., Huang, E., Zawistowski, J. S., Matsunami, H., Hale, L. P., and Marchuk, D. A. (2006). Neuronal expression of the Ccm2 gene in a new mouse model of cerebral cavernous malformations. Mamm Genome *17*, 119-128.

Plummer, N. W., Zawistowski, J. S., and Marchuk, D. A. (2005). Genetics of cerebral cavernous malformations. Curr Neurol Neurosci Rep *5*, 391-396.

Proctor, J. M., Zang, K., Wang, D., Wang, R., and Reichardt, L. F. (2005). Vascular Development of the Brain Requires {beta}8 Integrin Expression in the Neuroepithelium. J Neurosci *25*, 9940-9948.

Sahoo, T., Goenaga-Diaz, E., Serebriiskii, I. G., Thomas, J. W., Kotova, E., Cuellar, J. G., Peloquin, J. M., Golemis, E., Beitinjaneh, F., Green, E. D.*, et al.* (2001). Computational and experimental analyses reveal previously undetected coding exons of the KRIT1 (CCM1) gene. Genomics *71*, 123-126.

Sahoo, T., Johnson, E. W., Thomas, J. W., Kuehl, P. M., Jones, T. L., Dokken, C. G., Touchman, J. W., Gallione, C. J., Lee-Lin, S. Q., Kosofsky, B.*, et al.* (1999). Mutations in the gene encoding KRIT1, a Krev-1/rap1a binding protein, cause cerebral cavernous malformations (CCM1). Hum Mol Genet *8*, 2325-2333.

Serebriiskii, I., Estojak, J., Sonoda, G., Testa, J. R., and Golemis, E. A. (1997). Association of Krev-1/rap1a with Krit1, a novel ankyrin repeat-containing protein encoded by a gene mapping to 7q21-22. Oncogene *15*, 1043-1049.

Smith, M. J., Hardy, W. R., Murphy, J. M., Jones, N., and Pawson, T. (2006). Screening for PTB domain binding partners and ligand specificity using proteome-derived NPXY peptide arrays. Mol Cell Biol *26*, 8461-8474.

Sophie Béraud-Dufour, R. G., Corinne Albiges-Rizo, Pierre Chardin, Eva Faurobert, (2007). Krit1 interactions with microtubules and membranes are

regulated by Rap1 and integrin cytoplasmic domain associated protein-1. FEBS Journal *274*, 5518-5532.

Sorkin, A., McClure, M., Huang, F., and Carter, R. (2000). Interaction of EGF receptor and grb2 in living cells visualized by fluorescence resonance energy transfer (FRET) microscopy. Curr Biol *10*, 1395-1398.

Stainier, D., Fouquet, B., Chen, J., Warren, K., Weinstein, B., Meiler, S., Mohideen, M., Neuhauss, S., Solnica-Krezel, L., Schier, A.*, et al.* (1996). Mutations affecting the formation and function of the cardiovascular system in the zebrafish embryo. Development *123*, 285-292.

Stainier, D., Lee, R., and Fishman, M. (1993). Cardiovascular development in the zebrafish. I. Myocardial fate map and heart tube formation. Development *119*, 31-40.

Uhlik, M. T., Abell, A. N., Johnson, N. L., Sun, W., Cuevas, B. D., Lobel-Rice, K. E., Horne, E. A., Dell'Acqua, M. L., and Johnson, G. L. (2003). Rac-MEKK3-MKK3 scaffolding for p38 MAPK activation during hyperosmotic shock. Nat Cell Biol *5*, 1104-1110.

Uhlik, M. T., Temple, B., Bencharit, S., Kimple, A. J., Siderovski, D. P., and Johnson, G. L. (2005). Structural and Evolutionary Division of Phosphotyrosine Binding (PTB) Domains. Journal of Molecular Biology *345*, 1-20.

Verlaan, D. J., Davenport, W. J., Stefan, H., Sure, U., Siegel, A. M., and Rouleau, G. A. (2002). Cerebral cavernous malformations: mutations in Krit1. Neurology *58*, 853-857.

Wang, H. R., Ogunjimi, A. A., Zhang, Y., Ozdamar, B., Bose, R., and Wrana, J. L. (2006). Degradation of RhoA by Smurf1 ubiquitin ligase. Methods Enzymol *406*, 437-447.

Wang, H.-R., Zhang, Y., Ozdamar, B., Ogunjimi, A. A., Alexandrova, E., Thomsen, G. H., and Wrana, J. L. (2003). Regulation of Cell Polarity and Protrusion Formation by Targeting RhoA for Degradation. Science *302*, 1775-1779.

Whitehead, K. J., Chan, A. C., Navankasattusas, S., Koh, W., London, N. R., Ling, J., Mayo, A. H., Drakos, S. G., Marchuk, D. A., Davis, G. E., and Li, D. Y. (2009). The cerebral cavernous malformation signaling pathway promotes vascular integrity via Rho GTPases. Nat Med *15*, 177-184.

Whitehead, K. J., Plummer, N. W., Adams, J. A., Marchuk, D. A., and Li, D. Y. (2004). Ccm1 is required for arterial morphogenesis: implications for the etiology of human cavernous malformations. Development *131*, 1437-1448.

Wiesner, S., Ogunjimi, A. A., Wang, H. R., Rotin, D., Sicheri, F., Wrana, J. L., and Forman-Kay, J. D. (2007). Autoinhibition of the HECT-type ubiquitin ligase Smurf2 through its C2 domain. Cell *130*, 651-662.

Willem H Mager, M. S. (2002). Novel insights into the osmotic stress response of yeast. FEMS Yeast Research *2*, 251-257.

Wittchen, E. S., Worthylake, R. A., Kelly, P., Casey, P. J., Quilliam, L. A., and Burridge, K. (2005). Rap1 GTPase Inhibits Leukocyte Transmigration by Promoting Endothelial Barrier Function. J Biol Chem *280*, 11675-11682.

Wojciak-Stothard, B., and Ridley, A. J. (2002). Rho GTPases and the regulation of endothelial permeability. Vascular Pharmacology, Endothelial Hyperpermeability in Vascular Leakage *39*, 187-199.

Xu, Y. L., Zhao, J. Z., Wu, B. Q., Zhong, H. H., Wang, S., and Heng, W. J. (2003). [A novel Krit-1 mutation in Han family with cerebral cavernous malformation]. Zhonghua Bing Li Xue Za Zhi *32*, 220-225.

Yamashita, M., Ying, S. X., Zhang, G. M., Li, C., Cheng, S. Y., Deng, C. X., and Zhang, Y. E. (2005). Ubiquitin ligase Smurf1 controls osteoblast activity and bone homeostasis by targeting MEKK2 for degradation. Cell *121*, 101-113.

Yang, J., Boerm, M., McCarty, M., Bucana, C., Fidler, I. J., Zhuang, Y., and Su, B. (2000). Mekk3 is essential for early embryonic cardiovascular development. Nat Genet *24*, 309-313.

Zawistowski, J. S., Serebriiskii, I. G., Lee, M. F., Golemis, E. A., and Marchuk, D. A. (2002). KRIT1 association with the integrin-binding protein ICAP-1: a new direction in the elucidation of cerebral cavernous malformations (CCM1) pathogenesis. Hum Mol Genet *11*, 389-396.

Zawistowski, J. S., Stalheim, L., Uhlik, M. T., Abell, A. N., Ancrile, B. B., Johnson, G. L., and Marchuk, D. A. (2005). CCM1 and CCM2 protein interactions in cell signaling: implications for cerebral cavernous malformations pathogenesis. Hum Mol Genet *14*, 2521-2531.

Zhang, J., Clatterbuck, R. E., Rigamonti, D., Chang, D. D., and Dietz, H. C. (2001). Interaction between krit1 and icap1alpha infers perturbation of integrin beta1-mediated angiogenesis in the pathogenesis of cerebral cavernous malformation. Hum Mol Genet *10*, 2953-2960.

Zhang, J., Clatterbuck, R. E., Rigamonti, D., and Dietz, H. C. (2000a). Cloning of the murine Krit1 cDNA reveals novel mammalian 5' coding exons. Genomics *70*, 392-395.

Zhang, J., Clatterbuck, R. E., Rigamonti, D., and Dietz, H. C. (2000b). Mutations in KRIT1 in familial cerebral cavernous malformations. Neurosurgery *46*, 1272-1277; discussion 1277-1279.

Zhang, X. A., and Hemler, M. E. (1999). Interaction of the integrin beta1 cytoplasmic domain with ICAP-1 protein. J Biol Chem *274*, 11-19.

Zhu, J., Motejlek, K., Wang, D., Zang, K., Schmidt, A., and Reichardt, L. F. (2002). beta8 integrins are required for vascular morphogenesis in mouse embryos. Development *129*, 2891-2903.